POLITECNICO DI TORINO

Dipartimento di ENERGIA

Warsaw University of Technology

Faculty of Electrical Engineering

Corso di Laurea Magistrale in INGEGNERIA ELETTRICA

Tesi di laurea magistrale

Wind turbine overview. Mismatch assessment between manufacturer's power curve and on-site measurements during wind turbine operation

Supervisor:

Prof. Filippo Spertino …….

Erasmus+ thesis tutor:

Dr. inż. Mariusz Kłos …….

Candidate:

Francesco Buttau

Mat. 216/036

Academic year 2016-2017

Table of Contents

We are only seeking Man.
We have no need of other worlds.
We need mirrors.
We don't know what to do with other worlds.

Stanisław Lem, *Solaris*

Introduction to part 1

Wind turbine overview

On part 1, I described some of the features of the realization of an inland wind energy utilization project, such as a single wind turbine, or a wind farm. The document includes a brief description of the wind power history, in my opinion extremely important considering the impact of wind energy on human civilization, and that today's wind application are nothing more than the direct descendants of the glorious windmills.

A discussion regarding the physical principles of wind conversion, and on the nature of the wind resource itself follows. Once the wind has been characterized, it is necessary to consider and quantify the energy obtainable, the *energy yield*, with respect to the wind conditions. Finally, a more specific discussion on the choice of the generator is presented.

Part 1 is a theoretical, expositive part that I mainly produced during my Erasmus+ 2016 studies at Warsaw university of Technology. It should be seen as a support and a formal basis for part2, which I carried out in 2017 at Politecnico di Torino, exploring some of the concepts of part 1 into an original work.

Chapter 1.1: Wind power history

1.1.1 Windmills

For centuries, the power of the wind has been a useful resource in different locations of our planet. The first example of its usage dates back to the 1st century AD, when Heron of Alexandria invented an organ powered through a windwheel[1].

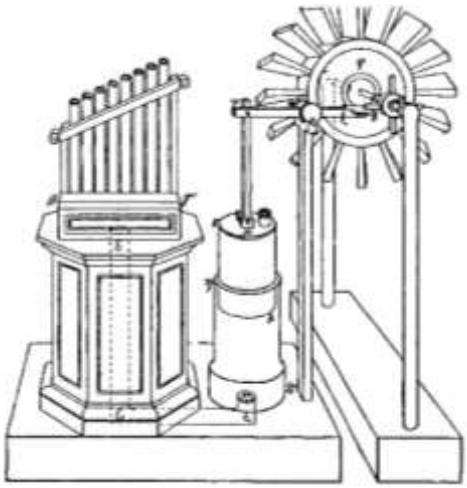

Figure 1: **Reconstruction of Heron's windwheel.**
Source: Wikimedia *https://upload.wikimedia.org/wikipedia/commons/5/5f/Heron's_Windwheel.jpg* consulted on 30/06/2017.

As many inventions and power applications in the classical Age, Heron's windwheel was meant to amaze the audience, to delight people, in a positive way clearly related to the concept of "deus ex machina" typical of the Hellenic world.

To have any economical large scale wind power application we have to wait till the Middle Ages, in China (difficult dating) and in Seistan (Afghanistan) documented in 644 and 945 A.D., as simple windwheel structures with a vertical axis[2] were used as mills.

Windmills, as watermills, had their scope into allowing grain milling and, in general, to provide mechanical power, used to feed water pumps, for fulling of cloth, for operating bellows and forges, thus pushing the ironworking. In the classical ages, human and animal force were rather used to obtain this kind of power: this fact postponed the success of both windmills and watermills.

---

[1] V.Marchis, *Storia delle Macchine, p.21*
[2] Hau, *Wind Turbines fund., p.2*

In Europe, especially in the northern part of the continent where winds are strong and constant, wind power finds a wide application in the second part of the XIII century, documented in Normandy, in England, and in the Flanders region. Windmills will spread rapidly through the Old Continent, to end up even in Palestine, where they were effectively used as a power source in the besieged towns[3].

Figure 2: **Dutch "Wipmolen".**
Source: Door Quistnix at nl.wikipedia, CC BY-SA 2.5,
https://commons.wikimedia.org/w/index.php?curid=3665728 **consulted on 01/08/2016.**

In the beginning of the XV century, in Holland, windmills started being used for effectively pumping water, while the population built dikes, thus reclaiming parts of land from the sea. These machines were called "Hollow Post Windmills" or "wipmolen", they had pyramidal base and they contained a simple mechanism of cog wheel, willower and shaft, to power the operating machine.

[3] V.Marchis, *Storia delle Macchine, p.23-24*

Figure 3: **Greek tower mill, with "yawing".**
Source: Hau, wind turbines fund, p.8.

In the Mediterranean area tower windmills were developed, introducing first the concept of “yawing”, with a manual repositioning of the windwheel to a certain number of fixed position, in order to be oriented on the same direction of the wind.

1.1.2 Impact of wind power from the Middle Ages till the XX century

Wind power utilization had a growing importance and influence throughout the last 800 years. Once mostly instruments for milling cereals, windmills found a wide range of applications, surprisingly adapting and developing through history, even in competition with the steam engine boom during the XIX century.

The importance of wind energy in the Middle Ages is testified by laws issued by the feudal lords, whom imposed taxes for "wind rights", as much as wood usage, water usage, or any other kind of natural resource usage.

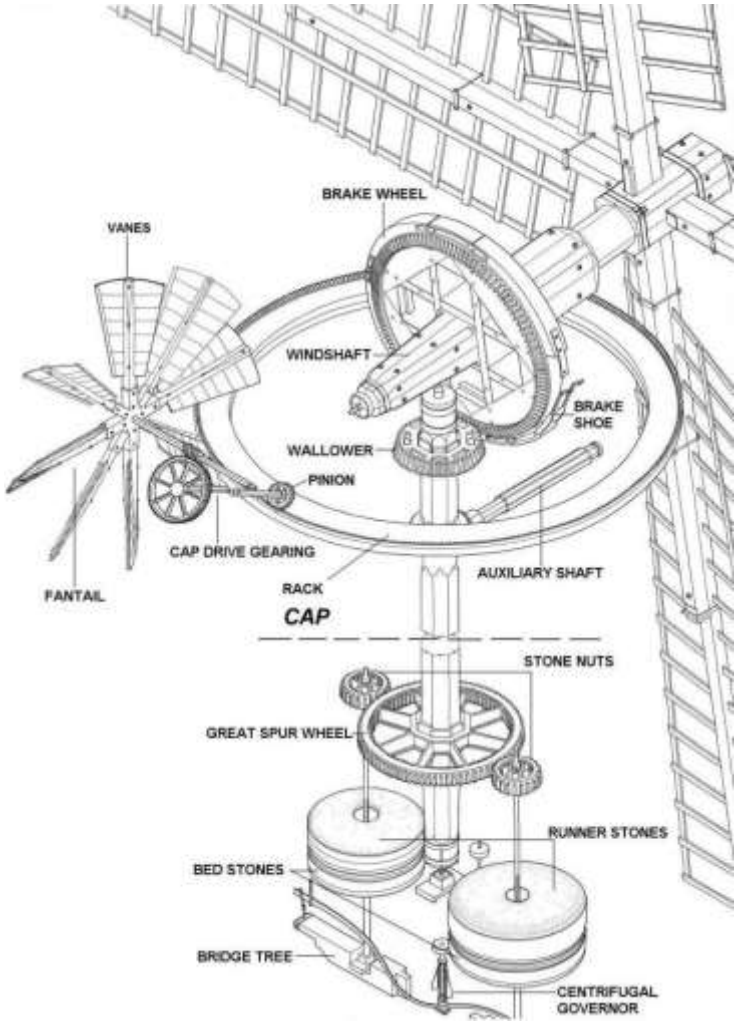

Figure 4: **18th century windmill scheme**
Source: *http://gerald-massey.org.uk/windmills/c_chapter_03.html* consulted on 02/08/2016.

In the Netherlands, after a successful application of windwheels for powering water pumps since the XV century in order to drain and recover lands from the sea, wind power starts to be

used as a source for feeding industrial processes, and it can be recognized as one of the key factor for the creation of the Netherland's great commercial and exporting tradition[4].

As a "modern" important example, in 1904, 11% of industrial energy in the Netherlands was still provided by windmills, and Germany had 18.000 units installed[5].

Figure 5: **American wind turbine, XIX century-today.**
Source: Pinterest https://s-media-cache-ak0.pinimg.com/236x/3d/bc/63/3dbc634df3baa5316c09eebf525371f8.jpg consulted on 30/06/2017.

In the U.S., during the XIX, the Halladay wind turbine was used to pump water. It was able to both yawing and blade pitching. In the XX century, a simpler American wind turbine will take its place, much cheaper but only being able of rotating on its vertical axis.

In the end, windmills will find their final decline in the first part of the XX century, with the rise of electrification[6].

On these historical basis, modern electrical wind turbines can be considered as direct heirs of the traditional wind power utilization that pushed economic development in different regions of the world through the centuries.

[4] Hau, *Wind Turbines fund., p.13*
[5] Ackermann, *Wind Power in P.S., p.25*
[6] Hau, *Wind Turbines fund., p.13*

1.1.3 Wind and Electrification

The historical contest of electrification, at the end of the XIX century, was that the urban centres of the developed countries were supplied by electrical plants, while the energy supplying of rural areas was much more complex and it would require part of the XX century, especially in the wide distances of the United States.

The connection between windmills and electrical wind turbines can be tracked back to 1891, when Poul la Cour, under the encouragement of the Danish government, connected a wind turbine to a dynamo[7]. His system provided energy to small isolated grids in rural areas together with diesel and steam-turbine generators, reaching the impressive number of 120 wind turbines installed in 1918. Yawing was possible.

Figure 6: **Poul La Cour first wind turbine prototype, 1891.**
Source: *https://isaacbrana.wordpress.com/2010/06/28/historical-background-of-the-wind-power/* consulted on 30/07/2017.

After the first flight of the Wright brothers in 1906, aerodynamics will develop at an incredible pace[8]. In the scenario of World War I, planes development pushes this science ahead, and after 1920 some extremely important theoretical contributions are written, by Betz and Glauert in Germany[9]. After 1931, prototypes were designed, and some were built in Germany and the USSR.

[7] Hau, *Wind Turbines fund., p.24*
[8] V.Marchis, *Storia delle Macchine, p.286*
[9] Hau, *Wind Turbines fund., p.29*

Figure 7: **Russian WIME D-30 (100 kW) operating 1931-1942.**
Source*: http://jagoanbelajarprimamedica.blogspot.it/2013/05/sejarah-kincir-angin.html* consulted on 02/08/2016.

It is worth to mention the "Jacobs wind charger", a DC wind powered generator, 3 bladed 4m diameter, 1.8-3 kW of power which had a huge success in the U.S., being sold in thousands of units between 1920 and 1960, and, much more than successful or failed big prototypes, contributed to feed rural areas with electrical energy[10]. Analogies with the "American wind turbine" water pump diffusion are evident.

Noticeable that one of his successful models even operated in the Antarctic for more than 2 decades with no maintenance[11].

Figure 8: **Marcellus Jacobs with a model of his turbines.**
Source: *http://www.motherearthnews.com/renewable-energy/wind-power-history-zmaz73ndzraw.aspx consulted* on 30/06/2017.

[10] Hau, *Wind Turbines fund., p.33*
[11] Hau, *Wind Turbines fund., p.33*

Once again in the U.S., another commercial attempt was made by engineer Palmer Cosslett Putnam.

Putnam, in collaboration with the Morgan Smith Company and scientists and technicians from the MIT of Boston, designed and built an impressive prototype in the state of Vermont, with a rotor diameter of 53.3 m, 1.25 MW of rated power, and a tower height of 35.6 m.

Despite a successful deployment and energy production for almost 4 years, the turbine broke down due to a rotor-blade fracture. The results of this experiment were used by Putnam to propose a bigger commercial version of his prototype, but unfortunately his price of wind energy production was 1.5x higher than the affordable price (125$/kW), thus putting an end on his ambitions[12].

Figure 9**: Smith-Putnam wind turbine.**
Source: NASA *https://www.dvidshub.net/image/861453/smith-putnam-wind-turbine-display* consulted on 02/06/2016.

More prototypes will follow in the US, in Denmark, in France, with limited success.

In Germany, Ulrich Utter proposed a quite innovative model, the W-34, which resembles in many ways contemporary wind turbines: aerodynamically refined rotor in glass fibre material, compensation for asymmetrical wind load (with teetering movement), light weighted structure. However, the project was quit after ten years due to a limited hours of energy productions, and limited funding.

[12] Hau, *Wind Turbines fund., pp.34-35*

Figure 10: **W-34 Hutter wind turbine, 1958-68.**
Source: *http://www.heiner-doerner-windenergie.de/ewindenergie.html* consulted on 02/06/2016.

In conclusion, all these prototypes failed to find a commercial application mainly because of their complexity and high costs, especially compared to energy prices, and due to little scientific rigorous development and coordination. Only simpler, cheaper models made their way through the market, in a way which resembles the diffusion of windmills through history: a well-known, robust structure, and the possibility of feeding energy (in this case electrical) in a simple, easy way to remote areas. However, with more developed electrification and cheap electrical energy available from the grid, all models were out-of-date.

1.1.4 After the energy crisis (1973)

A key year in the history of wind power is certainly 1973 when, because of the arab-israelian war, producers of the OPEC organization stopped the oil delivery to the major importing countries, including Europe and the United States. The West, shocked and surprised, found itself in the middle of a big energy crisis, as the oil price risen of multiple times: this fact somewhat mined a widespread opinion that energy was cheap, available and somewhat independent from geopolitical events. In this chaotic scenario, reducing dependence from oil exporters seemed very appropriate, and the US started a massive funding of wind power research. After the abandoning of the APOLLO projects, NASA was looking for new field of interests, and an interest in wind research came naturally. With 200m $ of government funding, many private companies take part into the project: the MOD series will be installed and tested between 1975 and 1987.

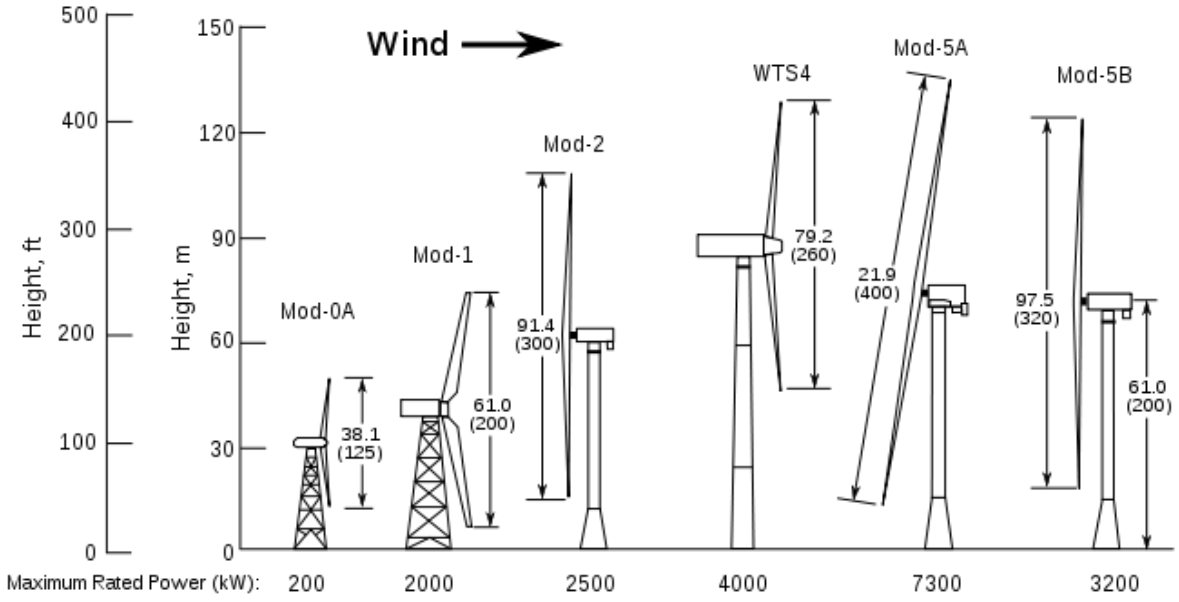

Figure 11: **NASA MOD wind turbines comparison.**
Source: Wikipedia
https://en.wikipedia.org/wiki/History_of_wind_power#/media/File:Wind_generator_comparison.svg **consulted on 04/08/2016**

At the same time, in many European countries big prototypes were also built. The most notable example is the West Germany's "*Growian"*. Growian was built thanks to a federal development project started in 1974, and with important theoretical contribution by State wind research departments and, amongst other authors, by Hutter: the design was based on the precedent experience of the W-34 turbine of the '50es. After some technical discussions about the size of the rotor, the nominal power and the height of the new prototype, with no little influence of

political reasons a 3MW solution was chosen. Unfortunately, due to many technical problems, including structural and vibrational issues difficult to model at the time's state-of-the-art scientific development, the "*Growian"* will not be a success.

Figure 12: **Installation of the Growian, 1983.**
Source*:* ***http://www1.wdr.de/stichtag/stichtag7866.html*** **consulted on 30/06/2017.**

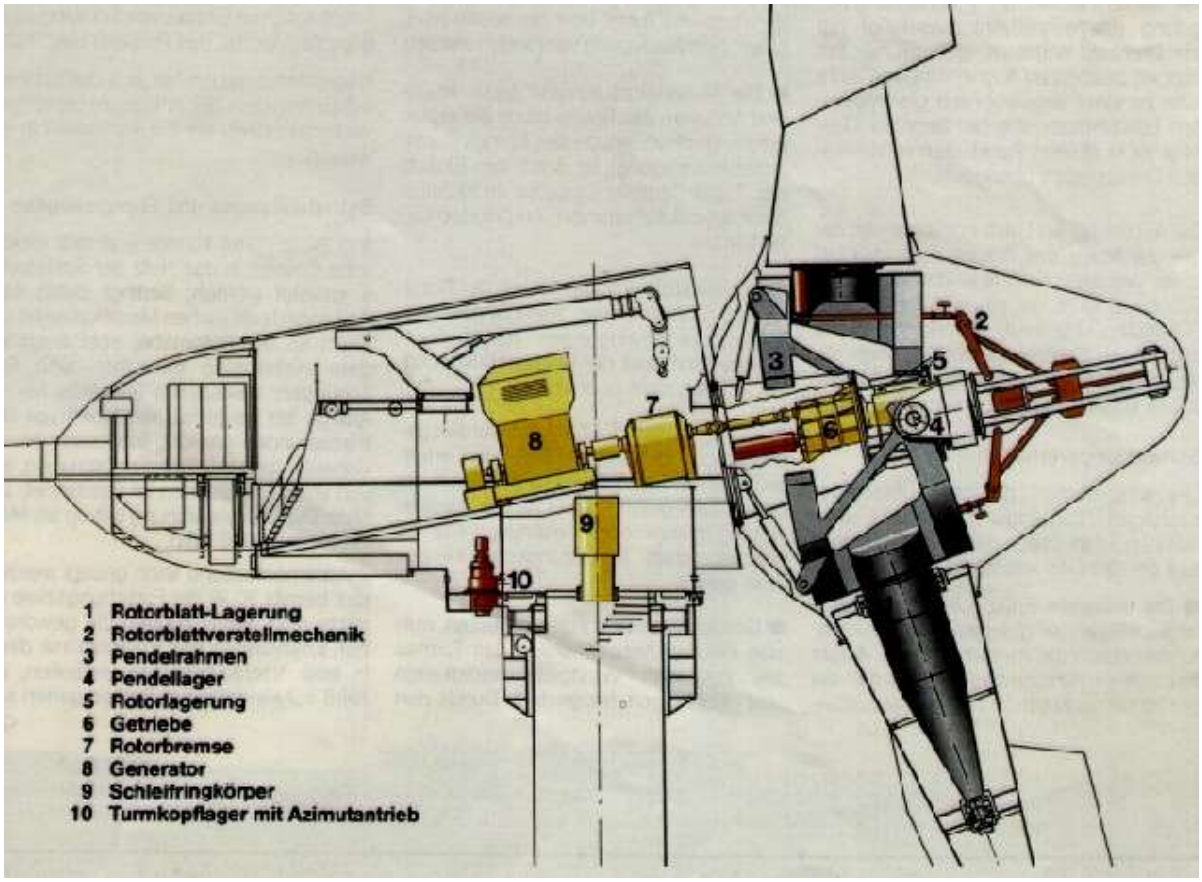

Figure 13: **GROWIAN scheme.**
Source: *http://www.heiner-doerner-windenergie.de/eGROWIAN.html* **consulted on 30/06/2017.**

Growian specifics[13]:

- Electric power, ratet: 3 MW
- Cut in speed: 5.4 m/s, cut off speed: 24.0 m/s, rated speed: 12.0 m/s
- 2 rotorblades, diameter: 100.4 m, rotor speed: 18.5 rpm at rated wind speed
- Steel shell case, steel tower height: 100 m, tower mass: 350 tons
- Rotational speed/power control with pitch control, direct acting inverter
- Asynchronous generator, doubly fed, nominal out 3443 kVA, nominal PF with inverter 0.95, 6,3 kV, 50 Hz

[13] *http://www.heiner-doerner-windenergie.de/eGROWIAN.html* consulted on 04/08/2016

1.1.5 The Danish experience

In Denmark, after the 1973 energy crisis, not only the installation of prototypes began, but also the commercial diffusion of smaller wind turbines, following the already present tradition of the country in stand-alone wind power applications. These small turbines, rated 50-60 kW and with a rotor diameter of 15-16 m[14], found success because of a well-tested and reliable technology, use in organized small communities, rural and territorial energy transmission issues, and, last but not least, a very important fiscal policy by the government (30% of purchase value of the turbine till 1985). After 1986, with much less fiscal benefits, the sector managed to stay alive thanks to cheaper technology (due to the technical experience of the precedent 10 years), already commissioned units, and, yet, geographical characteristics of rural areas.

1.1.6 The first wind farms in the U.S.A.

After the 1973 energy crisis, federal governments in the United States realized the importance of investing in new supply sources and, in the scenario of high energy prices, they decided to heavily sustain the private sector with fiscal incentives for the building and utilization of wind farms (up to 50% of the investment costs in 1985[15]).

In particular, at the end of the ’70, costs of construction for traditional power plants risen significantly, due to more strict regulations on safety and environment preservation. Nuclear plants were (and are) extremely expensive to build, traditional plants were much more costly than before, energy prices in general were high, so, for energy providers, the possibility of buying energy from private producers was sees as an opportunity. This situation, combined with public fiscal incentives, brought to the building of the first big wind farms in California.

California was a very interesting playground for wind energy production, with special natural conditions, a high temperature variation between day and night which brings a constant strong wind from afternoon till late night, contributing to cover the evening energy request peak of the country. For this time of the day, payment conditions were quite favourable. The annual mean wind reaches 9 km/h California’s windy areas.

[14] Hau, *Wind Turbines fund., p.57*
[15] Hau, *Wind Turbines fund., p.58*

At first, small U.S. manufactured turbines up to 100 kW were installed, but on the long time these machines proved to be unreliable, due to the lack of technical and development experience of American producers.

Figure 14: **Californian 40kW units wind farm in the '80s.**
Source: Wikimedia *https://commons.wikimedia.org/wiki/File:Wind_energy_converter5.jpg* consulted on 30/06/2017

In the meantime, Danish manufacturer accumulated a very important experience and, being able to produce and sell cheap and reliable turbines, they decided to hit the U.S. market.

The favourable moment lasted till the end of the ’80, when fiscal bonuses expired and the entire sector forced to survive on its own real economical possibilities: with some struggling, American wind power sector survived. During all the ’90, wind farms were built, even if with a fading trend, thanks to lower manufacturing costs, and already-existing energy agreements granted to the old farms the right to survive.

At the end of the ‘90, the curtain seemed to fell down the American wind power sector, but the New Millennium brought higher energy prices and a new environmental mentality, contributing to the continuation of the success of the American wind farms also outside California, eventually reconnecting with the success of the European wind power sector, which in the meantime found huge diffusion throughout the Old Continent.

Chapter 1.2: Wind energy conversion physical principles

1.2.1 Betz Law[16]

A fundamental physical analysis of the extraction of mechanical power from an air flow is due to Albert Betz. Despite his model is quite simplified, with lossless converter and frictionless air flow, it represents a milestone in the wind power theory, and it is still usable today for rough calculations.

The kinetic energy of a volume of air can be expressed as:

$$E = \frac{1}{2}mv^2 \ [Nm]$$

Where m is the mass of the air volume, v is its speed.

The volume flow is:

$$\dot{V} = v\,A \quad [\frac{m^3}{s}]$$

Where A is a cross-section of the air flow tube.

The mass flow is:

$$Q = \rho\, v\, A \quad [\frac{kg}{s}]$$

Where ρ is the air density.

Substituting m with Q, we obtain the (kinetic) power of the air flow:

$$P = \frac{1}{2}\rho v A v^2 \ [W]$$

The extraction of mechanical power comes at the expense of kinetic power:

$$P = \frac{1}{2}\rho(A_1 v_1^3 - A_2 v_2^3) \ [W]$$

Combined with the equation of mass continuity:

$$\rho v_1 A_1 = \rho v_2 A_2$$

[16] Hau, *Wind Turbines fund., pp.79-83*

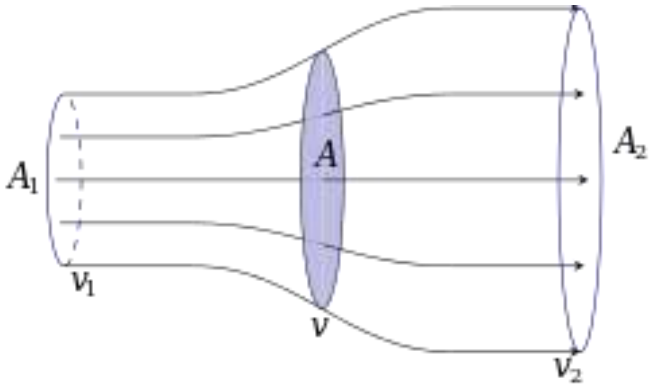

Figure 15: **Betz tube.**
Source:Wikipedia
https://en.wikipedia.org/wiki/Betz%27s_law#/media/File:Betz-tube.svg **consulted on 14/0872016**

With a substitution, for the mechanical power we obtain:

$$P = \frac{1}{2}Q(v_1^2 - v_2^2) = \frac{1}{2}\rho v_1 A_1(v_1^2 - v_2^2)$$

Apparently the maximum power is obtained for $v_2 = 0$. This does not make physical sense, as it would not admit any air flowing through the converter.

We look for the ideal $\frac{v_2}{v_1}$ coefficient.

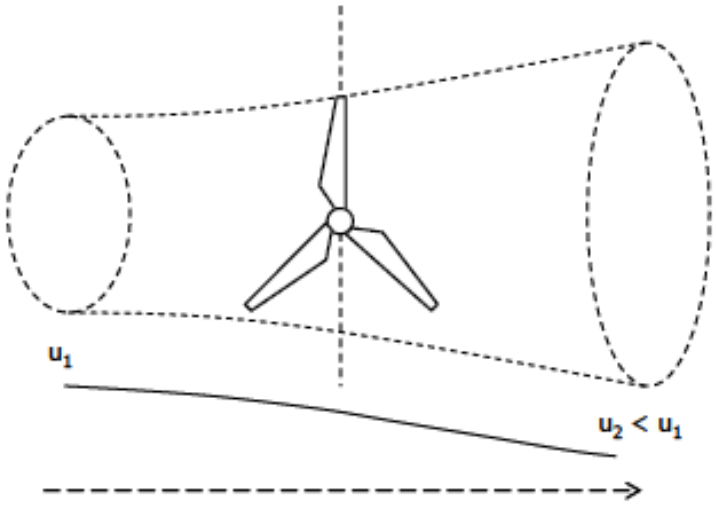

Figure 16: **Betz tube, speed and section variations.**
Source: Spertino, material from Generazione fotovoltaica ed eolica di energia elettrica course.

Applying the momentum conservation law:

$$F = Q(v_1 - v_2)$$

This force is applied on the converter which, for the equilibrium of forces, opposes an equal and opposite force. v' is the wind speed at the converter section: for flowing through the converter, the air applies the power:

$$P = Q(v_1 - v_2)v'$$

Equating this power and the mechanical power expression:

$$\frac{1}{2}Q(v_1^2 - v_2^2) = Q(v_1 - v_2)v'$$

Then:

$$v' = \frac{1}{2}(v_1 + v_2)$$

With a substitution in the mass flow, where A_{conv} is the air flow section on the converter:

$$Q = \rho A_{conv} v' = \frac{1}{2}\rho A_{conv}(v_1 + v_2)$$

Rewriting the mechanical power equation explicating the mass flow:

$$P = \frac{1}{2}Q(v_1^2 - v_2^2) = \frac{1}{4}\,\rho A_{conv}(v_1 + v_2)(v_1^2 - v_2^2)$$

The total kinetic power of the incoming air flow is:

$$P_0 = \frac{1}{2}\rho A_{conv} v_1^3$$

We can obtain an ideal power coefficient c_p, which expresses the unitary amount of power (or energy) theoretically extractable from an air flow according to Betz's model.

$$c_p = \frac{P}{P_0} = \frac{\frac{1}{4}\,\rho A_{conv}(v_1 + v_2)(v_1^2 - v_2^2)}{\frac{1}{2}\rho A_{conv} v_1^3}$$

Explicating c_p from $\frac{v_1}{v_2}$:

$$c_p = \frac{P}{P_0} = \frac{1}{2}\left[1 - \left(\frac{v_2}{v_1}\right)^2\right][1 + \frac{v_2}{v_1}]$$

Plotting in Matlab this function, we obtain

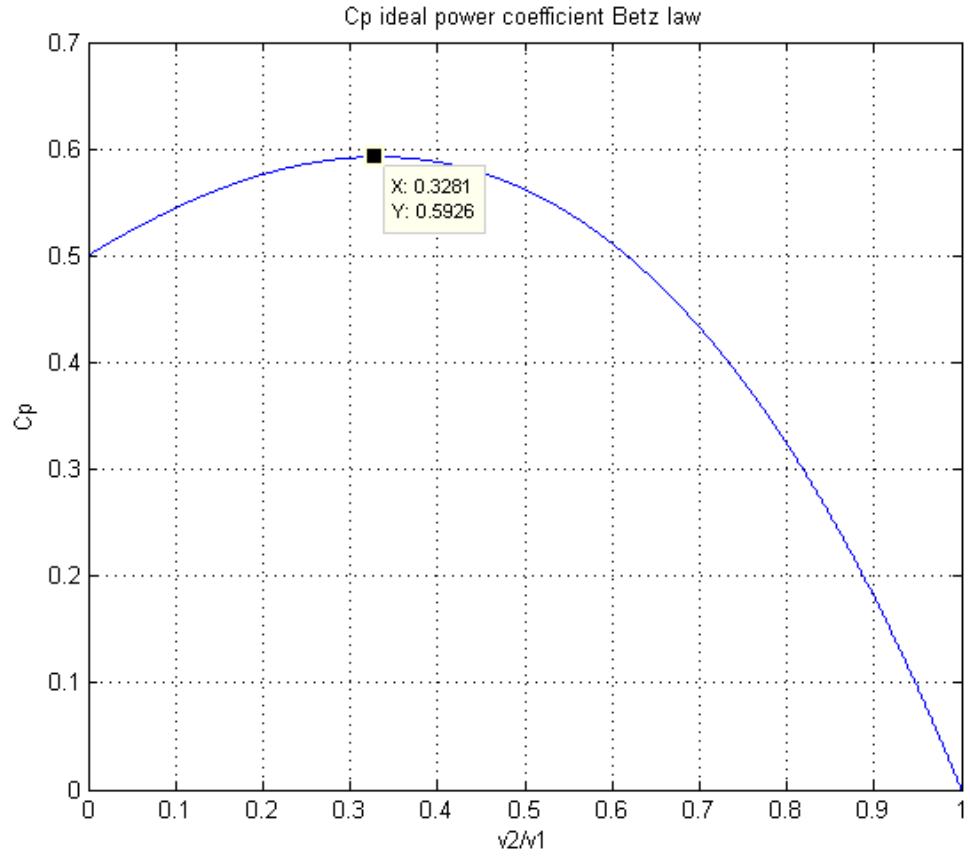

Figure 17: **Betz law Cp coefficient plotted using MATLAB**

- Cp max= 0.5926, with $\frac{v_2}{v_1} = 0.321 \sim 1/3$
- $v' = \frac{2}{3} v_1$

These are the ideal conditions for the production of mechanical power from the wind. In particular, Cp max value clearly expresses the concept that 1/3 of wind energy can't be extracted, not even in simplified theoretical models.

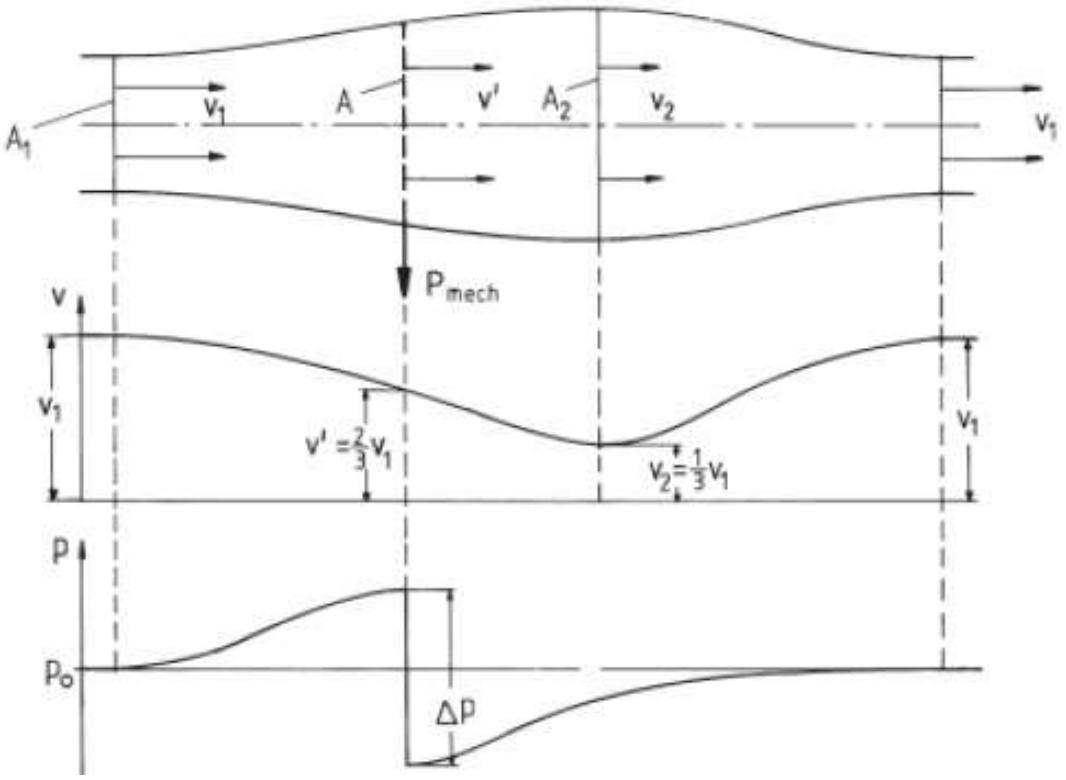

Figure 18: **Betz tube section, speed, pressure variations.**
Source: Hau, Wind Turbines fund., p.83.

1.2.2 Blade theory

To obtain a better reference for the description of Cp, we introduce the tip speed ratio λ:

$$\lambda = \frac{V}{U} = \frac{\omega R}{U}$$

Where V is the tip speed of a blade, U is the wind speed, ω is the angular speed of the rotor and R is the radius (length) of a blade.

Plotting Cp with λ as variable, we obtain:

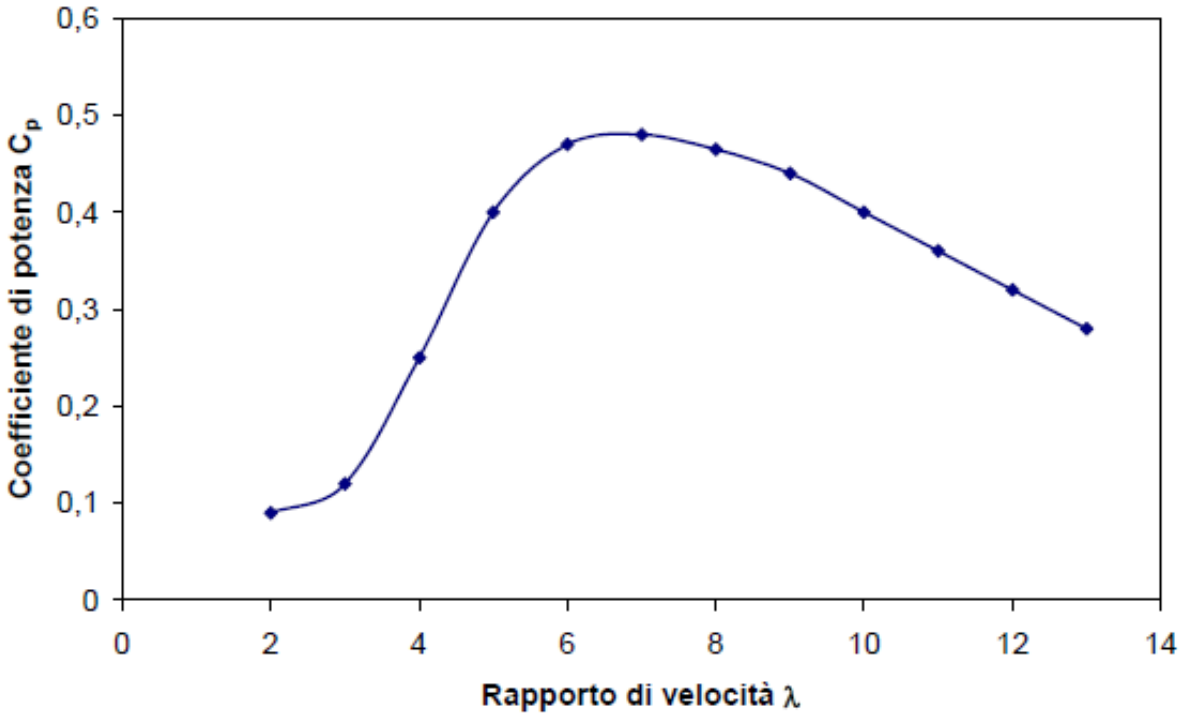

Figure 19: **Cp power coefficient in terms of λ.**
Source: Spertino, notes from gen. elt. Energy PV and Wind Power class.

The reasons of this trend will be described through cinematic and dynamic blade triangles. According to this function, it's easy to understand that, regulating λ, the blade can work at maximum Cp and, regulating V tip speed according to U wind speed, λ can be kept constant allowing a maximum Cp regulation for a variable speed turbine.

For Betz theory, we can write[17]:

$$c_p = \frac{P}{P_0} = \frac{P_{mech}}{\frac{1}{2}\rho A U^3}$$

Where P_{mech} is the ideal mechanical power obtainable. Combined with λ and plotted:

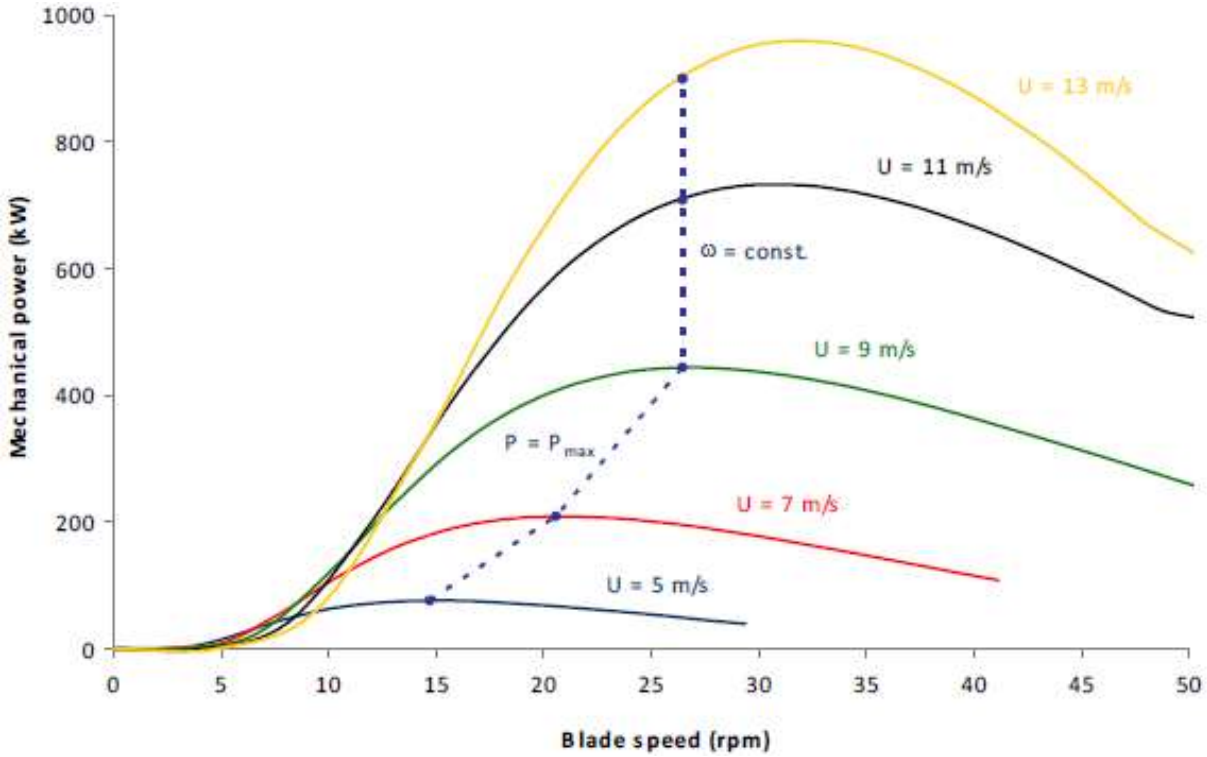

Figure 20: **Mechanical power of the rotor in terms of blade speed and wind speed. Source: Spertino, material from Generazione fotovoltaica ed eolica di energia elettrica course.**

P_{max} is analytically described as:

$$P_{max} = C_{Pmax}\frac{1}{2}\rho\pi R^5 \frac{1}{\lambda_{max}^3}\omega^3$$

With a square dependence from ω. After a certain blade speed value, the regulation is ω constant for not violating the technical limits of the wind turbine.

[17] Spertino, notes from gen. elt. Energy PV and Wind Power class

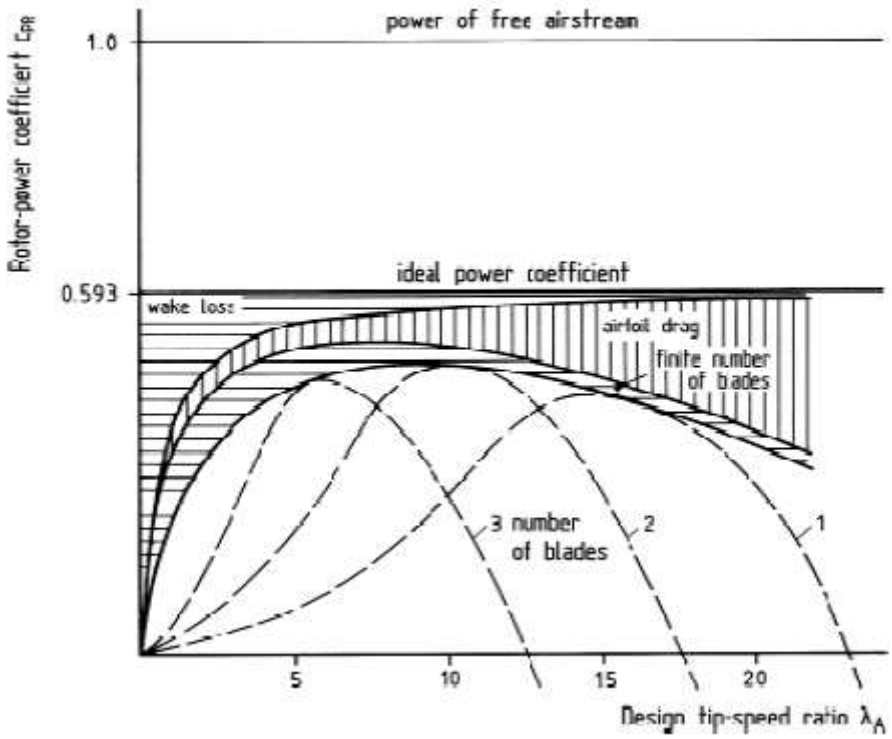

Figure 21: **Cp in terms of tip speed and of n° of blades, compared to the ideal Cp. Source: Hau, Wind Turbines fund., p. 95.**

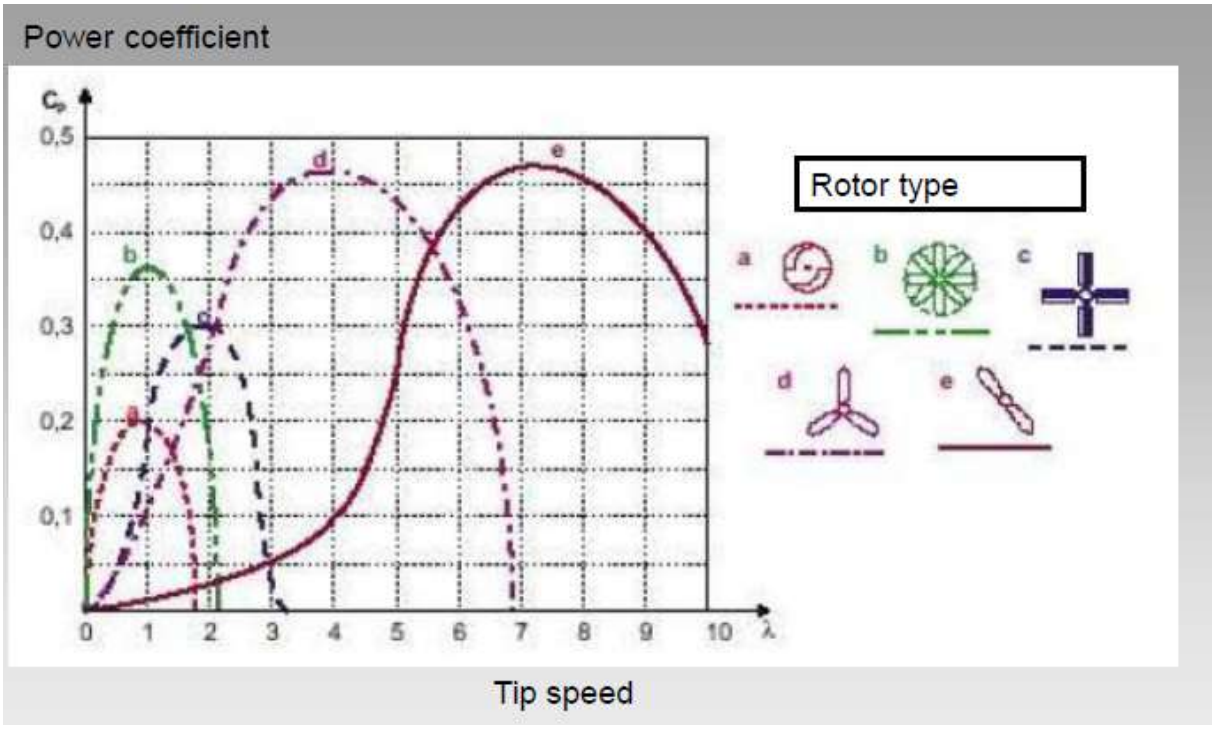

Figure 22: **Cp in terms of tip speed and rotor typology. Source: Rosłaniec: Energy conversions (university course), Warsaw university of technology, Warsaw 2016.**

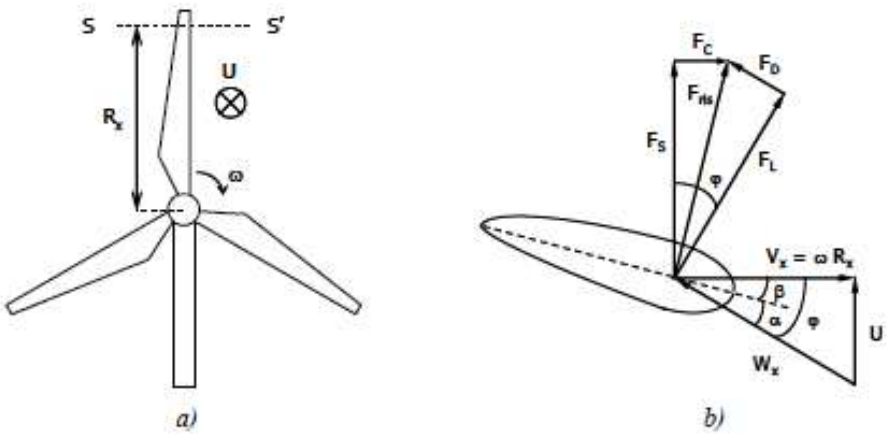

Figure 23: **Cinematic and dinamic triangles on a blade section.**
Source: Spertino, Spertino, material from Generazione fotovoltaica ed eolica di energia elettrica course.

Taking into consideration the universally used wind turbine with horizontal axis, we focus on a blade section SS', in order to describe the blade theory. This section is similar to an airplane wing section.

The cinematic triangle is composed of:

- U is the wind speed, referred to a global coordinate system. V_x is the speed of the section. $W_x = U - V_x$ is the relative wind speed, integral to the local blade-rotating coordinate system.
- α is the angle of attack, between the chord and W_x. β is the blade pitch angle, between V_x and the chord. $\alpha + \beta = \varphi$. $ctg(\varphi) = \frac{V_x}{U} = \lambda$

Thanks to the action of the wind speed on the blades, different forces act on the system:

- F_L is called lift. F_D is called drag. $F_L + F_D = F_{ris}$
- F_{ris} can be decomposed into F_C tangential force and F_S axial force, thrust.
- $F_C = F_L sen\varphi - F_D cos\varphi$ is responsible for the mechanical shaft torque. The drag contribution is negative.
- $F_S = F_L cos\varphi + F_D sen\varphi$ the thrust is caused both by the drag and the lift, but the lift contribution is higher. The thrust can be seen as a force which tries to "deflect" the tower
- $F_L \propto C_L(\alpha) W_x^2$. C_L is the lift coefficient, and it is proportionally increasing with α up to 15°, then it decreases again due to the incoming *stall* phenomena.

- $F_D \propto C_D(\alpha)W_x^2$. C_D is the drag coefficient, and it is always proportionally increasing with α.

The *stall* is caused by the creation of air vortex on the backward side of the blade, at a certain α for a definite or higher wind speed U.

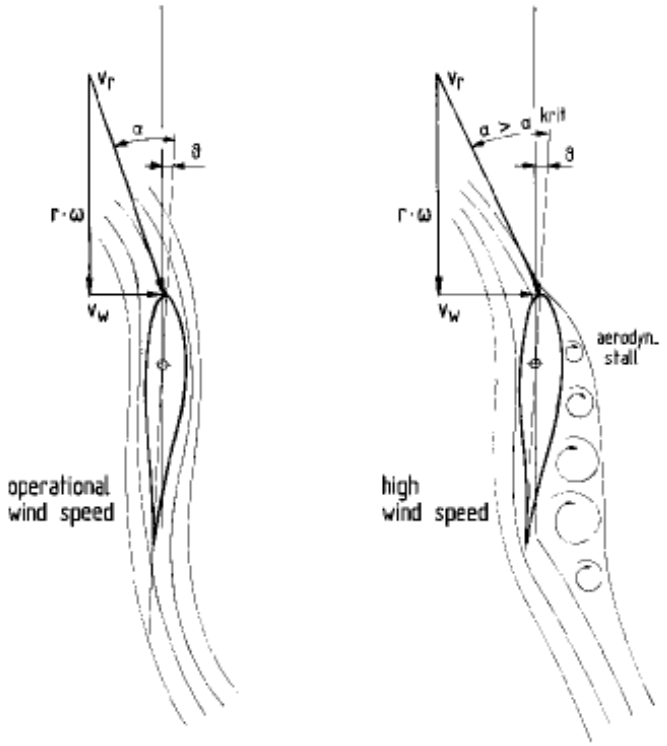

Figure 24: **Aerodynamic stall for a fixed pitch blade, due to the increased wind speed. Passive stall regulation.**
Source: Hau, Wind Turbines fund., p.112.

1.2.3 Power and torque management through blade regulations

The torque responsible for the rotation of the rotor can be regulated in *active* or in *passive* way.

- *Active* regulation, towards the stall or towards the feathered position. The pitch angle variates through mechanical actuators to reach one of these 2 states.
- *Passive* regulation, towards the stall. The pitch angle of the blade is fixed, the stall is achieved naturally in case of increased wind speed.

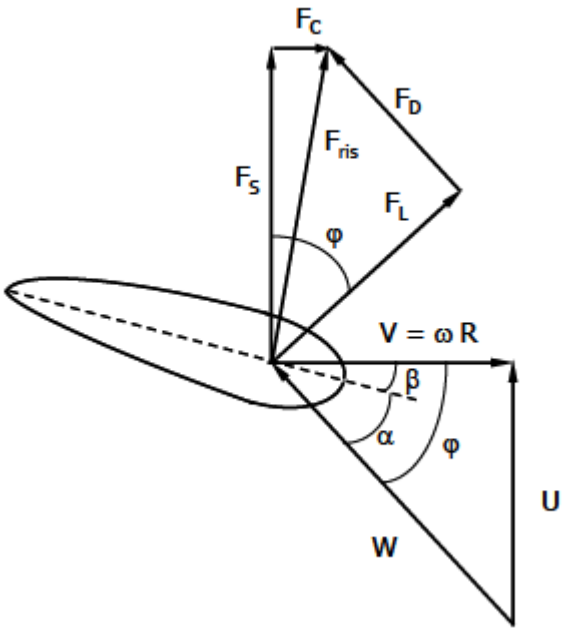

Figure 24: **Passive stall regulation.**
Source: Spertino, notes from gen. elt. Energy PV and Wind Power class.

In the case of passive stall regulation, U module is increased, causing an higher f and an higher α. C_L is reduced, while C_D is increased: going towards the stall condition, F_L/F_D is diminished. F_D module is higher than in the non stall condition, compared to F_L module. The composition of forces will result in a smallerF_C, thus reducing the mechanical torque. As the regulation is passive, the blade is in a fixed position, and the angle β is constant.

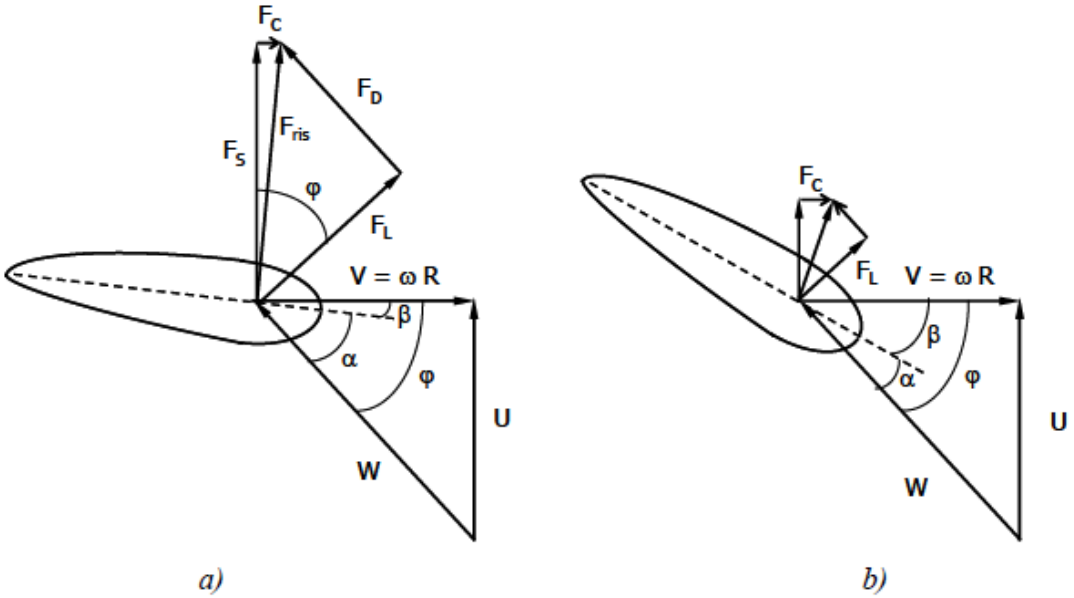

Figure 25: **a) active stall regulation; b) active regulation to the feathered position. Source: Spertino, notes from gen. elt. Energy PV and Wind Power class.**

In the case of *active stall regulation*, the stall condition is obtained thanks to the pitch control: the blade is rotating around itself, reducing the pitch angle β. As the cinematic triangle is constant (φ is constant), this will result in an increased value of α, which brings to the stall condition for the same reasons of the passive stall regulation. F_C is reduced, and thus the mechanical torque.

In the case of *active regulation to the feathered position,* the blade turns on itself on the opposite direction, in order to reduce α: both C_L and C_D are significantly reduced. F_L and F_D are reduced too, and also their sum F_{ris}. F_{ris} components are the smallest possible in the final feathered position state, for a chosen wind speed: F_C is low, thus reducing the mechanical torque applied; F_S, the thrust, is lower too, avoiding to create stresses on the tower structure.

Power regulation is mainly done through the previously described methods. It is indeed present a regulation through the variable speed of the rotor, if the system and the electrical generator allows it, but yet the main mean of regulating power is through the torque applied by the wind on the blades.

A continuously active pitch control towards feather position allows a fine regulation of power, once that the *rated wind speed* is reached. On the contrary, active stall regulation results in

arougher control of power, nevertheless being a faster method as the angle variation for reaching the *critical aerodynamic angle of attack* (when stall happens) is smaller.

The feather position is very useful in case of high wind speed, as the thrust to be counter-balanced by the tower is much lower, for a determined wind speed, compared to the normal operating pitch position: this fact allows the proper design and construction of light-weight turbine structures.

The feather position is very useful in case of high wind speed, as the thrust to be counter-balanced by the tower is much lower, for a determined wind speed, compared to the normal operating pitch position: this fact allows the proper design and construction of light-weight turbine structures.

In case of *passive stall regulation*, the blades are not able to rotate on their longitudinal axis, and the pitch angle can't be change. *Stalling* occurs naturally at a certain wind speed: the turbine is carefully designed to reach the *critical aerodynamic angle of attack* for a certain wind speed U. The power decreases for higher wind speeds. However, the structure has to be carefully designed also to withstand stress situations due to very high wind speeds: for big values of α, after *stalling* happened, the mechanical power transmitted to the rotor starts to rise again. Even with a non-rotating rotor, the thrust (coincident with U, if $\omega = 0$) is very high, and it has to be adequately opposed by all the structure and by the tower: lightweight structures are no longer admitted.

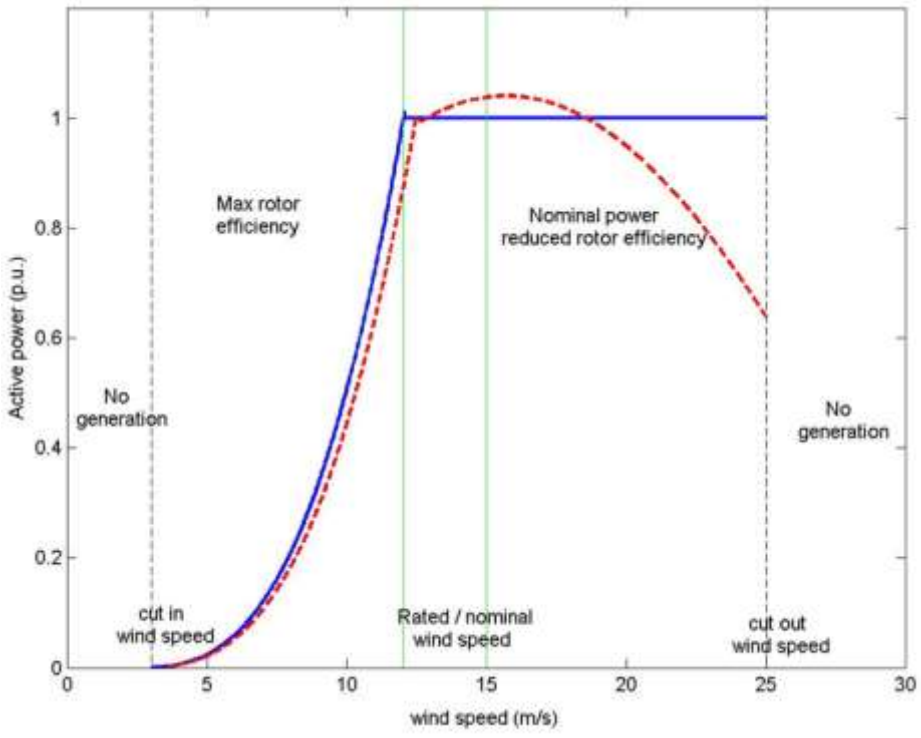

Figure 26: **BLUE: active pitch feather regulation RED: active stall regulation. Source: *http://www.intechopen.com/books/wind-farm-impact-in-power-system-and-alternatives-to-improve-the-integration/modeling-and-simulation-of-a-12-mw-active-stall-constant-speed-wind-f* consulted on 16/09/2016, Authors: Mihet-Popa, Groza.**

Chapter 1.3 The wind

The wind's primary cause is the solar energy, the solar irradiation: sunrays heats the Earth's surface, causing warm masses of air to rise high from the ground, thus generating air currents as they move to cooler regions. The Earth is not homogenous in its surface: oceans, plains, hills, mountains influence the presence of wind, creating morphological areas which allows air currents to accelerate, creating sheltered valleys. Seas and oceans, in particular, represents huge thermal capacities, being warmer or colder than lands in different moments of the day, or in different seasons: this thermal gradient is the cause of the strong wind activities typical of the coastal areas[18].

Different heights are interested by different wind speeds also because they can be immersed in higher wind *layers*, so mountainous areas are usually windier.

In the end, Earth's rotational movement causes Coriolis forces with greatly influences wind speed layers and air currents presents above our planet's surface.

The final model depicted is of great complexity and difficult to describe, let alone to be forecasted.

There is evidence that mean wind speed does not variate significantly on a long-term period, such as 30 years, even if the possibility that current human-induced climate changes could influence wind activities has to be taken into consideration[19].

[18] Handbook wind energy, Wiley p.9
[19] Handbook wind energy, Wiley p.12

1.3.1 Wind variations

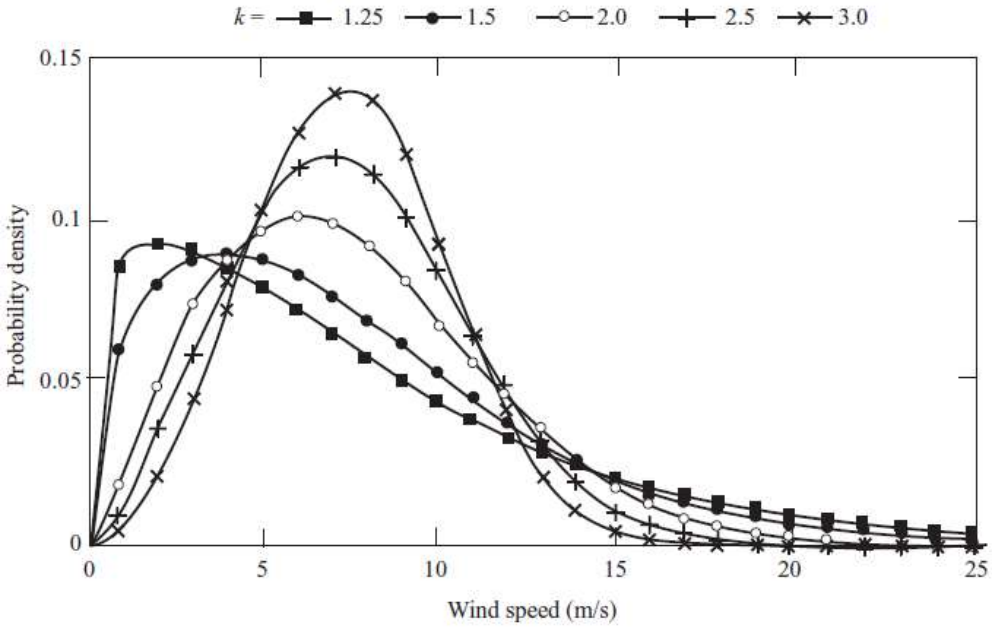

Figure 27: **Weibull wind distributions.**
Source: Handbook wind energy, Wiley p.13.

The wind resource variations are well approximated and modelled by the Weibull probability density function:

$$f(U) = k\frac{U^{k-1}}{c^k}\exp\left(-\left(\frac{U}{c}\right)^k\right)$$ [20]

Where k is a shape parameter (variability above the mean), c is a scale parameter, U is the wind speed.

The mean wind speed, usually considered for a yearly period, is:

$$\bar{U} = \int_0^\infty U\, f(U) dU$$ [21]

c and k are described with the relation:

$$\bar{U} = c\Gamma(1 + \frac{1}{k})$$ [22]

[20] Handbook wind energy, Wiley p.12
[21] Handbook wind energy, Wiley p.12
[22] Handbook wind energy, Wiley p.12

Low k values indicates high wind speed variations through the year. A Weibull function with k=2 is called Rayleigh function, and it is the common choice for the description of many geographical sites.[23]

Due to the seasonal nature of the wind, sometimes a "bi-Weibull" distribution function is used to describe regions characterized by wind behaviours strongly dependent from the period of the year:

$$\phi(U)_{bi-W} = 1 - [F_1 \exp\left(-\left(\frac{U}{c_1}\right)^{k_1}\right) + (1 - F_1)F_1 \exp\left(-\left(\frac{U}{c_2}\right)^{k_2}\right)$$

The cumulative wind speed frequency distribution φ represents, for a certain value of wind speed, the percentage of time, in a year, in which the wind speed is lower than the selected value.

$$\phi = 1 - \exp[-\left(\frac{U}{c}\right)^{k}]$$

In which the parameters are the same of $f(U)$.

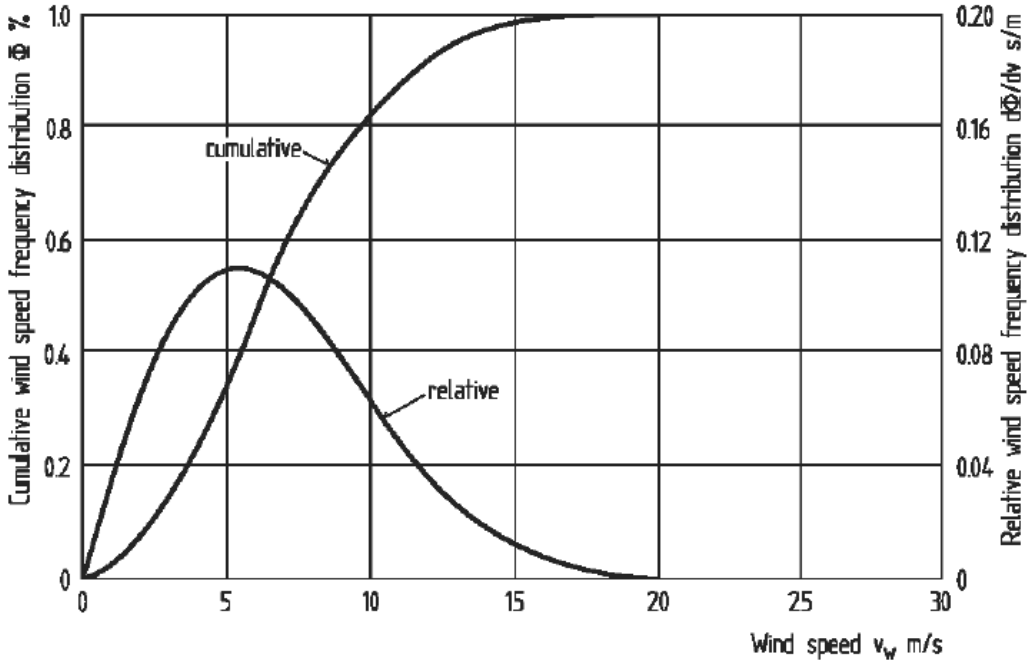

Figura 28: **Wind speed frequency distribution for the island of Sylt (Germany), k=2.0, measured at an elevation of 10 m.**
***source: Hau,* Wind Turbines fund., p.119.**

[23] Handbook wind energy, Wiley pp.12-13

1.3.2 Wind speed and altitude

At any location, wind speed is greatly dependent from the height from the ground: the friction of the air against the earth slows down the gas mass. Ideally, the speed is 0 at ground level and it rises to the final value at the "*atmospheric boundary layer*.

The first area, right above the ground and up to 20-150 m is called *Prandtl layer,* characterized by ground friction and heat-induced currents.

Above it, we locate the *Ekman Layer,* largely frictionless, and of noticeable influence for turbines higher than 100m. The logarithmic simplified laws does not take into account this layer, characterized by a higher wind speed if compared to the one modelled by the simple logarithmic model. Besides, also Coriolis forces due to the planet's rotation starts to have influence on the wind.

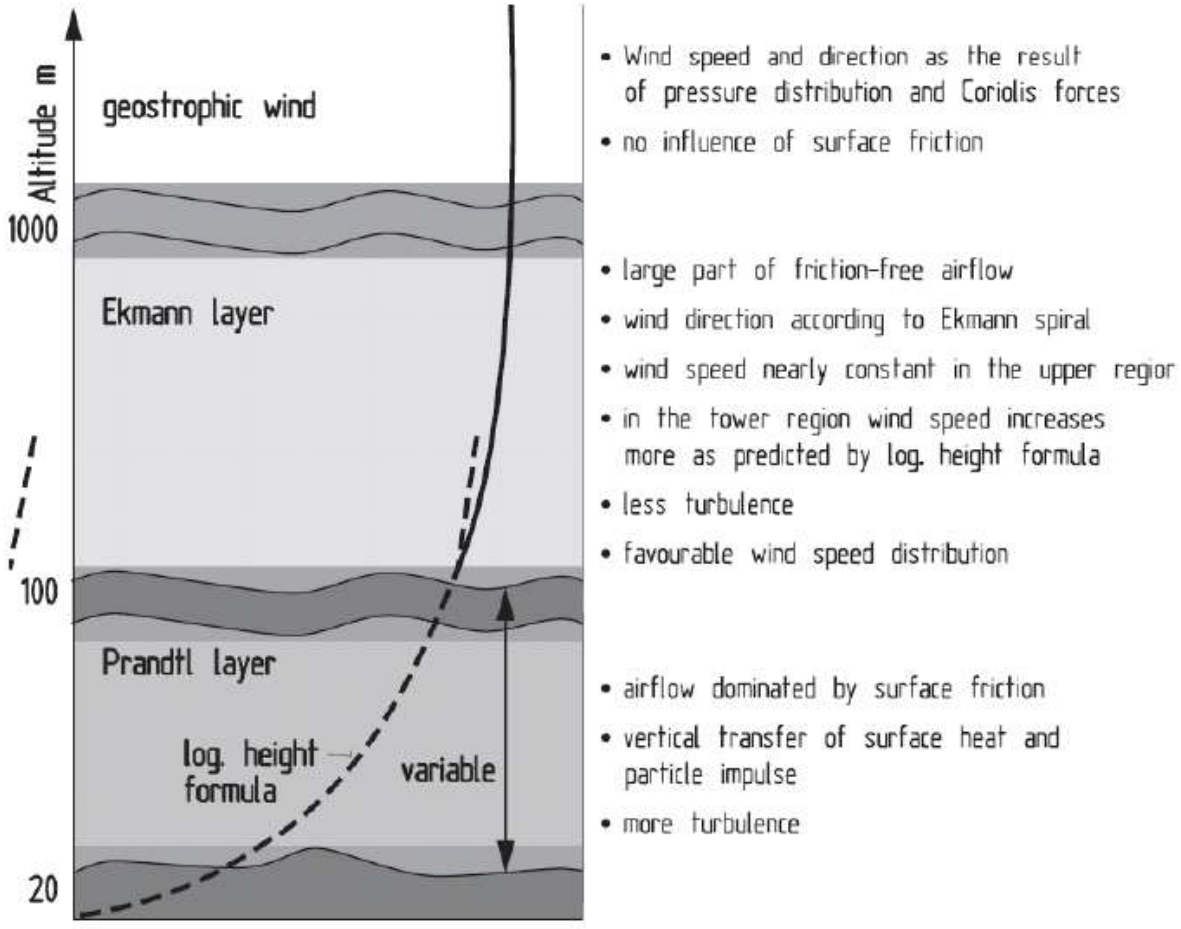

Figure 29: **Wind layers in terms of altitude from the ground.**
Source: Hau, Wind Turbines fund., p.521.

1.3.3 Wind speed related to height and terrain roughness

Ground "roughness" is defined by the *roughness length* z_0 $[m]$: the rougher the terrain, the higher z_0.

Type of Terrain	Roughness length z_o (m)
Cities, forests	0.7
Suburbs, wooded countryside	0.3
Villages, countryside with trees and hedges	0.1
Open farmland, few trees and buildings	0.03
Flat grassy plains	0.01
Flat desert, rough sea	0.001

Figure 30: **z0 roughness lenght for different types of grounds. Source: Hau, Wind Turbines fund., p.17.**

A valid engineering estimation of wind speed in the *Prandtl layer* can be obtained through the *Logarithmic Height Formula*[24]*:*

$$\overline{U_H} = \overline{U_{ref}} * \frac{\ln\frac{H}{z_0}}{\ln\frac{H_{ref}}{z_0}} \ [^m/_s]$$

Where $\overline{U_H}$ $[\frac{m}{s}]$ is the average wind speed at elevation H [m] , $\overline{U_{ref}}$ $[\frac{m}{s}]$ is the average wind speed at reference elevation H_{ref} $[m]$, and z_0 $[m]$ is the roughness length.

Ekman layer is not properly modeled through this formula, typically resulting in higher wind speed than those obtained for a determined H. Therefore, this method is not suggested for calculations about turbines higher than 80 m.

[24] Hau, *Wind Turbines fund., p.523*

1.3.4 Daily and seasonal variations of wind speed

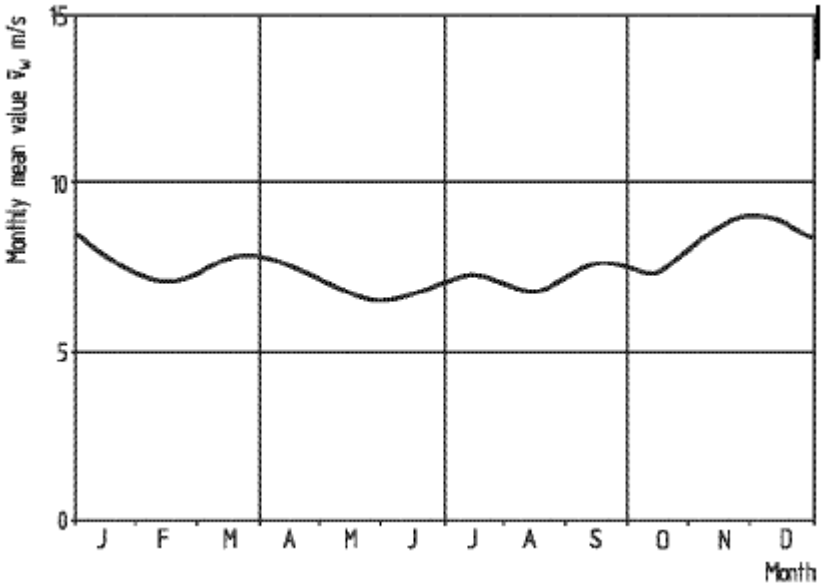

Figure 31: **Wind speed average value in terms of months.**
Source: Hau, Wind Turbines fund., p.525

Wind speed is subjected to important variations during the 24-hours, as wind is primary caused by solar irradiation: at night, wind tends to slow down. In this process, the presence and vicinity of sea and land has great influence, because of thermal effects.

In particular areas, such as California, the superposition of hours of higher power demand and hours of higher wind speed determined and determines the success of wind farms in the region.

Low-pressure mass fluctuations through the atmosphere has influence in wind speed, determining higher mean speeds in the winter season.

1.3.5 Turbulences

Wind turbulences are caused by earth friction against the air masses, and by temperature gradients which are prone to cause ascendant air flows, eventually generating the turbulence. The phenomena is, possibly enhanced by topographical peculiarities, such as hills, canyons, etc. *Turbulence is the instantaneous, random deviation of the wind speed*[25].

Known the mean wind speed (usually calculated on 10-min or 1-hour interval), the instantaneous wind speed can be written as:

$$u(t) = \overline{U} + u_\tau(t) \quad [m] \quad ^{26}$$

Where $\overline{U}$ is the mean wind speed, and $u_\tau(t)$ is the fluctuating contribute.

The *turbulence intensity* describes the overall turbulence level, in a synthetic parameter:

$$I = \frac{\sigma}{\overline{U}}$$

where σ is the standard deviation in the turbulent wind speed variation Gaussian distribution.

[25] Hau, *Wind Turbines fund., p.529*
[26] Hau, *Wind Turbines fund., p.529*

1.3.6 Topography and obstacles

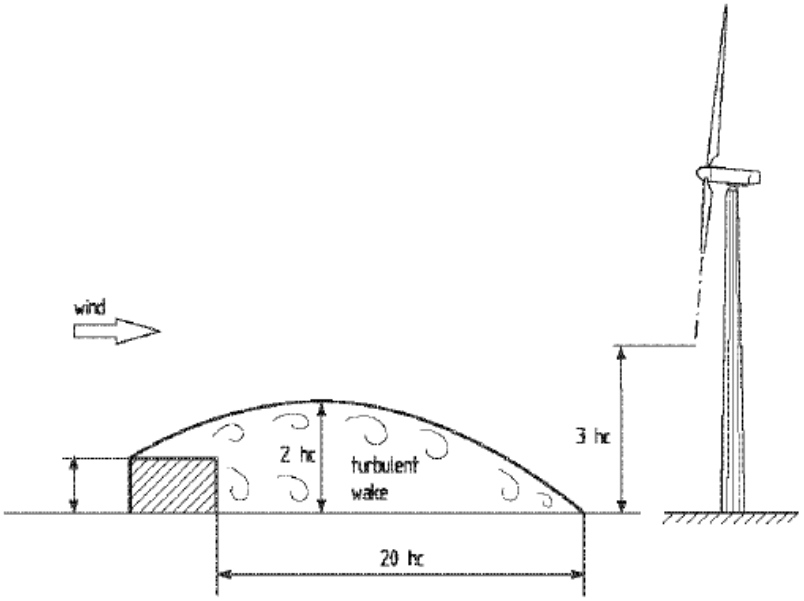

Figure 32: **Wind turbulence caused by an obstacle.**
Source: Hau, Wind Turbines fund., p.533.

Local topography has significant influence on wind speed and on the presence of turbulences: in particular, in the *logarithmic height formula* already enounced, the *terrain roughness* z_0 is the most relevant parameter. z_0 can be obtained from standard charts, but in presence of complex terrain, with the possible presence of land, water and forests, its determination is harder: the computational methods of the *European wind atlas* can be effectively used for its estimation.

The presence of differences in elevation can be negative, but also positive in terms of wind speed if the turbine is positioned on mountain ridges or on hilltops, especially if characterized by relevant slopes.

Obstacles, such as trees, buildings etc., have strong local influence on turbulences, enough to undermine the investment plan of the wind turbine. On a simple model of the phenomena[27], if the obstacle height is h_c:

- Downwind, the turbulent *separation bubble* is approximately $2h_c$ high, and it extends up to $20h_c$.
- The turbine rotor should be placed sufficiently downwind than $20h_c$, and at a height of at least $3h_c$

[27] Hau, *Wind Turbines fund., p.533*

1.3.7 Wind measurements

Regarding the acquisition of wind data, there are 2 main possibilities:

- Use of theoretical models and wind atlas, such as the *European Wind Atlas*
- Direct measurements on-site

In many cases, these 2 methods are used and combined together, in order to obtain the best scenario-description.

The use of long-term meteorological data is an almost-obliged choice, as parameters such as the mean wind speed should be considered on a very long term basis, for example 30 years, thus being able to compare and elaborate different year's data.

Local on-site measurement are extremely useful because data provided by wind data are assessed for a large area, and they should be compared and completed with more detailed measures which can take into account local topography and roughness of the terrain. At least one-year measurements should be carried on, to provide a valid comparison to wind atlas data, and possible significant deviations of the most important parameters. Also, identifying the prevalent wind direction is important, especially for the design of wind farms. A *wind rose*, obtained with atlas, tools, or measured data, describes the mean wind speed in terms of direction.

Direct measurements are taken thanks to *anemometers*, coupled with a data recording and elaboration system. The instrument's rotor position is on a mast or a tower, at a height of 10 m. Wind speed measurements regarding higher heights are computed from that data, using the logarithmic law or more complex models. These measurements are valid as a term of comparison with the wind atlas data.

In the need of providing sufficiently reliable data in the absence of atlas data or, because of topography, lower height measurements can't offer a sufficient uncertainty-free description, a direct measurement at the rotor height is possible. However, the construction of a very tall anemometer support can represent a legal issue, depending on the country.

In the specific case of the design of high turbines and rotors, it is technically difficult to carry on direct measurements at a height of 80m or above. In this situation, radar based techniques are available for obtaining wind speed measurements.

Figure 33: **Wind-flagged tree indicating the main direction of the wind, on the island of Sardinia, Italy.**
Source: Renato Brotzu, sardegna digital library.

A valid, even if rough method, for checking the historical prevalent direction of the wind in windy regions, is observing the growing direction of trees.

Figure 34: **A wind vane and rotating cup anemometer.**
Source: *http://learningweather.psu.edu/node/10* consulted on 30/06/2017.

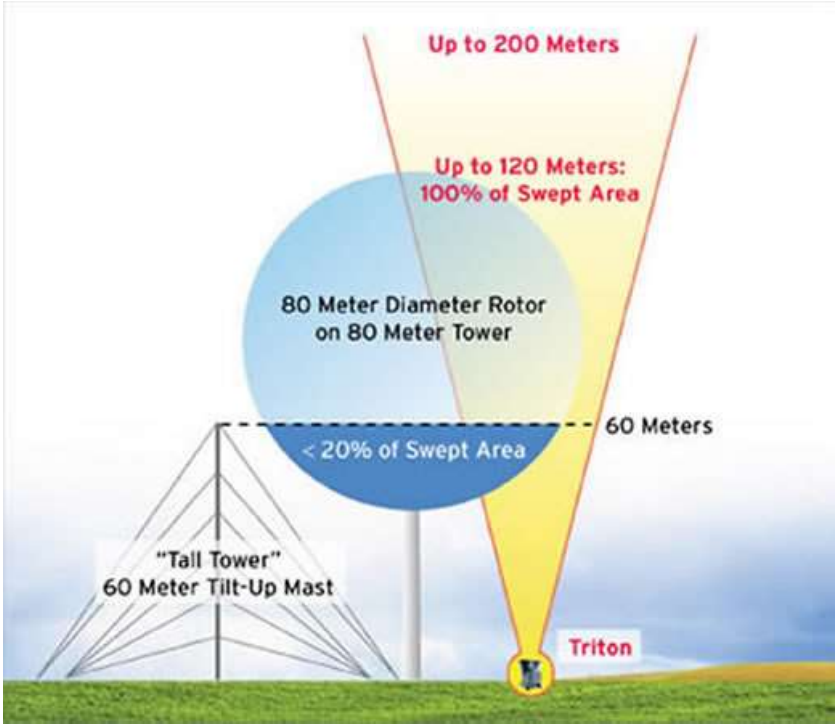

Figure 35: **Example of a SODAR wind-measuring system.**
Source: University of Massachusetts
https://www.umass.edu/windenergy/research/topics/tools/hardware/sodar **consulted on 20/08/2016.**

SODAR (sonic and detecting) radar measuring system can cover and measure wind speed at height impossible to reach with a mast tower.

Chapter 1.4 Energy yield and turbine size

In the case of wind turbines, the energy yield is not only related to the rated power of the generator, but the power curve has to be taken into consideration.

The most important component for determining the energy yield is obviously the main energy converter, from kinetic energy to mechanical energy, the turbine rotor. For a certain rotor, considering the wind distribution of the installation site, an optimal rotational speed has to be identified, or a limited range of rotational speeds in case of variable speed turbines. At this stage, a proper size of the generator is chosen, and all the main features about the design and the aerodynamics of the rotor, and all the control and operation system is determined. The efficiency of the whole energy conversion process is estimated.

After the rotor diameter and the tower height has been chosen, basing on the wind speed distribution, the rated power of the generator is chosen: it represents the maximum power generable by the turbine. This choice is strongly influence by economical evaluations (its cost rises with the size) and, in general, by all the manufacturing costs of the whole turbine.

1.4.1 Finding the best rotor speed

Once that the rotor and the generator rated power has been chosen, the proper rotational speed of the rotor should be specified. As it has been described in the precedent chapters, a rotor is characterized by a power coefficientC_{pr}, usually in terms of *tip speed ratio* λ.

It is useful to examine a chosen rotor's C_{pr} in terms of wind speed, for different rotational speeds. These curves are plotted together with *frequency distribution of wind speed* and *energy density of wind speeds*. It is worth to notice that the maximum of the *energy density* is located for higher wind speeds than the *frequency distribution* maximum.

The maximum energy density wind speed is located. That wind speed is characterized by the maximum C_{pr} coefficient.

In case of variable-speed operation, the maximum energy density wind speeds range is located, and, according to this range, the correspondent best C_{pr} rotor speeds curves are chosen, thus obtaining the rotor speed range

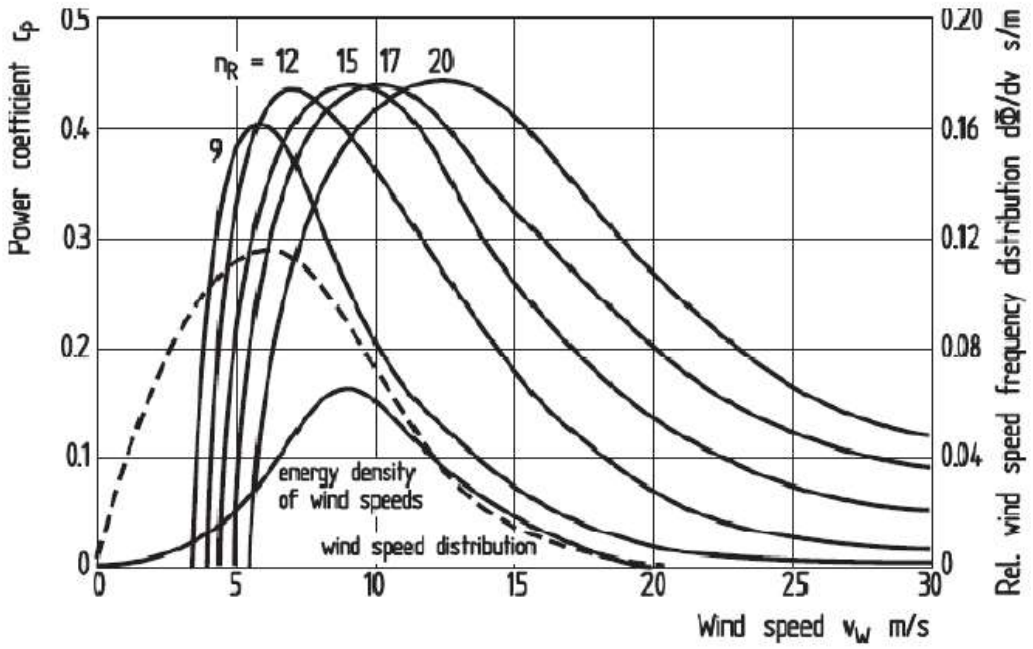

Figure 36: **Rotor Cpr in terms of rotor speed and wind speed. Energy density and wind speed distribution in terms of wind speed.**
Source: Hau, Wind Turbines fund., p.538.

.

It is important to underline the importance of available wind data and wind speed measurements carried on before this design stage: in fact, it is technically difficult to adjust the rotor speed on-site, once that the wind turbine is installed. Therefore, the rotor speed is exclusively determined during the design stage. Wind speed distribution and its related energy density must be accurate.

The wind speed which grants the maximum energy density is called *design wind speed* v_d.

For the final choice of the rotor speed, the calculation of the energy yield is necessary. Thus, we calculate the electrical power of the turbine:

$$P_{el} = \frac{1}{2} C_p \rho A_{rot} v^3$$

Where C_p is the power coefficient of the whole turbine, ρ is the air density, A_{rot} is the rotor-swept area, and v is the wind speed. C_p can be obtained from C_{pr} of the rotor, if the mechanical-electrical efficiency $\eta_{mech-elt}$ is known.

$$C_p = C_{pr} * \eta_{mech-elt}$$

Plotting P_{el} for different rotor speeds, and taking into consideration the upper limit given by the rated power of the electrical generator:

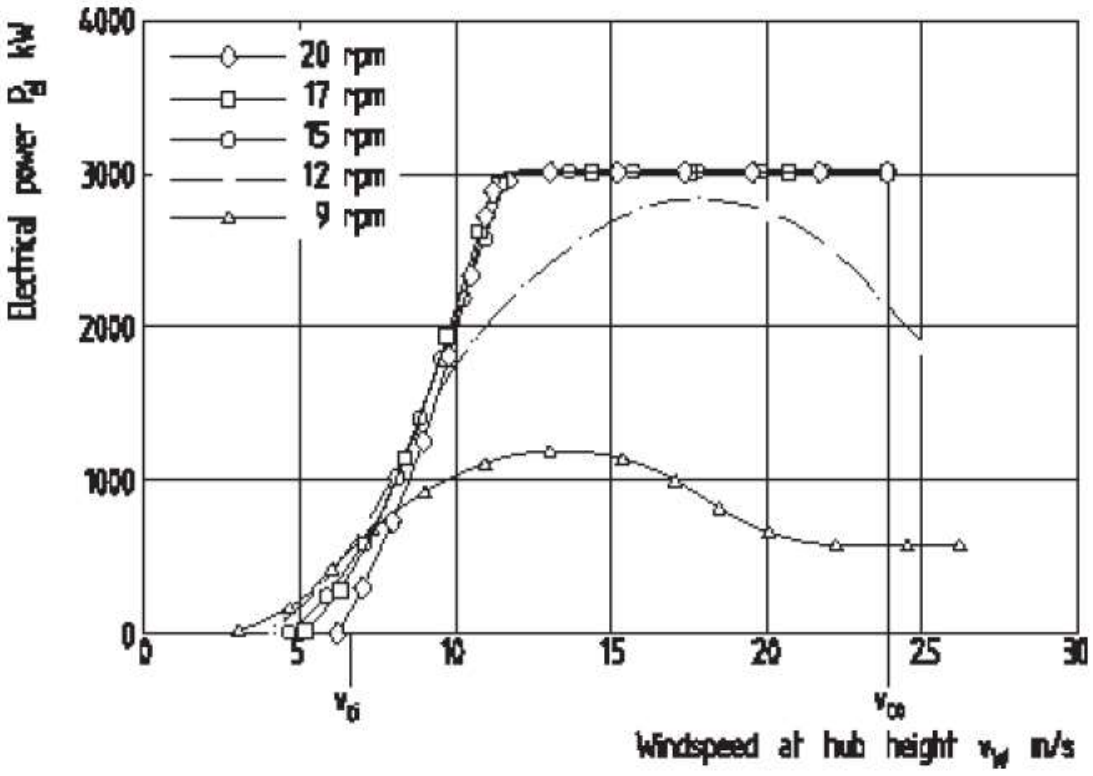

Figure 37: **Pel in terms of wind speed, for different rotor speeds.**
Source: Hau, Wind Turbines fund., p.552.

In the plot, the *cut-in wind speed* v_{ci} and the *cut-out wind speed* v_{co} are located.

From these P_{el} curves, the annual energy yield is computed:

$$E = \int_{v_{ci}}^{v_{co}} P_{el}(v)dt \cong \sum_{v_{ci}}^{v_{co}} P_{el}(v)\Delta t$$

The result is a scalar number, obtained for a single rotor curve, thus for a single rotor speed. Computing E for a range of rotor speeds, and plotting:

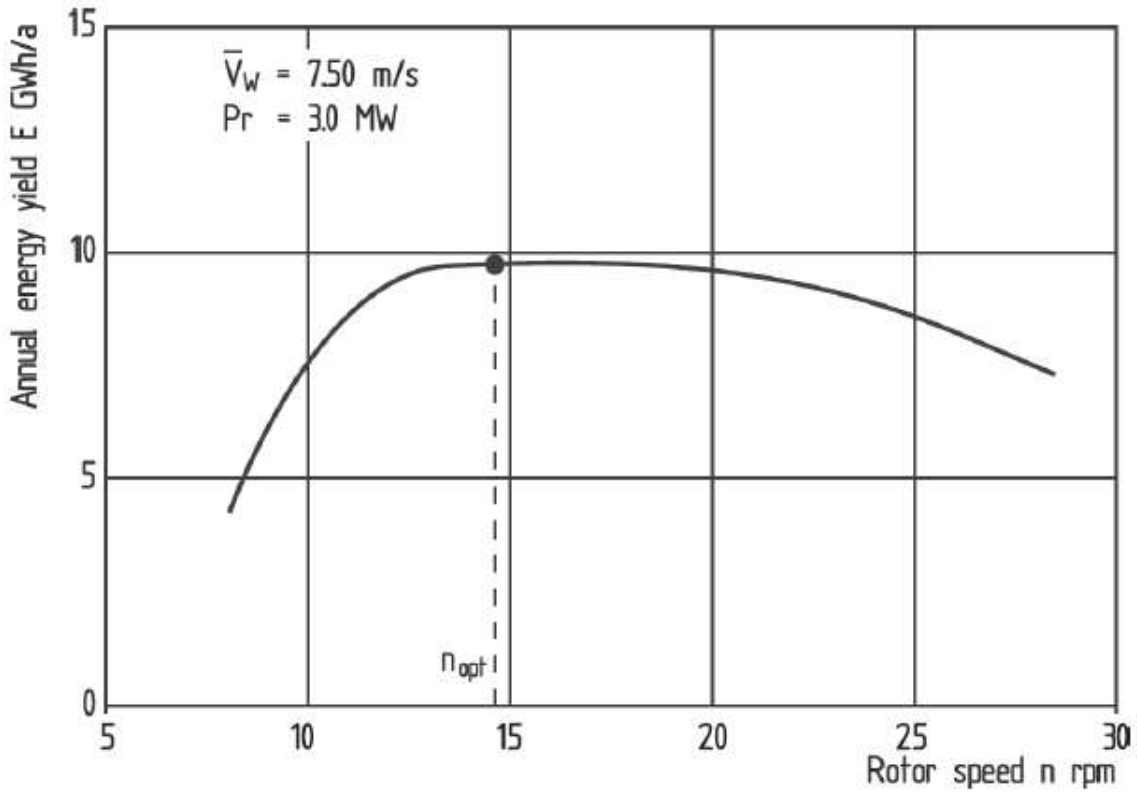

Figure 38: **Energy Yield in terms of rotor speed. Optimal rotor speed is located on the max of this function.**
Source: Hau, Wind Turbines fund., p.553.

The maximum of this function is located in correspondence of the optimal rotor speed.

1.4.2 Electromechanical energy conversion efficiency

The power coefficient of the turbine is obtained as:

$$C_p = C_{pr} * \eta_{mech-elt}$$

The *electromechanical efficiency* $\eta_{mech-elt}$ is influenced by:

- Gearbox efficiency
- Shaft, bearings frictional losses
- Electrical generator and inverter efficiency
- Transformer efficiency
- Wind turbine progressive wear during the operative life

The electromechanical efficiency tends to get higher for bigger turbines, because of more costly and carefully-designed components, and, in general, a more careful design of the whole system.

The choice of the electrical generator typology has also great influence on the whole efficiency, also. due to the presence or less of the gearbox.

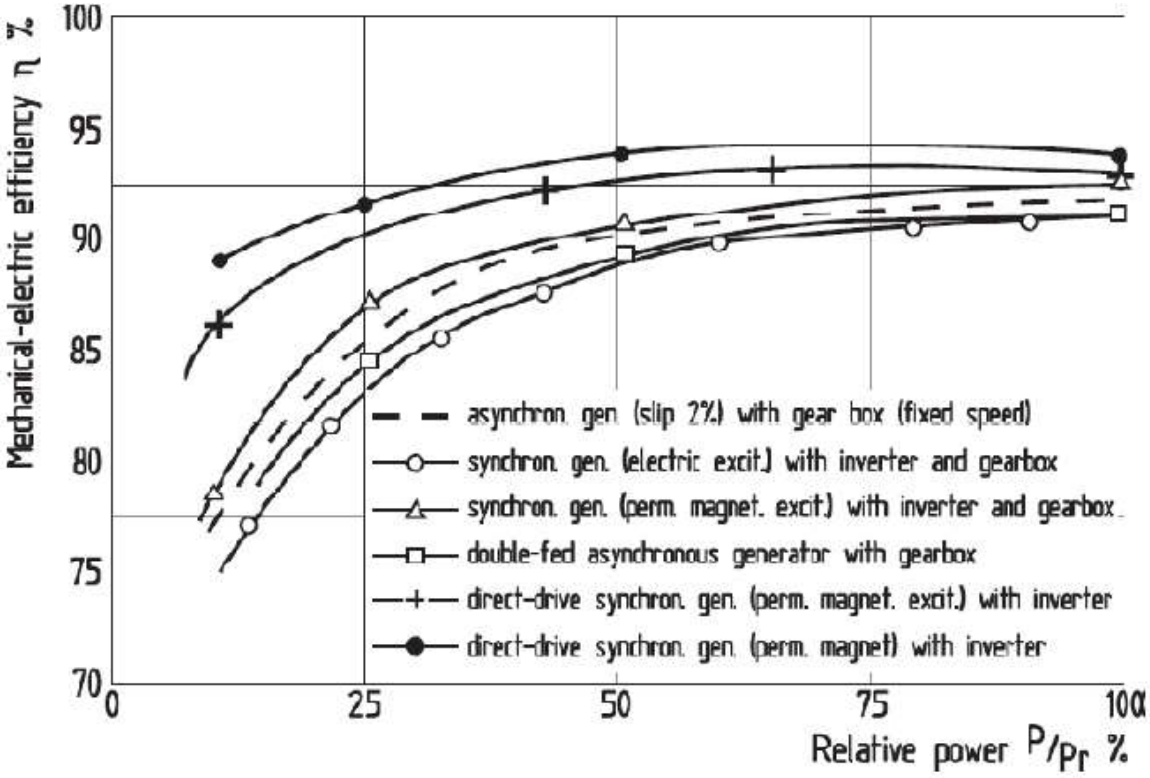

Figure 39: **Mechanical-electrical efficiency of a turbine with different generators and configurations, in terms of relative power (to the rated power).**
Source: Hau, Wind Turbines fund., p.559.

1.4.3 IEC definitions

The IEC 63400-2-1 Guideline gives some useful definitions related to the power curve:

- v_{ci} is the *cut-in velocity*, at which the turbine starts producing a power output. The rotor is already rotating before its reaching, to compensate for all the energy conversion process losses.
- v_R is the *rated wind velocity*. At this velocity, the rated power of the generator is reached. In the real, measured power curve, v_R is determined more or less approximately, because of turbulences and uncertainties of the real on-site conditions and of the turbine control.
- v_{co} is the *cut-out velocity.* it is the maximum wind speed that allows power delivering from the turbine.
- *Power* is assumed to be the net power, delivered as an output of the whole turbine system. The power line transformer is not included in the turbine system.
- The *standard atmospheric conditions*[28] are described by DIN 5450: air density 1,225 kg/m3 at MSL[29], temperature 15 C°.

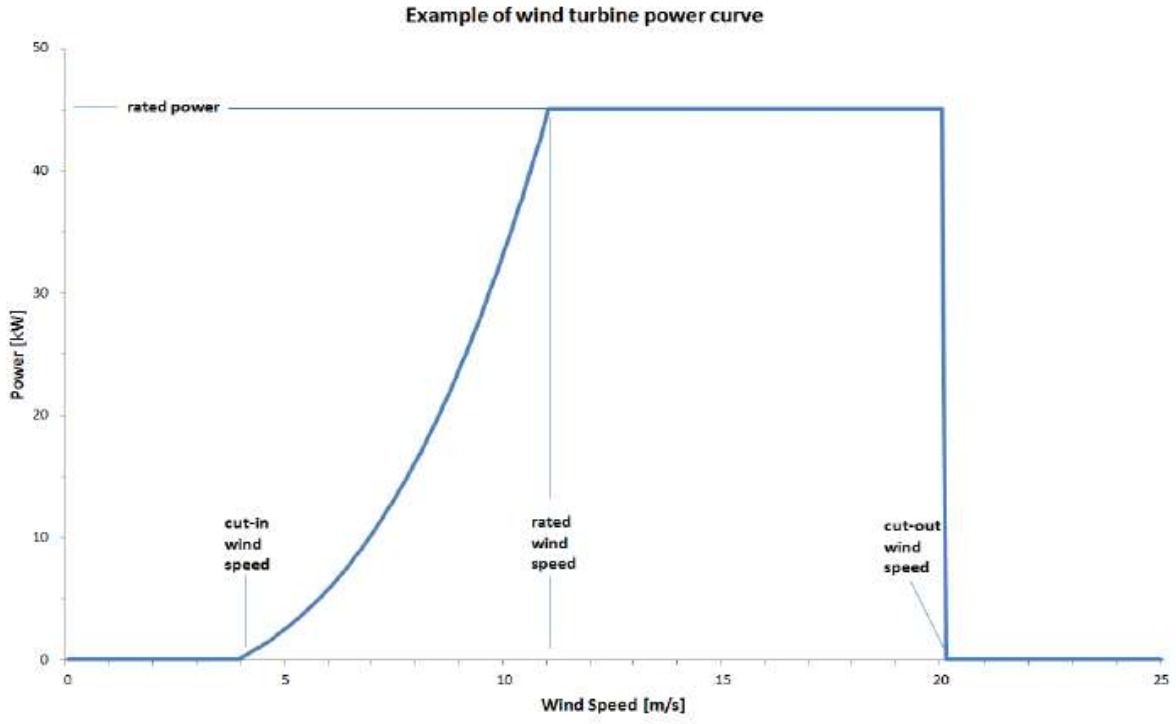

Figure 40: **Example of wind turbine power curve.**
Source: Rosłaniec: Energy conversions (university course), Warsaw university of technology, Warsaw 2016.

[28] $\rho_0 = 1.225 \frac{kg}{m^3}$, $T_0 = 15\ C°$, $P_0 = 1013.3\ mbar$
[29] Mean Sea Level

1.4.4 Air density variations and influence on the power curve

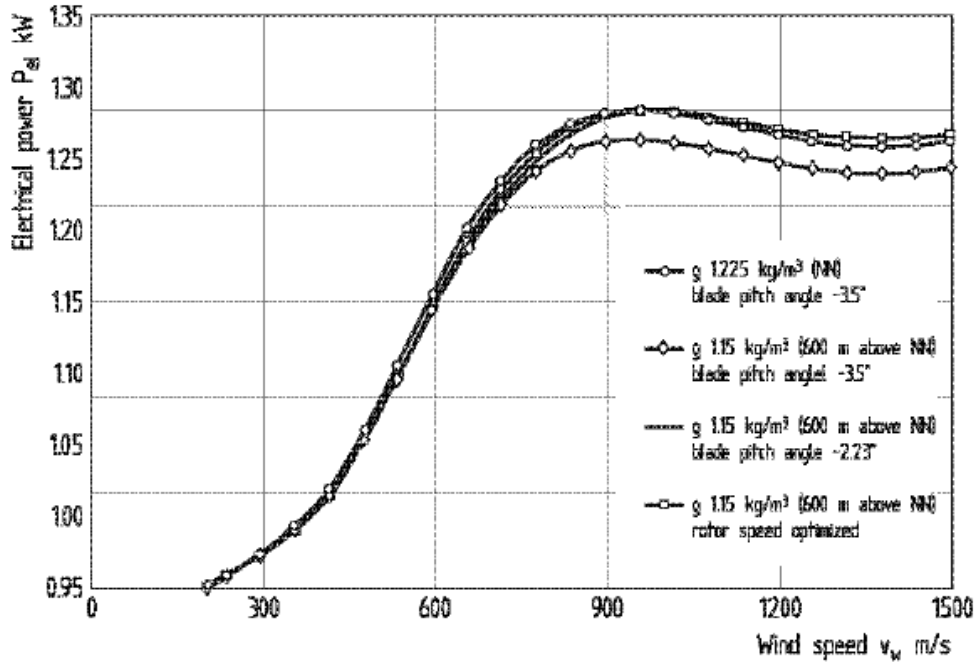

Figure 41: **Power curve of a stall-controlled turbine with pitch angle corrections. Source: Hau, Wind Turbines fund., p.571.**

Air density depends on altitude and temperature. The constructors provide power curves of the turbines for *standard atmospheric conditions,* and in some cases they could need a correction in terms of the actual on site conditions.

Air density can be calculated through the *Boltzmann barometric equation:*

$$\rho_H = \rho_0 \frac{T_0}{273.15 + t} \frac{P_H}{P_0}$$

Where ρ_H is the air density at height H above MSL. ρ_0, T_0, P_0 are *standard atmospheric conditions*, t is the temperature at height H.

In case of *stall controlled turbines,* the differences in the power curve are evident, and the energy losses on yearly basis can be up to 6%. With proper corrections of the blade pitch angle and rotor speed, they can be reduced to around 2%.[30]

In case of *blade pitch controlled turbines,* the changes in the power curve are less evident. However, due to the fact that the blade pitch angle is easy to change and that these turbines

[30] Hau, *Wind Turbines fund., p.572*

usually have variable rotor speed, corrections are applied, allowing a lossless operation for different air density conditions.

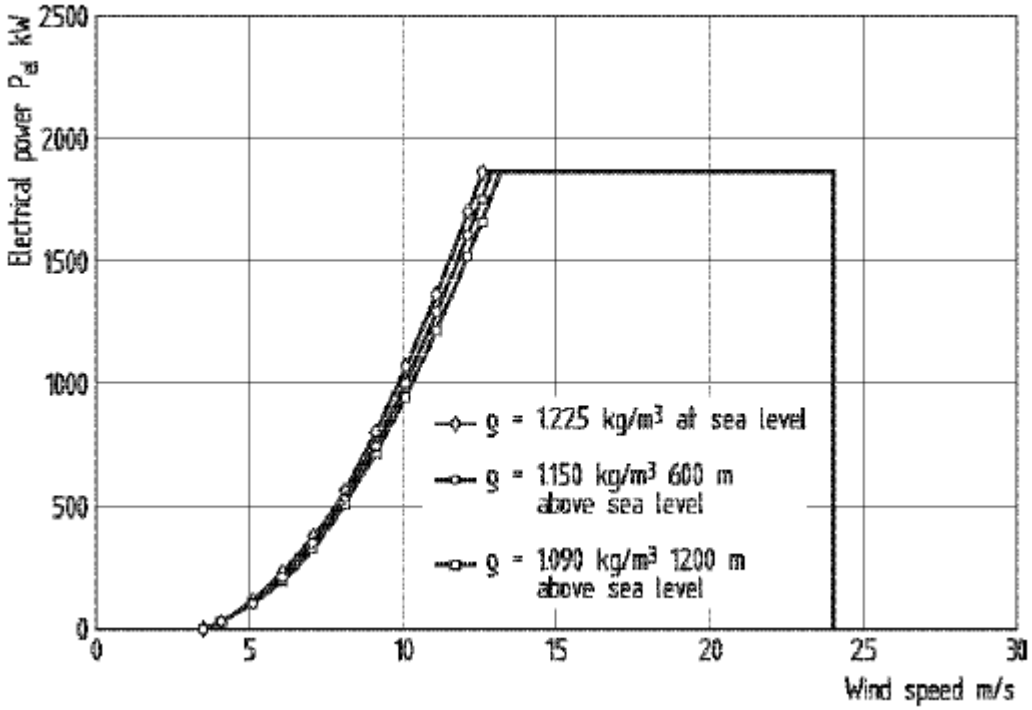

Figure 42: **Blade pitch controlled turbine power curve and relative corrections for different air density conditions.**
Source: Hau, Wind Turbines fund., p.573.

1.4.5 Turbulence influence on the power curve

In presence of turbulences, the power curve of a wind turbine can be influenced, even if not in a very important way. The air fluxes of the turbulence play a little role in increasing the air density, but their directions are not necessarily favourable with respect to the rotor-swept area. The effect on the power curve is a more or less evident rise for lower wind speeds, and a diminution for higher wind speeds. Regarding the effects on the annual energy yield, these are so limited that can be simply neglected. The main issue regarding turbulences is the turbine's withstanding of the structure load they cause.

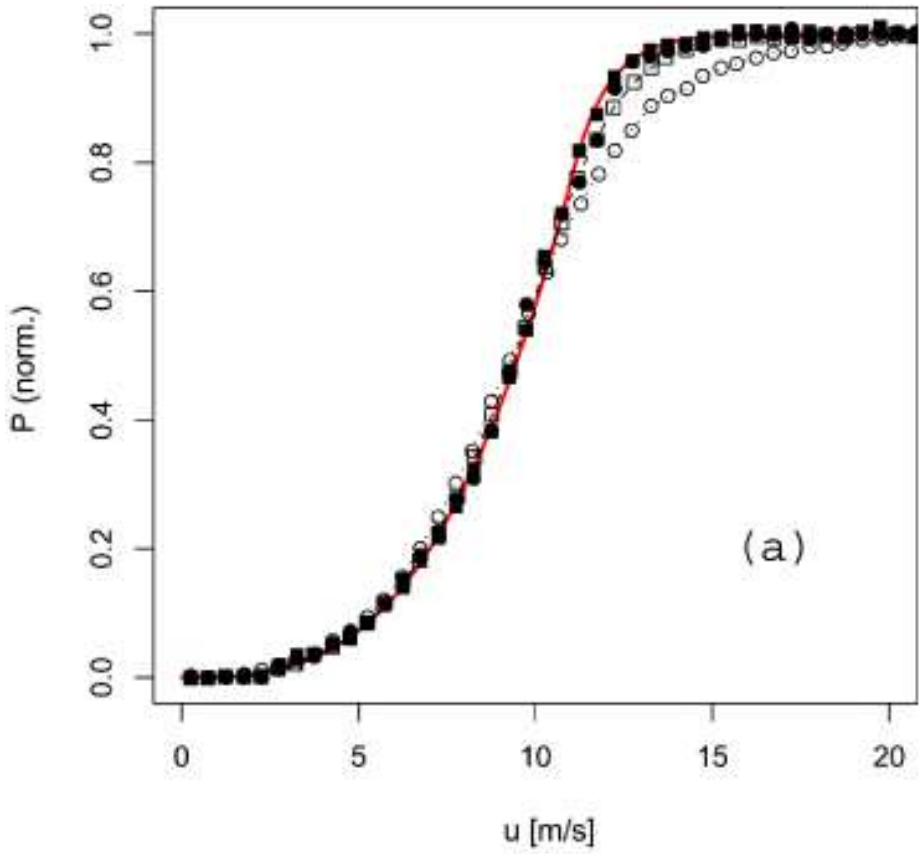

Figure 43: **Turbulence effects on the power curve, indicated in white**
Source: "How to improve the estimation of power curves for wind turbines" by Julia Gottschall and Joachim Peinke *http://iopscience.iop.org/article/10.1088/1748-9326/3/1/015005/fulltext/*

1.4.6 Blades soiling

The most damaging and dire environment effect on the energy yield of a wind turbine is soiling. Soiling of blades occurs very fast, in some months, and it is composed of dead bugs and dust. The influence of the specific site is relevant, being the sandy ambient the most problematic, and the forest-wood the least. Higher hubs are less subjected to soiling, as the blades are further from the ground. The effects on the dynamic of the blade are represented by a variation of the lift-drag actions, and an increased turbulent effect of the air flow. Stall-controlled turbines are the most penalized, because soiling variates their design parameters, and stalling happens for lower wind speeds than it should. Blade-pitch controlled turbines can withstand the phenomena to a greater extent, thanks to the adaptation of the pitch angle due to the control system, but an important power loss is anyway happening. Rotor blades washing, even if expensive, seems to be the only solution in those cases when soiling represents a relevant limitation to the turbine energy production.

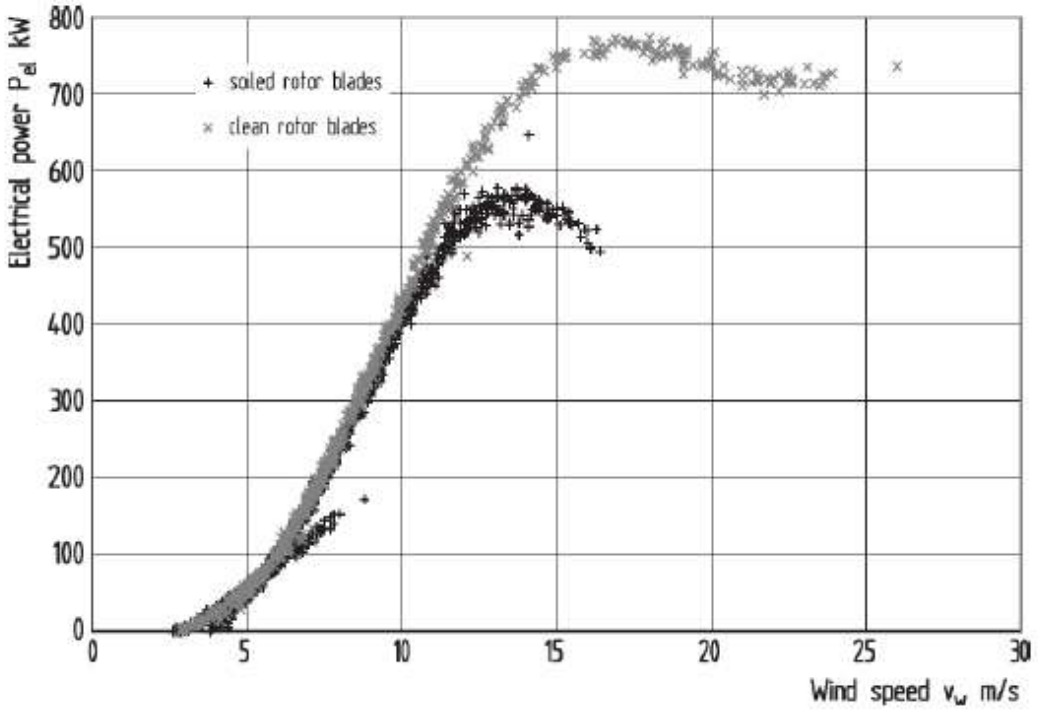

Figure 43: **Measured power curves of a soiled blades stall-controlled turbine and a clean one.**
Source: Hau, Wind Turbines fund., p.576.

1.4.7 Energy yield calculation

The annual energy yield is calculated with:

$$E = 8760 \sum_{v_{ci}}^{v_{co}} P_{el}(v)\Delta\phi \quad [31]$$

Where $\Delta\phi$ is the *cumulative frequency distribution*, and 8760 is the number of hours in a year.

A Δv interval is chosen, for example 1 m/s, and for every wind speed interval the corresponding $P_{el}(v)$) is read on the power curve, and it is multiplied with the corresponding $\Delta\phi$ from the cumulative frequency distribution function. Iteratively summing the results obtained for every wind speed interval Δv between v_{ci} and v_{co} produces the total energy yield.

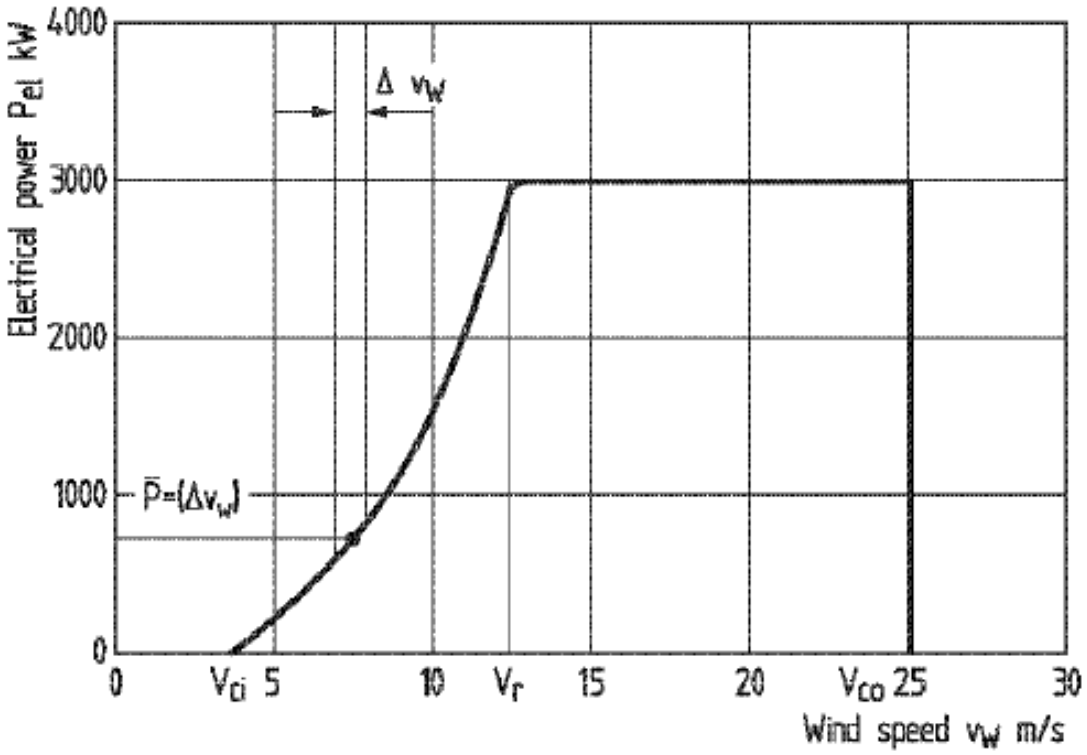

Figure 44: **Pel for a specific Δv interval, selected on the wind turbine power curve. Source: Hau, Wind Turbines fund., p.580.**

[31] Hau, *Wind Turbines fund., p.579*

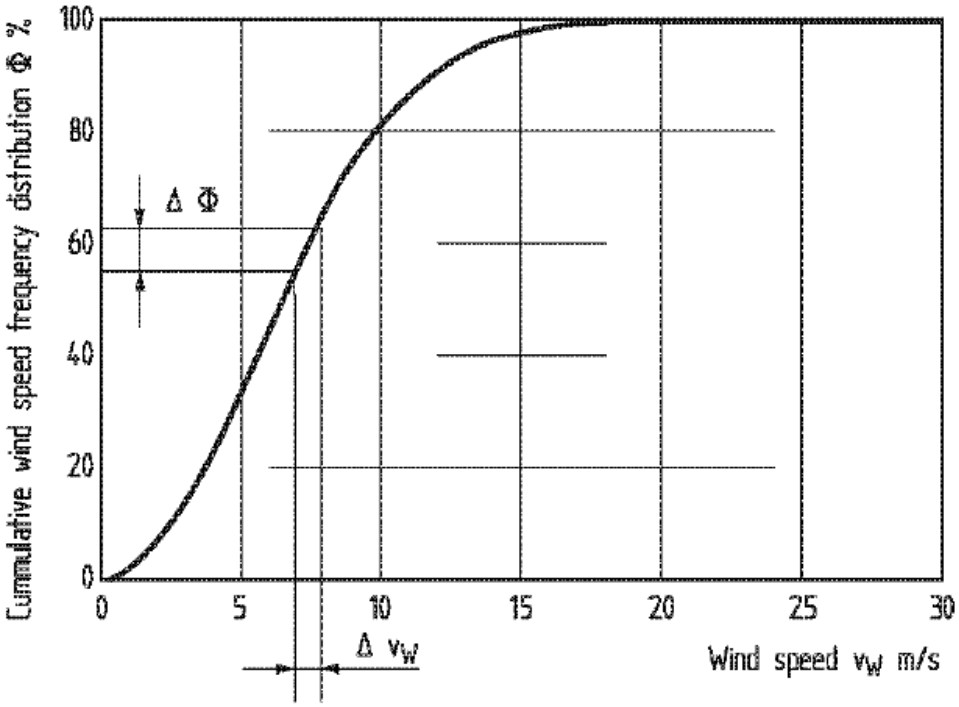

Figure 45: **$\Delta\phi$ selected for a specific Δv interval, on the cumulative wind speed frequency distribution function.**
Source: Hau, Wind Turbines fund., p.579

For every level of electrical power P_{el}, a representation in terms of load hours can be done. The area between the curve and the horizontal axis is equal to the annual energy yield. The *annual average power* can be obtained as

$$P_{avg} = \frac{E}{8760}$$

And it can be seen as the height of an equivalent rectangle of area E, with 8760 as base. For an intuitive representation of the annual energy yield, an equivalent rectangle of area E can be defined with height correspondent to P_{gen} (the rated power of the generator), and with base equal to the *equivalent full load hours*.

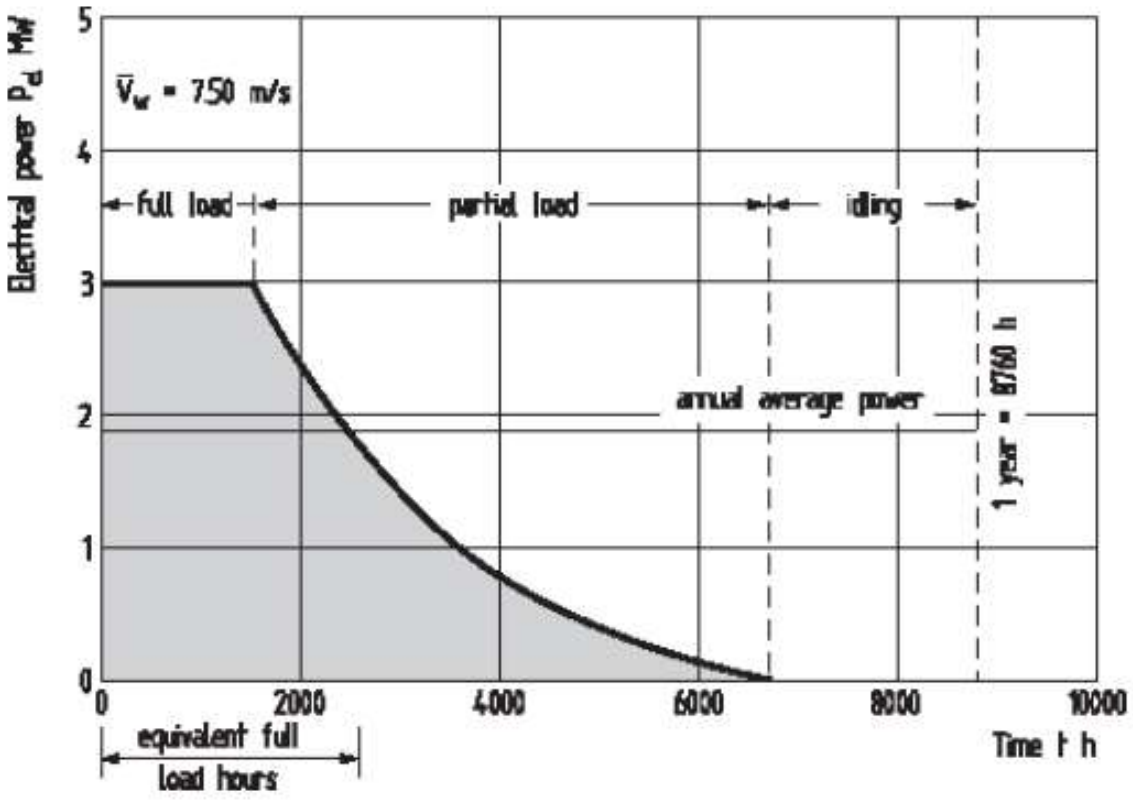

Figure 46: **Power duration curve. The area underneath the curve is the annual energy yield E. Source: Hau, Wind Turbines fund., p.581.**

1.4.8 Technical availability

For every energy plant, it is technically impossible to reach the maximum energy yield: maintenance and unplanned service interruptions reduce the maximum possible working hours. In particular, maintenance is absolutely necessary and fundamental for the proper operation of the facility.

The ratio of the effective annual working hours, to the theoretical maximum annual working hours represents the *technical availability:*

$$K_T = \frac{T_V}{T_N}$$

Where T_V is the *available time* and T_N is the *nominal time*. The available time can be written as:

$$T_V = T_B + T_R$$

Where T_B is the *operating time* (effective time of energy generation) and T_R is the *stand-by time* (on which the facility is operation-ready but it is not working).

In the specific case of wind turbines, the time which is <u>not</u> considered as a *non-availability* is the time due to[32]:

- Recovery time from routine maintenance.
- Standstill time due to intervention of the operator or of the authorities.
- Standstill time due to external causes (such as the hit of a lightning , blade icing, or electrical grid issues).
- Time when the wind speed is out of the *cut-in/cut-out* velocity range.
- "Trivial" standstill times limited to an annual small amount of hours (< 5 hours).

However, to forecast in a very precise way the *operating time* of a wind turbine is not easy. Therefore, it is widespread amongst the manufacturer's side to offer the wind turbine *warranty agreement* basing on a forecasted amount of energy which will be produced. In this legal agreement, it is quite obvious the importance of past and present wind measures and data for both the manufacturer and the operator, and of the effective annual operational data acquired and provided by the operator in order to obtain the possible "damages cash". These agreements

[32] Hau, Wind Turbines fund., p.585

can be seen as a way to eliminate part of the "uncertainties" of the economical operation of a wind turbine, due to the obvious not completely foreseeable nature of the wind resource.

A good reference scenario from economical point of view is to have a *technical availability* of 98%, with respect to a maintenance cost equal or inferior to the 10% of the turbine's income. Higher maintenance costs represents a bad economical factor[33].

From economical point of view, in order to have good terms of comparison, an important factor for any kind of power plant is the *capacity factor:*

$$c = \frac{\bar{P}}{P_r} = \frac{E}{P_r * 8760}$$

Where $\bar{P}$ is the mean power, P_r is the rated power, and E is the annual energy yield.

For the *equivalent full load hours:*

$$Equivalent\ full\ load\ hours = \frac{E}{P_r}$$

These 2 parameters can be effectively used as a term of comparison between wind turbines only if the turbines are approximately of the same size, and if their ratios $\frac{P_r}{A}$ (A is the rotor-swept area) are approximately equal or if a proper conversion on rated power is applied.

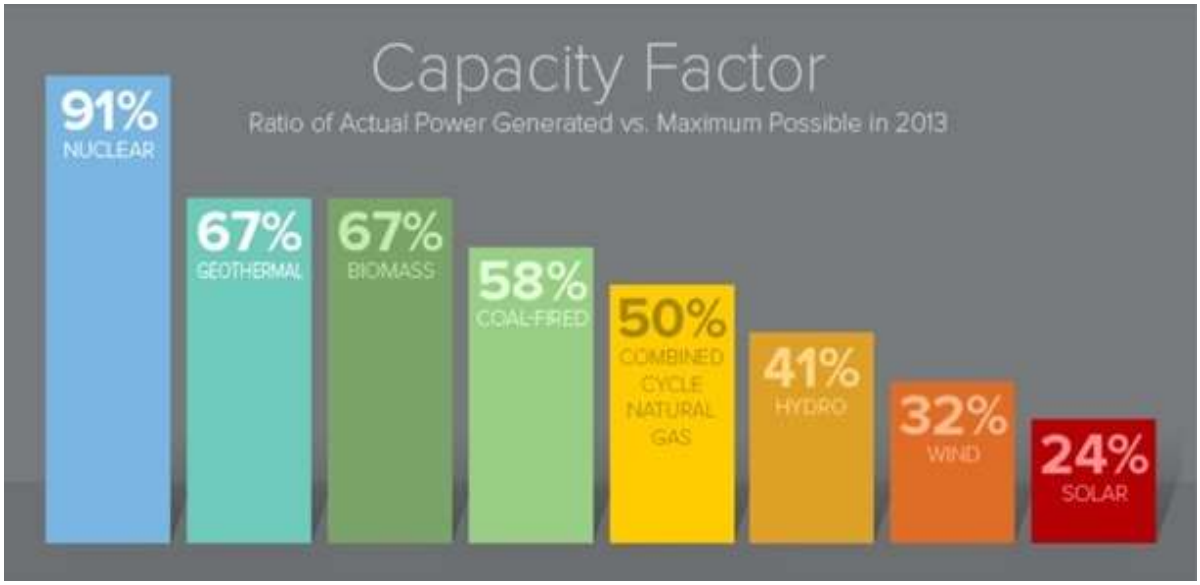

Figure 47: **Capacity factors for different power plants in the U.S. in 2013.**
Source: Nuclear Energy Institute. *http://ansnuclearcafe.org/2014/12/15/columbia-celebrates-three-decades-of-clean-electricity-production/#sthash.v1J1fZxS.dpbs* consulted on 24/08/2016.

[33] Hau, Wind Turbines fund., p.586

1.4.9 Safety deductions on the energy yield

As one of the most relevant factors of an important investment plan, the energy yield should be carefully examined, and possibly a percentage of it could be subtracted as a safety deduction.

In detail, the most relevant issues are:

- How the *power curve* has been obtained, if it responds to the actual installing conditions such as the height of the hub, if it is calculated from a prototype or from more "practical" installations, and if safety margins have already been applied.
- *Parking efficiency* in case of wind parks and *energy transmission losses to the grid* should be considered in the safety deductions too.
- *Wind forecast uncertainties* can be accounted, but it depends on how these data has been applied for the earlier calculation of energy yield, and if there is an effective probability of obtaining a significant reduction of the energy produced, or if positive and negative uncertainties somewhat tends to compensate.
- At last, an *overall safety deduction* can be applied if minor losses are presents, due to yawing and blade-pitching frequent hysteresis, turbulences, air density variation, limited soiling, and, in general, any hard-to-quantify secondary effect: these effects should be roughly quantified in terms of significance on the overall energy yield, and an *overall safety deduction* of 5% in case of limited influence, or of 10% in case of uncertainties for wind forecasting and the specific installation site, should be applied. It is important to underline that *safety deduction* are made on a computational effective evaluation, even if not too precise, and they should not be considered a way to correct "bad design and planning issues": this consideration is even more important for big projects and investments.

1.4.10 Choice of the rotor diameter and influence on the energy yield

The choice of the rotor diameter is not arbitrary, nor it can variates too much, for a determined size of the wind turbine. In fact, rotor diameter depends on the overall turbine dimension, and on its rated power. The key is to find the optimal rotor diameter for a certain situation: for a correct design of the turbine, the choice can't be far from the optimal parameter.

In particular, the *handbook wind energy, Wiley* (see bibliography) reports the results of a study conducted by Fuglsang and Thomsen in 1998[34]. The study is based on a 1.5 MW turbine, 60m of rotor diameter, fixed rotor speed, with stall regulation, installed on land. The aim was to obtain the cost of the components of a geometrically similar turbine, for a size variation of structure and components in terms of rotor diameter.

Table 6.1 Component costs expressed as a percentage of total machine cost for a 1.5 MW, 60 m diameter, fixed speed, stall-regulated wind turbine on land (from Risø-R-1000, Fuglsang and Thomsen, 1998)

Component	Cost as a percentage of total	Component	Cost as a percentage of total
Blades	18.3%	Controller	4.2%
Hub	2.5%	Tower	17.5%
Main shaft	4.2%	Brake system	1.7%
Gearbox	12.5%	Foundation	4.2%
Generator	7.5%	Assembly	2.1%
Nacelle	10.8%	Transport	2.0%
Yaw system	4.2%	Grid connection	8.3%
		TOTAL	100%

Figure 48: **Component costs for an example turbine based on the indicated study. Source: Handbook wind energy, Wiley p.327, from Cost optimisation of wind turbines for large-scale offshore windfarms, Fuglsang and Thomsen, Risø 1998.**

[34] Cost optimisation of wind turbines for large-scale offshore windfarms, Fuglsang and Thomsen, Risø 1998

In particular, for all the components except generator, controller and grid connection, the cost is expressed as:

$$C_1(D) = 0.8C_T\left(0.9\left(\frac{D}{60}\right)^3 + 0.1\right) \quad 35$$

Where $C_1(D)$ is the cost of the scaled component, C_T is the cost of the base machine component, and D is the diameter of the scaled machine. There is a cube proportionality for costs, in terms of diameter.

The controller cost is supposed to be constant for any diameter. For the generator, and the grid connection:

$$C_2(D) = 0.158C_T\left(0.9\left(\frac{D}{60}\right)^2 + 0.1\right) \quad 36$$

Where $C_2(D)$ is the cost of the scaled component, C_T is the cost of the base machine component the diameter of the scaled machine. There is a square proportionality for costs, in terms of diameter.

On the basis of this model, of different sites with peculiar terrain roughness z_0, assuming a hub height equal to the rotor diameter, it is possible to plot the *energy cost index*:

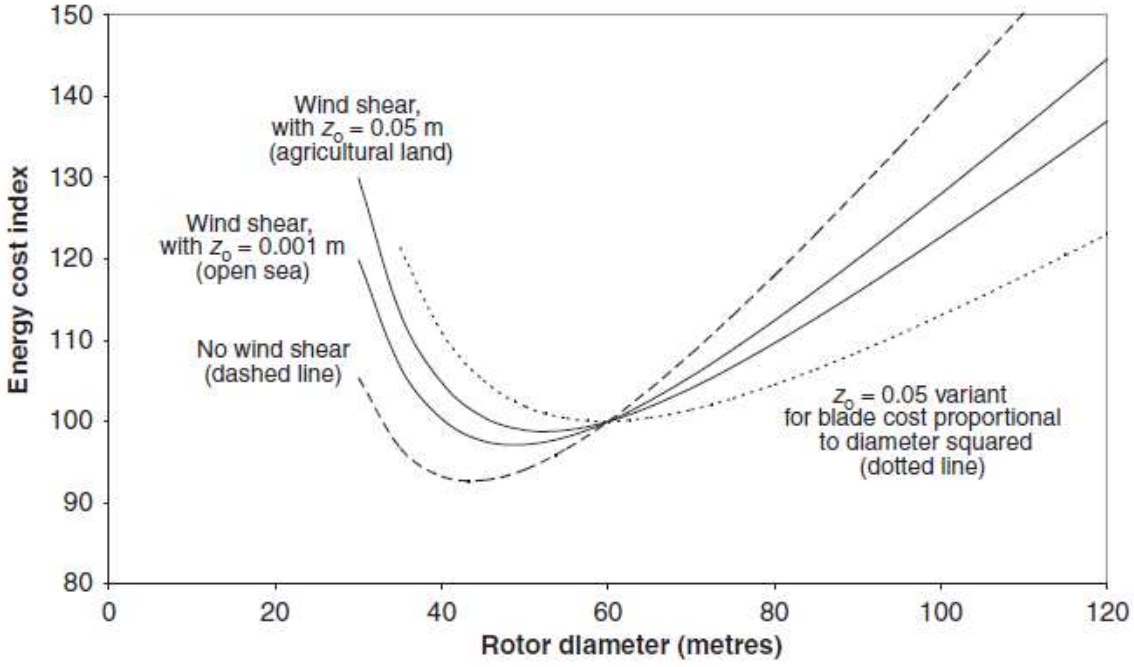

Figure 49: **Energy cost index of the example scaled turbine, in terms of rotor diameter, for different site parameters.**
Source: Handbook wind energy, Wiley p.328.

The plot shows how, for different sites, the lower energy cost index is reached for different rotor parameters. The concept of "*optimal",* non-arbitrary choice of the rotor diameter is strongly underlined.

Regarding the rotor speed, in the precedent chapters we saw how the optimal C_p is reached for a particular tip-speed ratio λ: in order to work on the maximum possible C_p, with a diameter variation also the rotor speed has to be changed.

1.4.11 Rotor diameter and rated power of the generator

A higher energy yield is obtained using a larger rotor, but to obtain a relevant improvement, as the rotor diameter increases, it's necessary to mount a generator with an appropriate rated power.

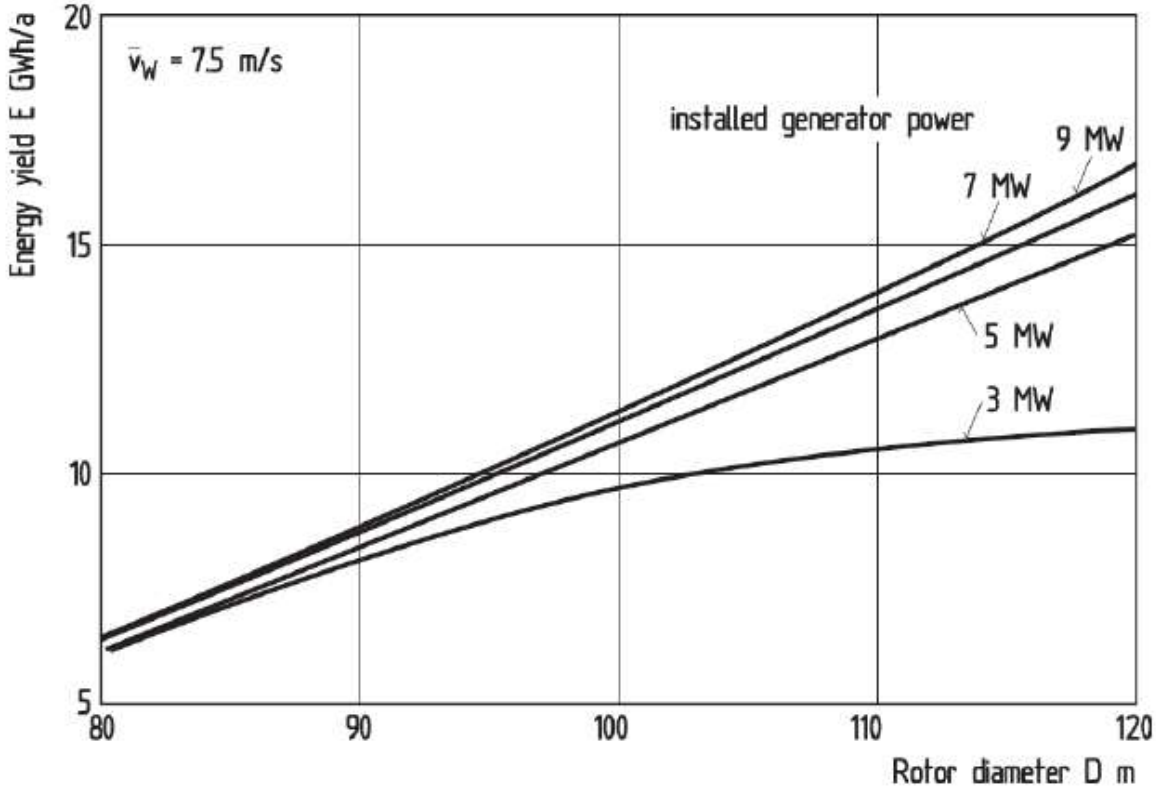

Figure 50: **Annual Energy yield of a specific turbine, in terms of rotor diameter and generator rated power.**
Source: Hau, Wind Turbines fund., p.594.

[35] Cost optimisation of wind turbines for large-scale offshore windfarms, Fuglsang and Thomsen, Risø 1998
[36] Cost optimisation of wind turbines for large-scale offshore windfarms, Fuglsang and Thomsen, Risø 1998

1.4.12 Variable rotor speed operation

Previously, I described how to find the optimal rotor speed for a particular wind speed frequency distribution. It is clear that there will occur variations in the mean wind speed, depending on the year analysed. However, the maximum energy yield obtainable for a certain mean wind speed, requiring a specific rotor speed to be achieved, it is not so dramatically different than the energy yield obtained if an optimal fixed rotor speed is adopted.

More specifically, adopting a variable rotor speed operation range from 40% to 100%, the corresponding positive increase in the energy yield would be in the range of 3-5%, not necessarily enough to justify the presence of an AC/DC-DC/AC inverter-based conversion system coupled with the generator[37].

The reasons of the widespread use of the variable rotor speed operation has to be found, together with this (relatively) small increase in the energy yield, in a reduced load on mechanical parts, reduced aerodynamical noise, and a better power output from electrical power quality point of view[38].

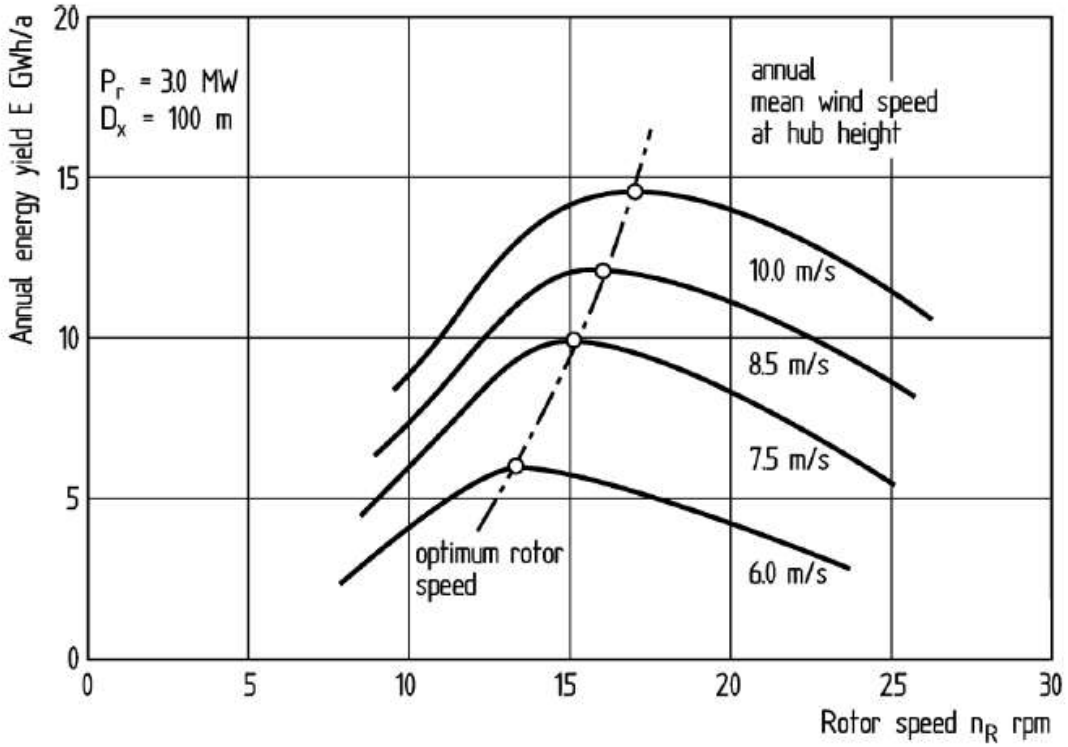

Figure 51: **Energy yield of an example turbine, in terms of rotor speed and mean wind speed Source: Hau, Wind Turbines fund., p.595.**

[37] Hau, Wind Turbines fund., p.586
[38] Hau, Wind Turbines fund., p.595

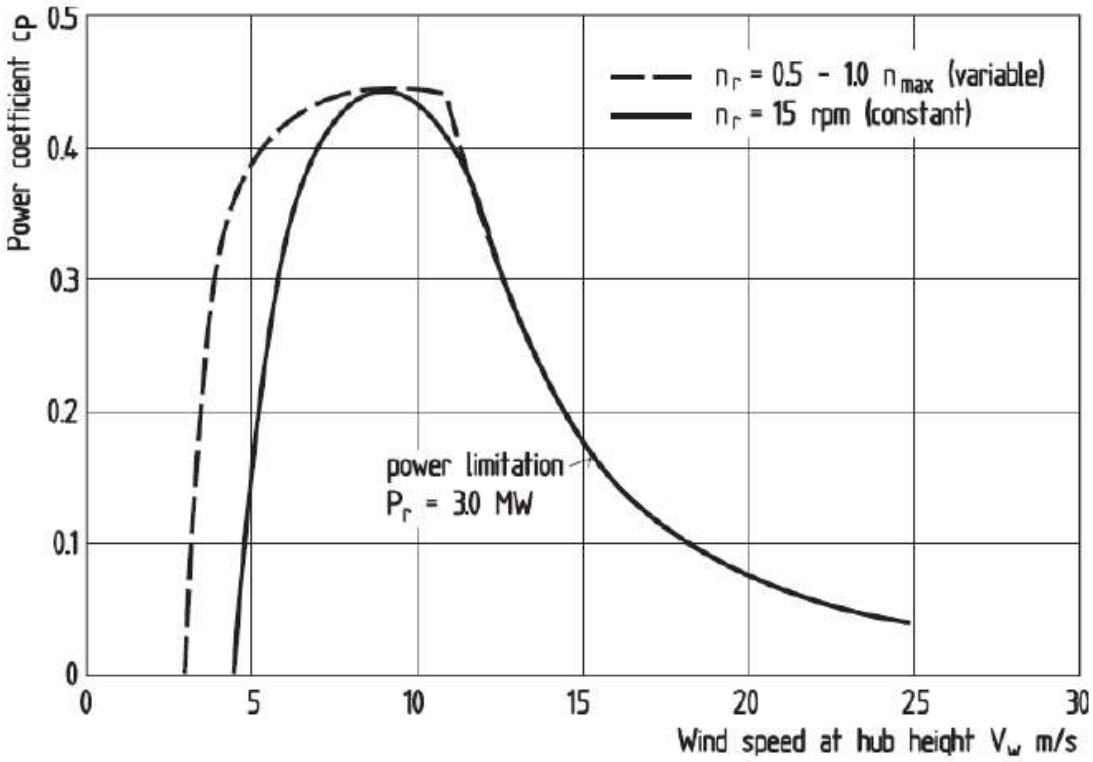

Figure 52: **Cp in terms of wind speed, for constant rotor speed and variable rotor speed. Source: Hau, Wind Turbines fund., p.596.**

In terms of Cp, on the chart we can observe how the most relevant improvements are obtained for lower wind speeds, less relevant from the *energy density function* point of view.

1.4.13 Hub height

A sufficient rotor height, given that stiffness, load, and vibrational structural issues of are faced, allows a better utilization of the site and thus, a higher annual energy yield. In particular, at higher heights the *mean wind velocity* gets higher, and, even if it is true for offshore marine sites, the tendency is more important for inland sites, characterized by a higher *roughness length* z_0. Once again, a cost/benefits evaluation should be made, taking into account the cost of the tower and the gain in terms of energy yield. At heights superior to 100m, careful estimation should be made due to the increased uncertainties of the *Ekmann Layer*.

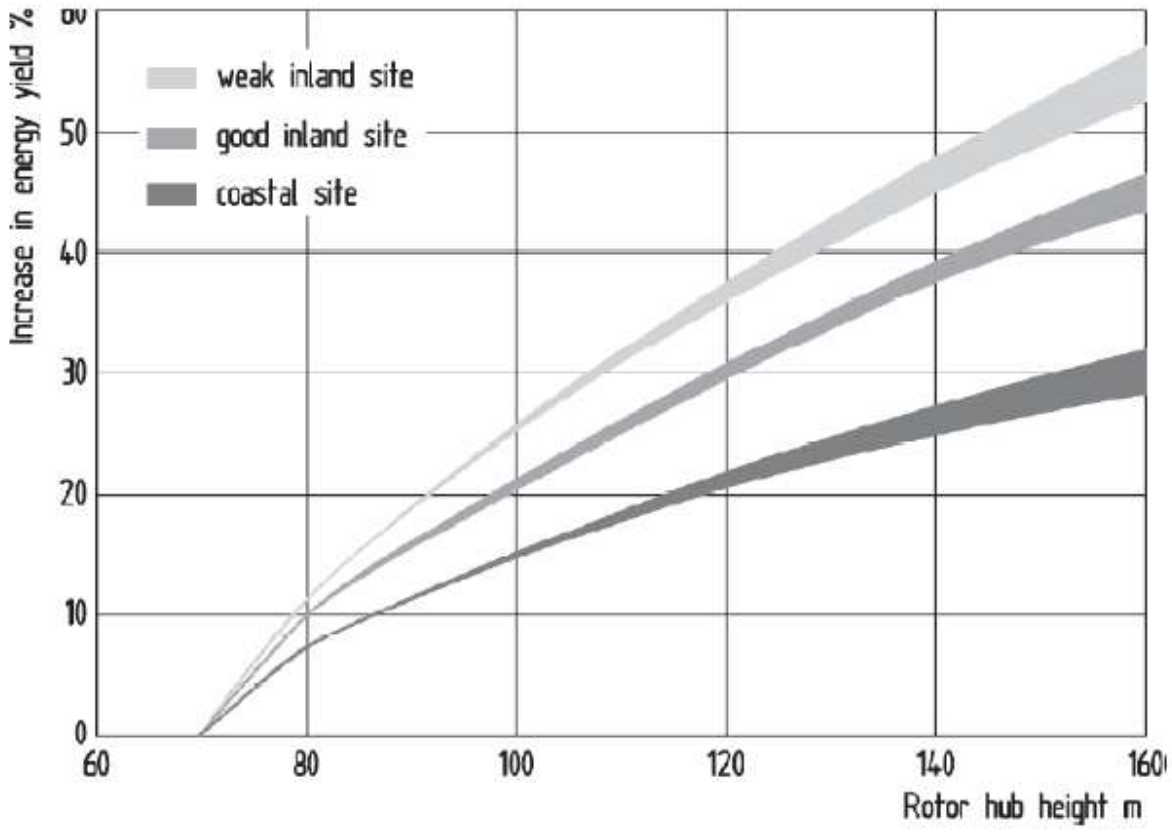

Figure 53: **Increase in energy yield for different sites, in terms of hub height. Source: Hau, Wind Turbines fund., p.600.**

1.4.14 Cut-in cut-out wind speed range

Cut-in and cut-out speeds choice is of very limited effects on the *energy yield*. In particular, the choice is made in order to:

- For the *cut-in speed*, the ideal choice is right above the wind speed needed to compensate the system losses. Some tolerance in higher direction is useful to avoid too frequent shut-in shut-out operation, thus avoiding hysteresis.
- For the *cut-out speed*, the limit is issued for safety reasons. At a certain wind speed (20-25 m/s) the rotor is stopped. Cut-out hysteresis can happen.

From the energy yield point of view, cut-in speed variations are of very limited influence, due to a very low energy content of low wind speeds. Cut-out speed variations are of limited influence because of the infrequent occurrence of such high wind speeds. The most important aspect is that control operation are settled in a way to avoid excessive cut-out hysteresis and possible useful operational time loss.

Chapter 1.5 Electrical generators and wind turbines configurations

1.5.1 Configurations

In state-of-the-Art wind turbines, different configurations are available, to respectively achieve fixed-speed operation or variable-speed operation.

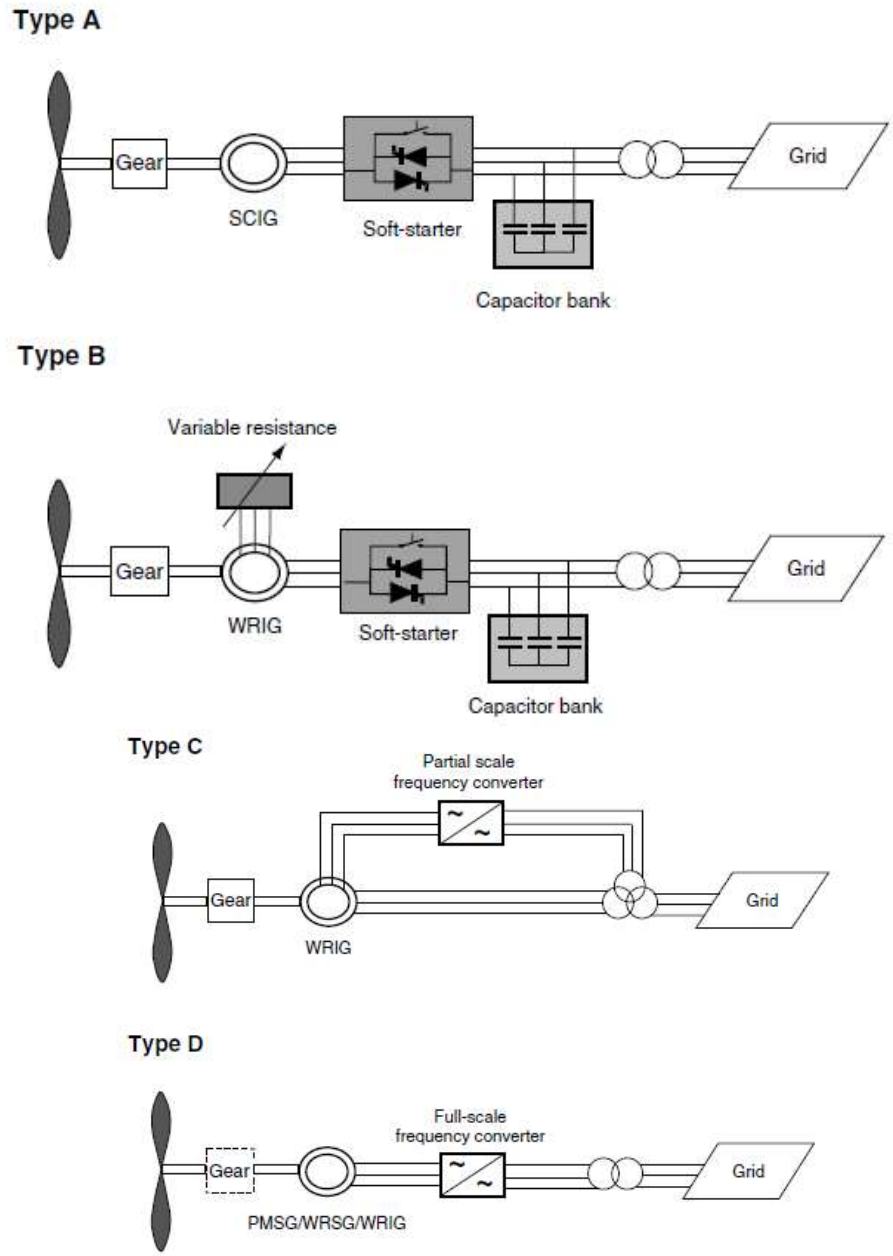

Typical wind turbine configurations. SCIG: squirrel cage induction generator; WRIG: wound rotor induction generator; PMSG: permanent magnet synchronous generator; WRSG: wound rotor synchronous generator. The broken line around the gearbox in the Type D configuration indicates that there may or may not be a gearbox

Figure 54: **Source: Ackermann, wind power in power syst. p.76.**

Fixed speed (type A)

In the fixed speed configuration, the SCIG (squirrel cage induction generator) is directly connected to the transformer, and therefore to the grid. The SCIG absorbs important quantities of reactive power, which have to be compensated with a capacitor bank. A soft starter can be present, in order to reduce inrush currents and consequent voltage disturbance that could affect the grid.

Power control can be present through a blade-pitch regulation, but anyway in this configuration the wind speed fluctuation, being faster than the control, will result in an electrical power oscillation, and also reactive power oscillations which could bring to voltage fluctuations.

This typology can use *passive stall control*, *blade-pitch control* and *active stall control.* More specifically, the best results in terms of power quality are obtained with the active stall control, at the cost of a higher price of both control mechanism and controller.

Limited variable speed with variable rotor resistance (type B)

In this configuration, the generator is a WRIG (wound rotor induction generator), where the rotor resistance can be controlled (dynamically by power electronics) to a limited extent, thus allowing a narrow regulation of slip. Consequently, load and power output can be regulated, with better power quality and reduced mechanical loads. However, the speed regulation is very limited and the system still needs reactive power compensation (capacitor bank) and possibly a soft starter.

The main drawbacks of this solution are its simplicity and its favourable cost/benefits ratio.

Variable speed, partial-scale frequency converter (doubly fed induction generator) (type C)

The DFIG (doubly fed induction generator) is basically a WRIG (wound rotor induction generator) with its rotor connected through slip rings to a partial-scale inverter. The inverter is rated around 30% of nominal power, and it allows a wide control of slip, and a better efficiency thanks to the possibility to transfer active power from the rotor to the grid. Moreover, it allows to control reactive power, thus eliminating the need of a capacitor bank. No soft-starter is needed. The rotor speed range is around 30-40% of the nominal value. This solution is very interesting from economical point of view, allowing speed regulation with a smaller inverter, with good efficiency and little drawbacks (slip rings and an additional protection for the rotor in case of grid faults).

Variable speed with full scale frequency converter (type D)

This configuration is characterized by the presence of a full scale inverter, connecting the generator to the grid. There is control of full range of active and reactive power, and improved electrical power quality. Synchronous generators such as WRSG (wound rotor synchronous generator) or PMSG (permanent magnet synchronous generator) are usually mounted, but it is possible to use a WRIG connecting both the rotor and the stator to the frequency conversion system. The presence of a gearbox can be avoided if a large diameter multipole generator is installed.

1.5.2 Wind farm solutions

In a scenery of widespread diffusion of wind farms on the electrical grid, with farms comparable to traditional power plants in terms of installed power, it is more and more important the controllability of these facilities. In particular, active and reactive power needs to be controlled, together with voltage and frequency, providing also a quick dynamical reaction in case of transients[39]. They should contribute to the stability of the grid. The mechanical control of the turbines is not apt to such dynamical operation, therefore the only solution lies in the use of power electronics, in different possible connections and configurations.

a) Every turbine is provided with its own frequency conversion system (partial scale in the case of WRIG), thus autonomously controlling its working point in an optimal way. After the transformer, power is transmitted through an internal AC network and then transferred to the grid. This configuration is the most used nowadays.
b) Every turbine is provided with a full scale rectifier, and the internal power link of the wind farm is DC. An AC conversion is operated to connect the wind farm to the grid. Every turbine has an autonomous rotor-speed control.
c) In this configuration, the control structure is centralized, and the turbines behaviour results separated from the grid. This solution is cheaper than having a dedicated full scale inverter system for each machine, in terms of power electronics. The main drawback is that speed control is the same for all the turbines, therefore reducing efficiency and energy yield, and possibly increasing mechanical and structural stress. An interesting possibility is to have an HVDC (high voltage direct current) link to connect the wind farm to the grid, particularly useful for offshore wind farms distant from the connection point.

[39] Ackermann, wind power in power syst. p.100

d) This configuration is similar to c), but a transformer is present at each turbine, transforming electrical parameters to grid standards. A central static compensation is applied through a VAR compensator such a STATCOM unit, improving both reactive power balance and electrical power quality.

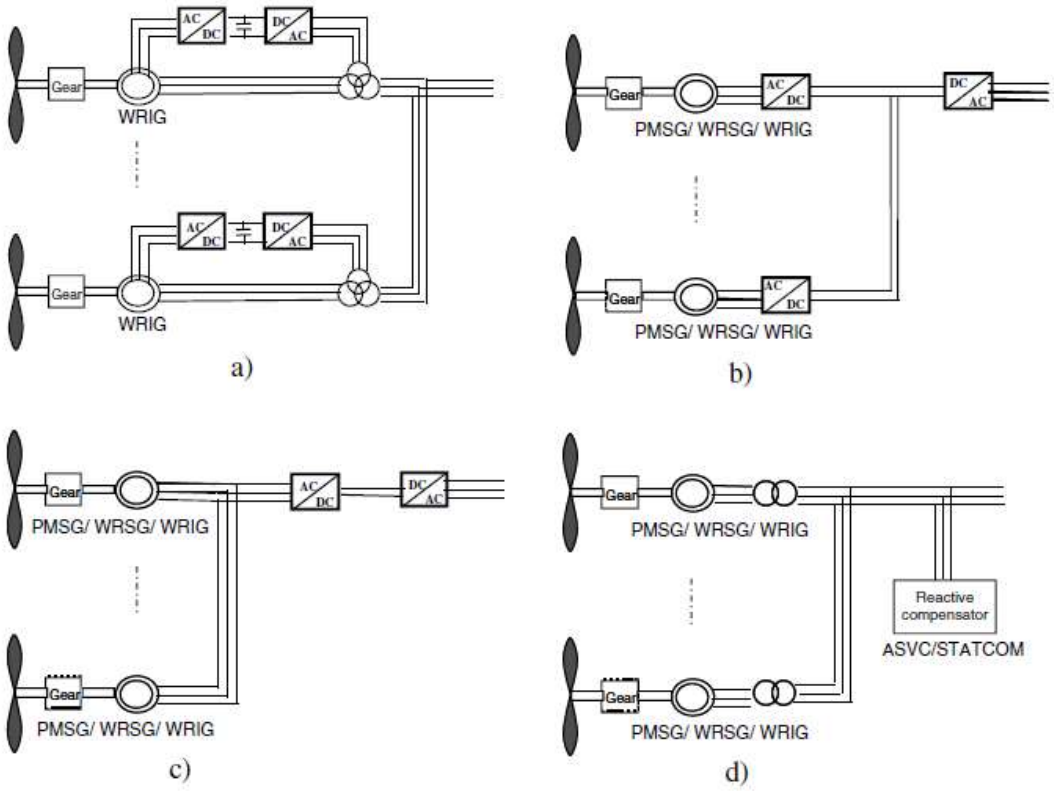

Figure 55: **Wind farms grid connection configurations.**
Source: Ackermann, wind power in power syst. p.76.

1.5.3 Electrical comparison

In order to obtain better terms of comparison, it is possible to evaluate costs and efficiencies of different electrical concepts of wind turbines. These data should be considered very carefully, as higher generator costs could bring to significant advantages from control and mechanical point of view, and produce an overall cheaper or economically more convenient investment.

Hau[40] provides data comparison for a reference turbine of 1500 kW, valid for a range of 0.5-3 MW turbines, with a cost analysis which includes the whole electrical apparatus of the turbine. In the efficiency data, transformer losses (1-2%), static reactive power compensation losses (0.8-1%) and harmonic filters losses (around 0.5%) have been excluded. They can be added if necessary.

The maximum efficiencies as mere values are of limited significance in a sector as the wind power, together with the rated power of a turbine.

Electrical efficiencies and approximate cost ratio of electric generator systems of wind turbines in the 0.5 to 3 MW power range

System	Typical speed range	Maximum efficiency	Approx. cost ratio
Induction generator (squirrel-cage rotor)	100 ± 0.5 %	0.965	100 %
Pole-changing two-speed induction generator	100 ± 0.5 % 66 ⅔ ± 0.5 %	0.965 0.945	110 %
Induction generator with oversynchronous cascade	100 + 30 %	0.95	150 %
Double-fed induction generator with inverter (AC-DC-AC)	100 ± 50 %	0.955	160 %
Synchronous generator (electric excitation)	100 ± 0	0.97	110 %
Synchronous generator (permanent magnet excitation)	100 ± 0	0.985	120 %
Synchronous generator with inverter (AC-DC-AC), electric excitation, perm. magnet excitation	100 ± 50 %	 0.945 0.96	 250 % 280 %
Direct-drive synchronous generator with inverter (AC-DC-AC), electric excitation, permanent magnet excitation	100 ± 50 %	 0.93 0.94	 400 - 450 % 300 - 350 %

Figure 56: **Source: Hau, Wind Turbines fund., p.426.**

[40] Hau, Wind Turbines fund., p.426

Regarding the energy yield, it's much more important to have a clear representation of efficiencies on a wide range of power, typical of real-site scenarios and different wind conditions:

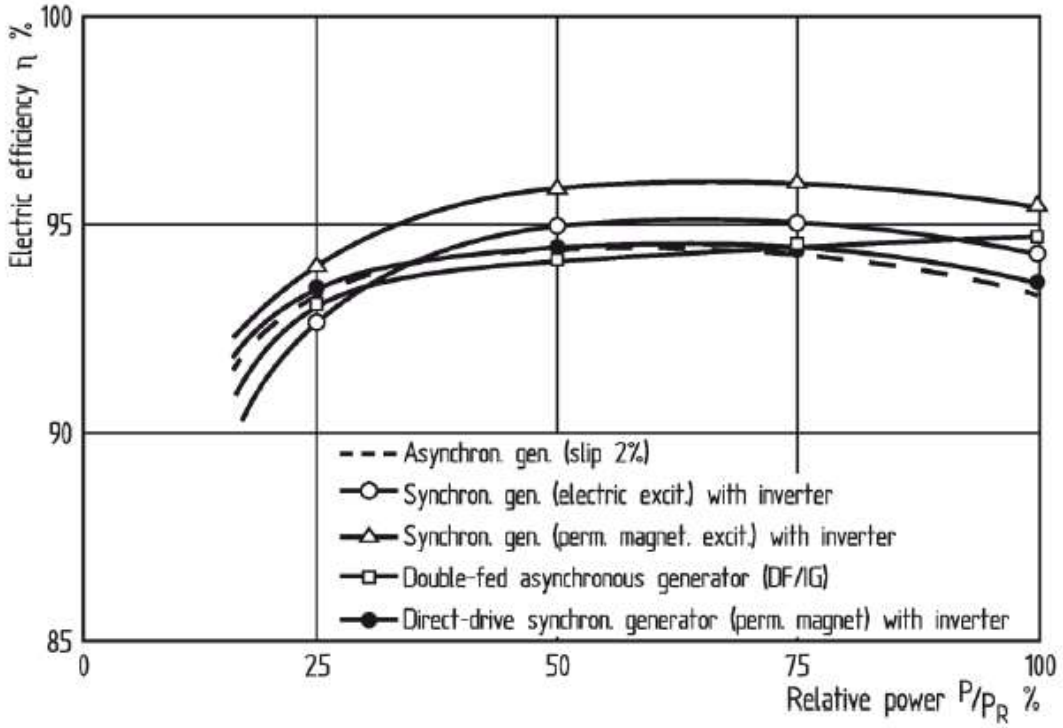

Figure 57: **Efficiency comparison of different generator-inverter systems, in terms of relative power.**
Source: Hau, Wind Turbines fund., p.427.

The PMSG with inverter is the most advantageous situation for every point on the power range, while the DFIG performs very well at rated power but it results in one of the worst efficiencies for powers inferior than 75%. Again, a cost-benefits approach should be used, with particular attention to the *frequency distribution function* of the specific installation site.

Part 2: Mismatch assessment between manufacturer's power curve and on-site measurements during wind turbine operation.

A practical case, with reference to a DFIG-equipped, inland installed wind turbine.

Introduction to part 2

In wind power generators, wind speed is linked to the produced electrical active power through the *power curve*, provided by the turbine manufacturer. Throughout the case, *electrical power* will be used as a synonymous of electrical active power.

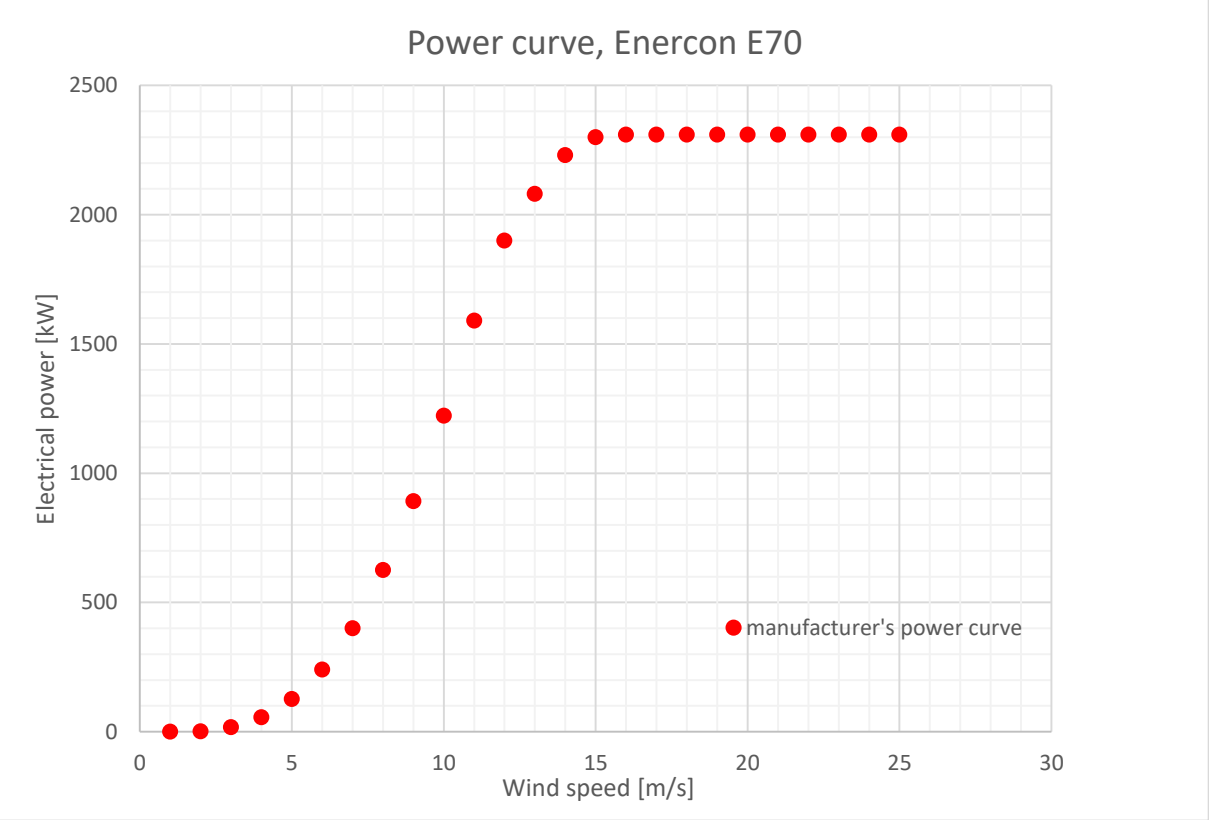

Figure 58 **Power curve, Enercon E70.**

The power curve is obtained by the manufacturer following IEC guidelines.[41] The electrical power is intended to be a net power, the total electrical power produced by the turbine, minus its internal electrical power utilization. The transformer is not included into the power balance.

The power curve represents the result of an experimental site test, conducted under the standard atmospheric conditions, at MSL (ρair=1.225 kg/m^3; Tair=15°C)[42]. Consequently, very often the curve is presented in form of points, which should be considered as the result of a standardized site test in defined conditions, thus affected by a certain degree of uncertainty. Obviously, the wind turbine won't produce the exact power curve results when deployed on a

[41] IEC 63400-12-1
[42] Hau, *Wind Turbines fund., p.561*

different topology site, with different ρair, Tair and turbulence. Part of this case study will be aimed at investigating the different behaviour of the wind turbine, with reference to the power curve, and its possible causes, including ρair variations and turbulence.

In particular, the wind speed considered in the power curve is the one at *turbine hub height*, in front of the turbine, ideally representing the unperturbed wind speed. In fact, it's the same wind speed which would be measured by an anemometer standing straight in front of the hub.

Wind turbines are commonly equipped with anemometric sensors on the back of the nacelle, providing a measure of wind speed and possibly its direction with reference to a section located *behind* the blades.

Evidently, the wind speed measured at the back of the nacelle is not the one referred by the turbine manufacturer in the *power curve*. As the Betz law describes, with reference to the hub front, after passing through the blades the air flow sections slightly expand, and the wind speed decreases, thanks to the extraction of kinetic energy operated by the turbine (which is, ultimately, an energy converter).

There is a general interest in obtaining an estimation of the unperturbed, front hub wind speed, also without the usage of a front hub anemometer. The following case will analyse the mismatch assessment between the manufacturer's power curve and on-site measurements during wind turbine operation.

In the case of turbines equipped with their native rear anemometric sensors, it is possible to obtain a valid estimation of the *front hub* wind, through different correction methods operated on the *back section* wind speed measurements. This mismatch assessment can be operated on full scale wind farms, providing that the correlation is obtained through properly filtered wind data (non-turbulent, front-hub equivalent).

- Ur [m/s] is the average 10 min wind speed measured by the sensor at the *rear section* of the wind turbine, on the back of the nacelle. Pscada=P(Ur) [kW] is the average electrical power measured by the SCADA system, with reference to Ur, in the same 10 min interval.
- Uanem [m/s] is the average wind speed measured by the station anemometer, in a 10 min interval. If Uanem>Ur and turb (Uanem)<0.18 , Uanem can be considered as equivalent to the unperturbed *front hub* wind speed.

In this case, two difference correction methods will be studied:

- A correlation between Uanem and Ur, with reference to the same 10 min time interval. A further correlation, based on the same time interval and on wind directions, can be found.
- A correlation between Ur, P(Ur), and the manufacturer power curve points. For different manufacturer's power curve points, a small power range is defined and, for each power range, an 5% non exceeding Ur wind speed is obtained through statistical methods. A linear correlation between 5% non-exceeding Ur wind speeds and Upc manufacturer's power curve wind speeds is found.

In our case, the experimental data are gathered with a sampling rate of around 1 second, and presented in form of 10 minutes mean values of wind speed and electrical power.

The correlations obtained will be used to address the mismatch between the Ur-P measured points and the manufacturer's power curve:

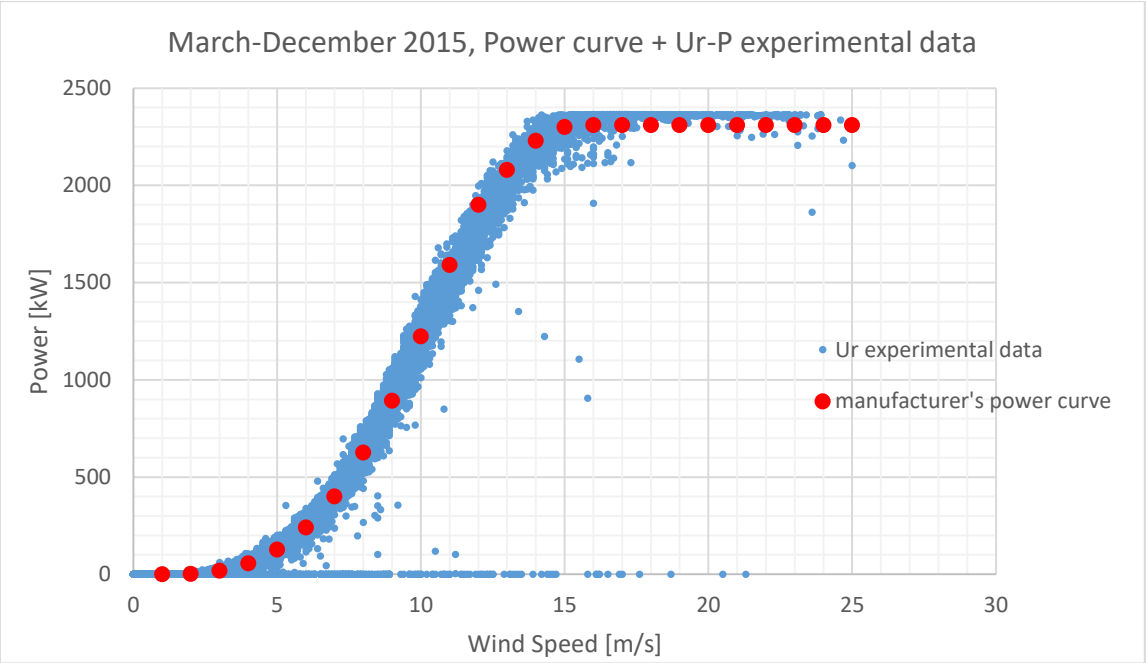

Figure 59*:* **March-December 2015, Power curve + Ur-P experimental data.**

Ideally, the mismatch addressing should produce a corrected result similar to the Uanem-P experimental char, where the actual unperturbed wind speed is plotted against the its related Pscada:

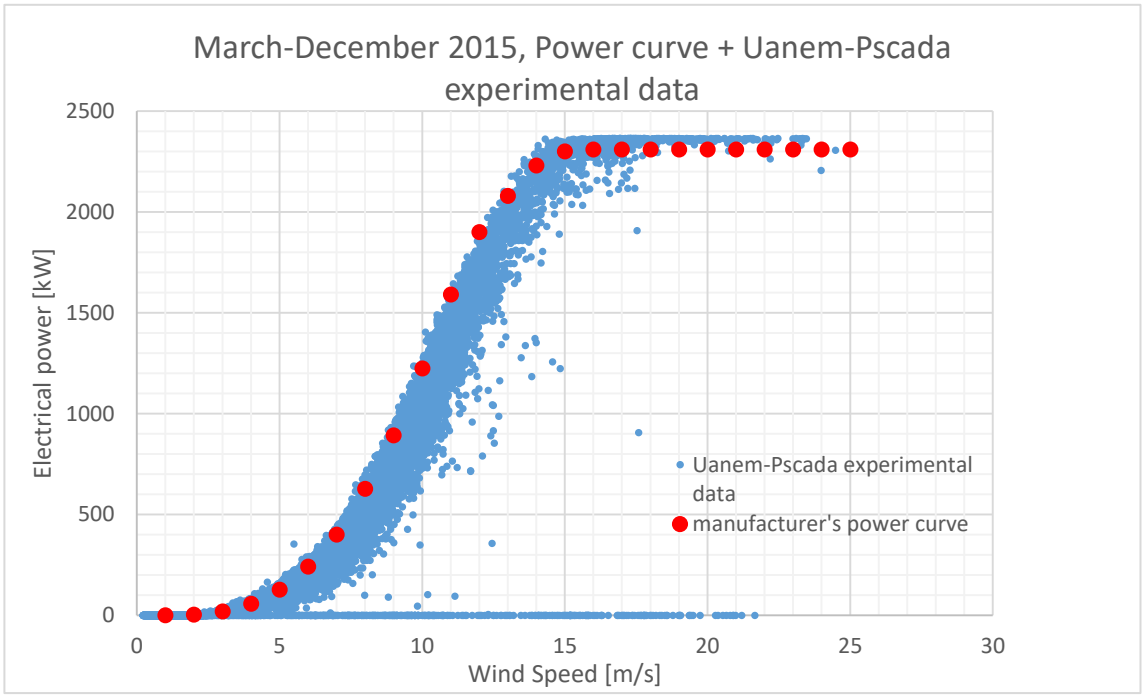

Figura 60**: March-December 2015, Power curve + Uanem-Pscada experimental data.**

On the study case, the primary energy resource, the on-site wind, will be studied and assessed, in terms of directions, frequency, average speed, and turbulence.

Finally, an efficiency experimental study will be produced, and it will be compared with an efficiency estimation obtained through the mismatch corrected wind speed. Both results will be compared with the manufacurer's power coefficient Cp:

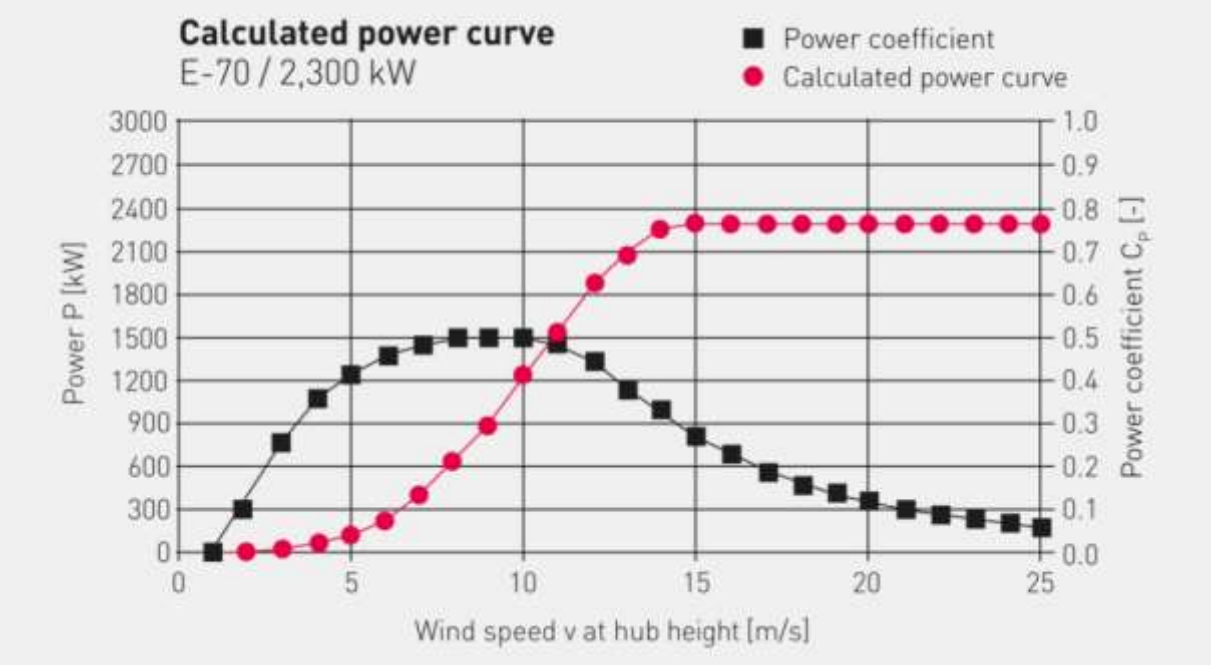

Figure 61: **Enercon E70 power curve and Cp power coefficient.**

Chapter 2.1: On-site measurements

On this study case, measurements are referred to one Enercon E70 wind turbine, 64m hub high, with a 71m rotor diameter and a nominal electrical power of 2300 kW. The turbine is part of a wind farm located on the island of Sardinia, Italy.

The site terrain is flat and rocky, with shrill vegetation, and it is located at an altitude of 779 metres on sea level. The *station anemometer sensors* are equipped on a meteorological tower, 156m distant from the turbine. The *Uanem wind speed sensor* is 64m above the ground, same as the turbine hub, while the *Danem direction sensor* is 62m above the ground. Temperature and pressure sensors are also mounted on the meteorological tower, at a height of 62m above the ground.

The experimental data, from the *Uanem wind speed sensor,* the *Danem wind direction sensor* and the *Ur wind speed sensor* (this one on the back of the turbine) are gathered with a sampling rate of around 1 second, and presented in form of 10 minutes mean values of wind speed and electrical power. Temperature and pressure are also gathered on a i 10 min intervals basis.

In this specific case, the wind direction measurements are only available for the *Danem wind direction sensor*. Regarding Uanem, the standard deviation with reference to the i interval is provided.

Chapter 2.2: Wind characterization

2.2.1 Direction, frequency, average speed

Given a certain period of time (in our study case April 2015, and the period March-December 2015), categorizing the *Danem* measurements into 16 directions ranges, it's possible to obtain the relative frequency and the absolute frequency of wind directions for the period.

Data can be summarized into a *wind chart*, and showed together with the *average* Uanem for each direction, in order to find the *main wind direction* for the defined time period.

The *Danem wind direction sensor* provides data in degrees, where the north direction (N) is defined as "0", and a clockwise convention is used.

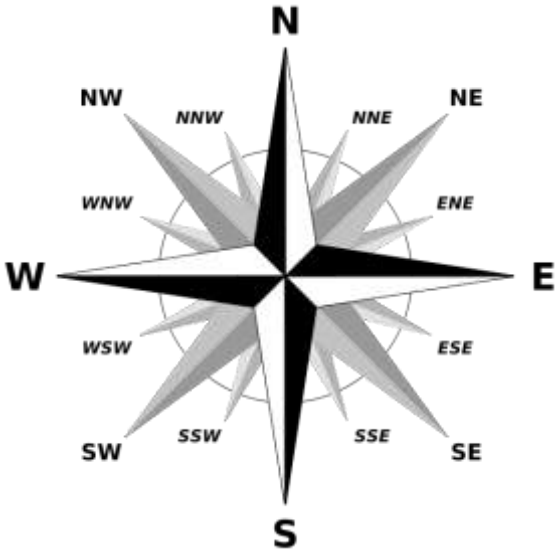

Figure 62: **A 16-points compass rose.**
Source:
https://en.wikipedia.org/wiki/Compass_rose#/media/File:Brosen_windrose.svg
consulted on 21/05/2017.

April, 2015						
wind, directions	16	range, degrees	22,5	Fabs(Danem)	Frel(Danem)	**Uanem,avg [m/s]**
	N	348,75	11,25	69	1,6%	3,06
	NNE	11,25	33,75	175	4,1%	5,81
	NE	33,75	56,25	325	7,5%	5,27
	ENE	56,25	78,75	208	4,8%	2,98
	E	78,75	101,25	147	3,4%	3,21
	ESE	101,25	123,75	172	4,0%	4,03
	SE	123,75	146,25	253	5,9%	4,77
	SSE	146,25	168,75	247	5,7%	5,65
	S	168,75	191,25	187	4,3%	3,90
	SSW	191,25	213,75	179	4,1%	3,31
	SW	213,75	236,25	105	2,4%	2,28
	WSW	236,25	258,75	208	4,8%	4,36
	W	258,75	281,25	338	7,8%	5,54
	WNW	281,25	303,75	957	22,2%	8,99
	NW	303,75	326,25	543	12,6%	7,04
	NNW	326,25	348,75	207	4,8%	3,91
n° of measurements			sum	4320	100%	
4320						

Table 1: **Frequency and wind speed direction assessment April 2015.**

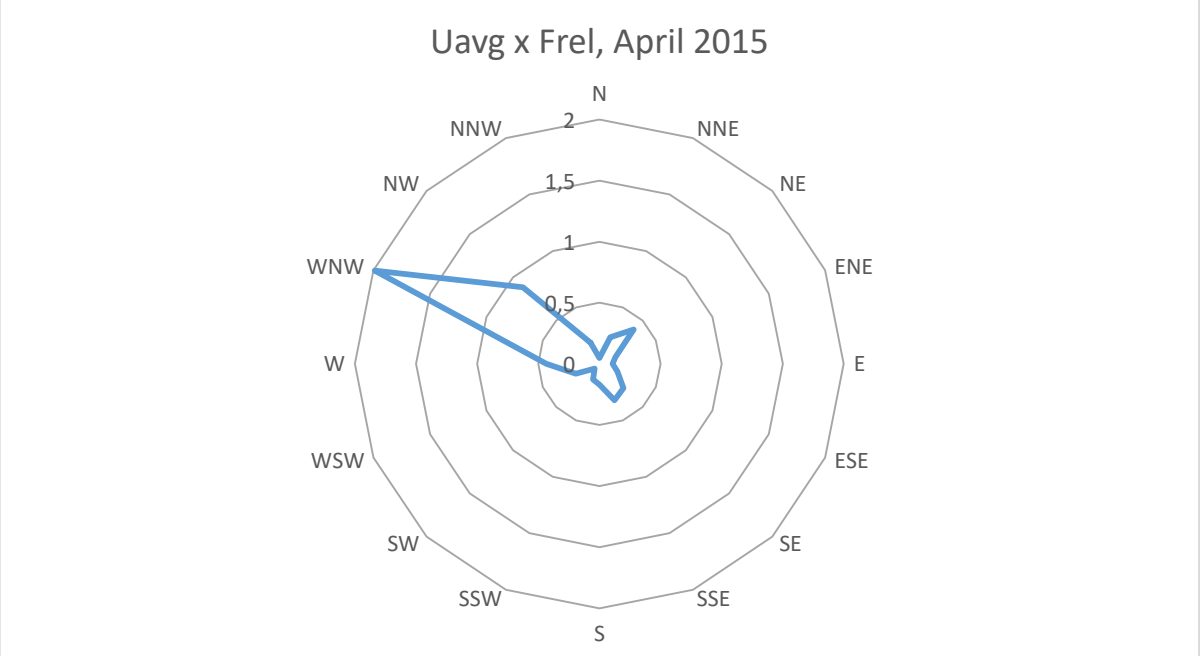

Figure 63: **Main direction chart, April 2015.**

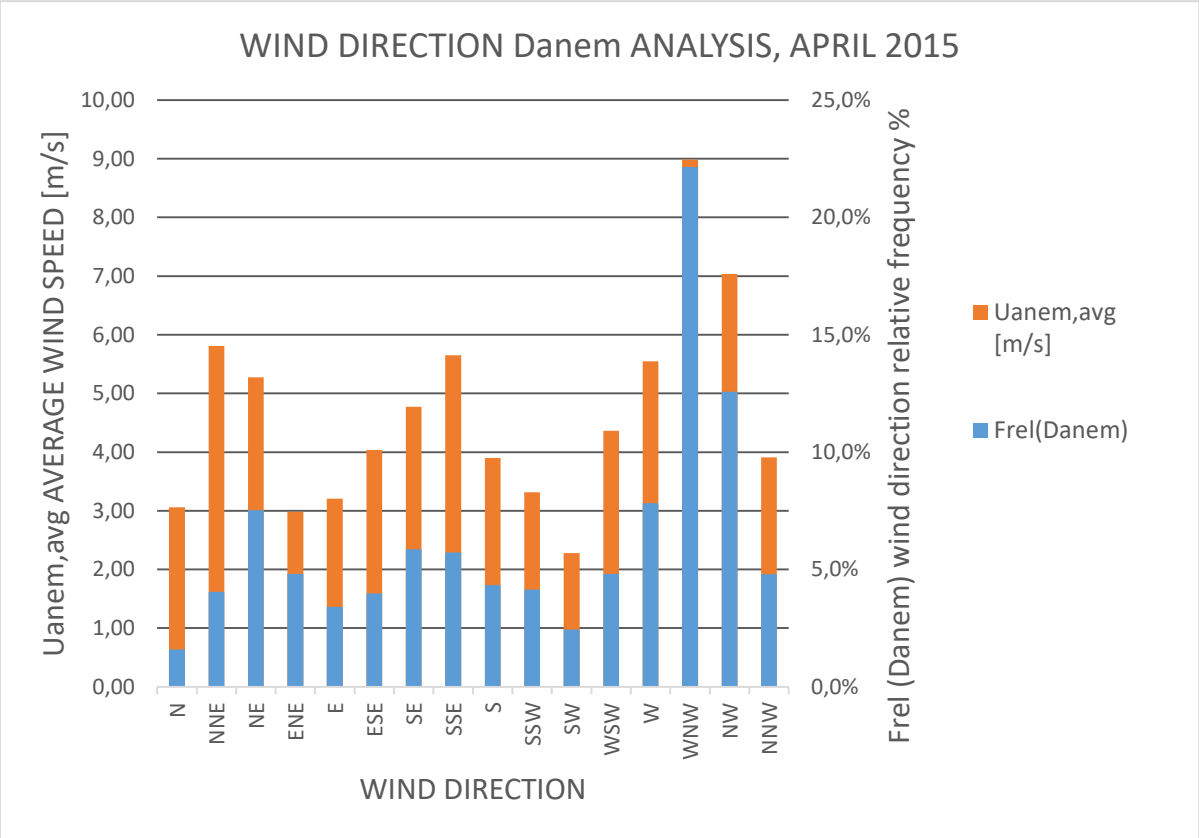

Figure 64: **Wind direction Danem Analysis, April 2015.**

For April 2015, data clearly shows how the WNW direction is the main direction, both in terms of frequency and average front hub wind speed.

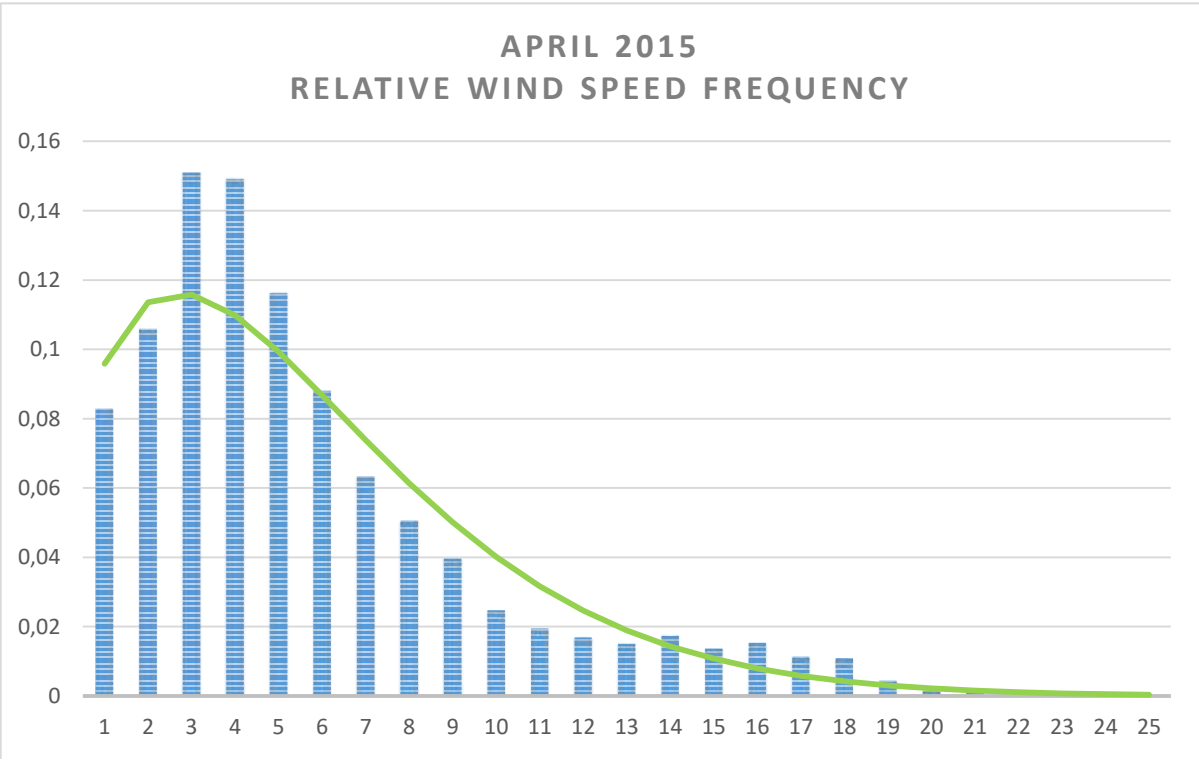

Figure 65: **Relative wind speed frequency, April 2015.**

March-December 2015						
wind, directions	16	range, degrees	22,5	Fabs(Danem)	Frel(Danem)	**Uanem,avg [m/s]**
	N	348,75	11,25	958	2,2%	3,92
	NNE	11,25	33,75	1525	3,5%	6,34
	NE	33,75	56,25	2279	5,2%	5,26
	ENE	56,25	78,75	2007	4,6%	3,20
	E	78,75	101,25	1513	3,4%	4,12
	ESE	101,25	123,75	1838	4,2%	5,58
	SE	123,75	146,25	3137	7,1%	6,98
	SSE	146,25	168,75	2271	5,2%	6,54
	S	168,75	191,25	1303	3,0%	3,70
	SSW	191,25	213,75	1373	3,1%	3,13
	SW	213,75	236,25	1351	3,1%	2,94
	WSW	236,25	258,75	2495	5,7%	4,79
	W	258,75	281,25	4956	11,2%	5,57
	WNW	281,25	303,75	8907	20,2%	7,24
	NW	303,75	326,25	6073	13,8%	6,28
	NNW	326,25	348,75	2078	4,7%	3,73
n° of measurements			sum	44064	100%	
44064						

Table 2: **Frequency and wind speed direction assessment March-December 2015.**

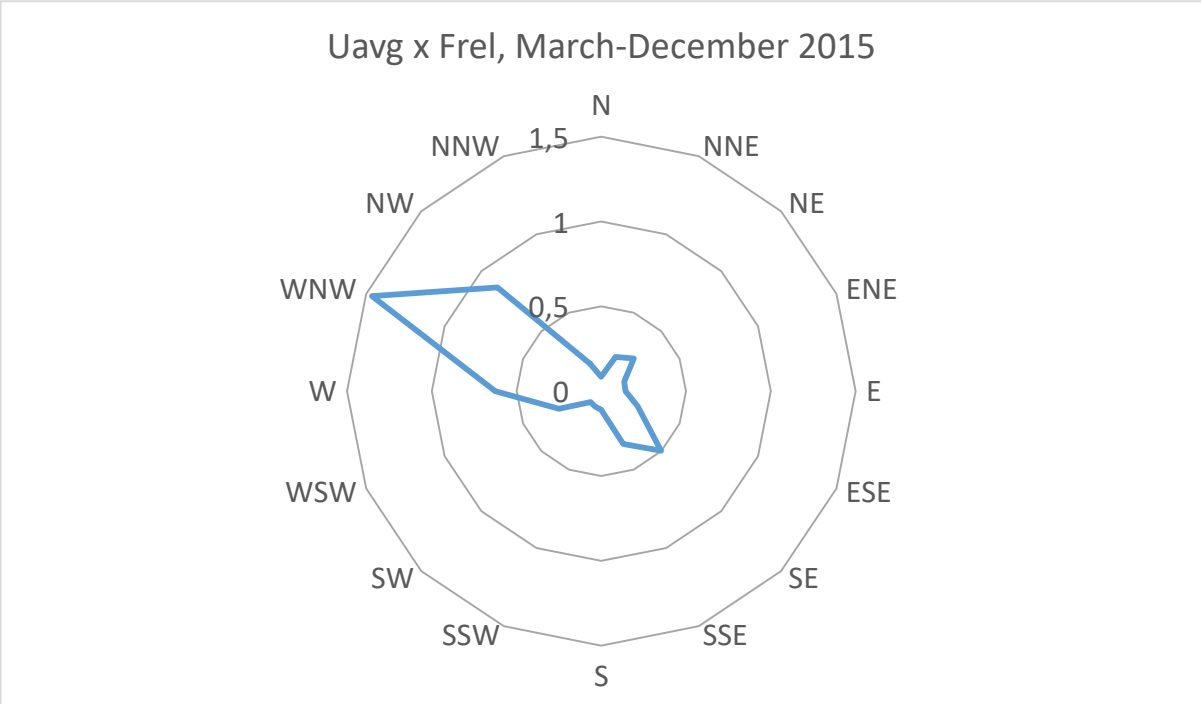

Figure 66: **Main direction chart, March-December 2015.**

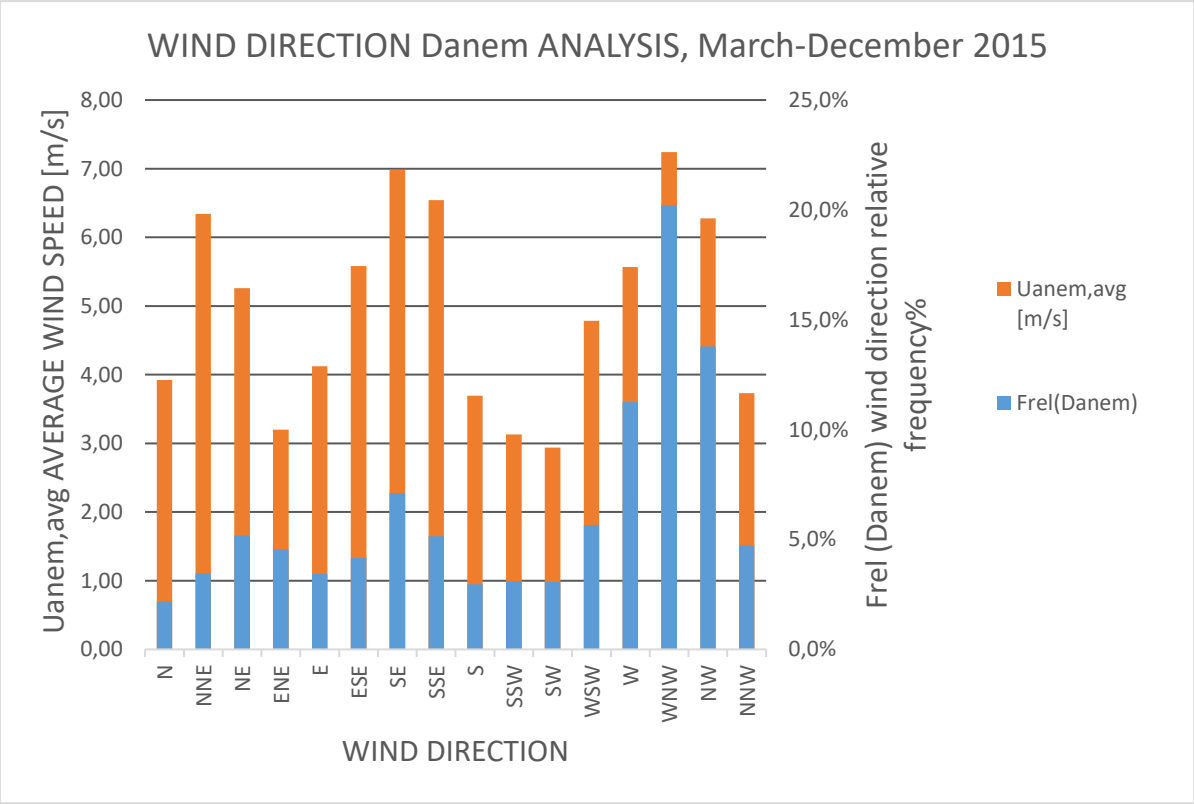

Figure 67: **Wind direction Danem Analysis, March-December 2015**

For March-December 2015, data clearly shows how the WNW direction is the main direction, both in terms of frequency and average front hub wind speed.

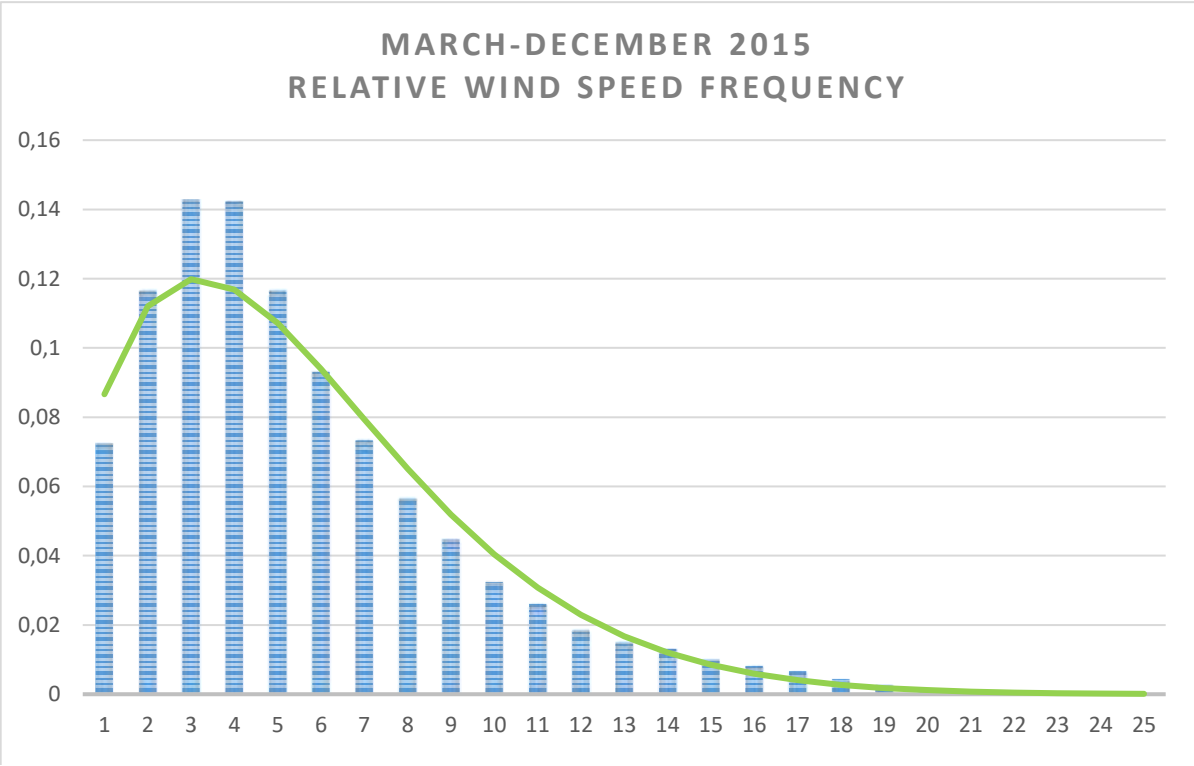

Figure 68: **Relative wind speed frequency, March-December 2015.**

2.2.2 Turbulence assessment

In order to obtain a valid correlation between Uanem and Ur wind speeds, it is necessary to discriminate turbulent and non-turbulent wind measurements.

Regarding Uanem, for each $Uanem_i$ measurement, wind turbulence $It(Uanem_i)$ is defined as:

$$It(Uanem_i) = \frac{\sigma(Uanem_i)}{Uanem_i}$$

Where $\sigma(Uanem_i)$ is the standard deviation of the $Uanem_i$ *station anemometer wind speed* measurement, based on the 10-min i interval.

As example, part of the excel worksheet is presented, regarding April 2015, and March-December 2015.

The turbulence limit chosen for the study case is 0,18. All the measurements exceeding a turbulence of 0,18 are automatically discarded.

April, 2015		
total measurements	4320	
non-turbulent meas	2728	63,15%

		APRIL, 2015			max turbulence index allowed			
RECORD	station anemometer				0,18			
RN								
	Uanem [m/s]	**σ (Uanem)**		**It(Uanem)**	**It (Uanem) <0,18**		**valid Uanem [m/s]**	**It <0,18 TRUE(1) FALSE(0)**
6955	14,14	1,644		0,1163	0,116265912		14	1
6956	14,86	1,437		0,0967	0,0967		14,86	1
6957	13,92	1,488		0,1069	0,1069		13,92	1
6958	12,92	1,751		0,1355	0,1355		12,92	1
6959	12,74	1,75		0,1374	0,1374		12,74	1
6960	10,92	1,652		0,1513	0,1513		10,92	1
6961	14,68	3,329		0,2268	0,0000		0,00	0
6962	21,99	2,758		0,1254	0,1254		21,99	1
6963	23,3	2,314		0,0993	0,0993		23,30	1
6964	22,89	2,378		0,1039	0,1039		22,89	1
6965	20,92	2,095		0,1001	0,1001		20,92	1
6966	20,21	1,854		0,0917	0,0917		20,21	1
6967	20,69	1,901		0,0919	0,0919		20,69	1

Table 3: **Turbulence assessment April 2015.**

March-December, 2015		
total measurements	44064	
non-turbulent meas	29437	66,81%

		MARCH-DECEMBER, 2015		max turbulence index allowed		
RECORD	station anemometer			0,18		
RN						
	Uanem [m/s]	**σ (Uanem)**	**It (Uanem)**	**It (Uanem) <0,18**	**valid Uanem [m/s]**	**It <0,18 TRUE(1) FALSE(0)**
2497	0,855	0,147	0,1719	0,171929825	0,855	1
2498	0,35	0,14	0,4000	0	0	0
2499	0,715	0,159	0,2224	0	0	0
2500	0,783	0,061	0,0779	0,077905492	0,783	1
2501	1,336	0,334	0,2500	0	0	0
2502	1,588	0,34	0,2141	0	0	0
2503	1,491	0,144	0,0966	0,096579477	1,491	1
2504	1,127	0,151	0,1340	0,133984028	1,127	1
2505	1,09	0,209	0,1917	0	0	0
2506	1,801	0,199	0,1105	0,11049417	1,801	1
2507	2,002	0,232	0,1159	0,115884116	2,002	1
2508	2,166	0,124	0,0572	0,057248384	2,166	1
2509	1,867	0,114	0,0611	0,061060525	1,867	1
2510	2,2	0,14	0,0636	0,063636364	2,2	1
2511	2,045	0,105	0,0513	0,051344743	2,045	1
2512	1,995	0,116	0,0581	0,058145363	1,995	1

Table 4: **Turbulence assessment March-December 2015.**

Chapter 2.3: Turbine rear wind speed-Pscada power curves: the mismatch.

Producing the Ur-Pscada chart, plotted together with the manufacturer's power curve, permits to underline the experimental data mismatch with reference to that curve. The mismatch is produced by the fact that the Ur is measured on the back of the turbine, after the *kinetic energy extraction* by the wind converter. The aim of the procedure is to correct the Ur, in order to obtain an estimation of the unperturbed front hub wind speed, and produce a power curve and an efficiency assessment referred to the primary energy source (the actual wind present on the site).

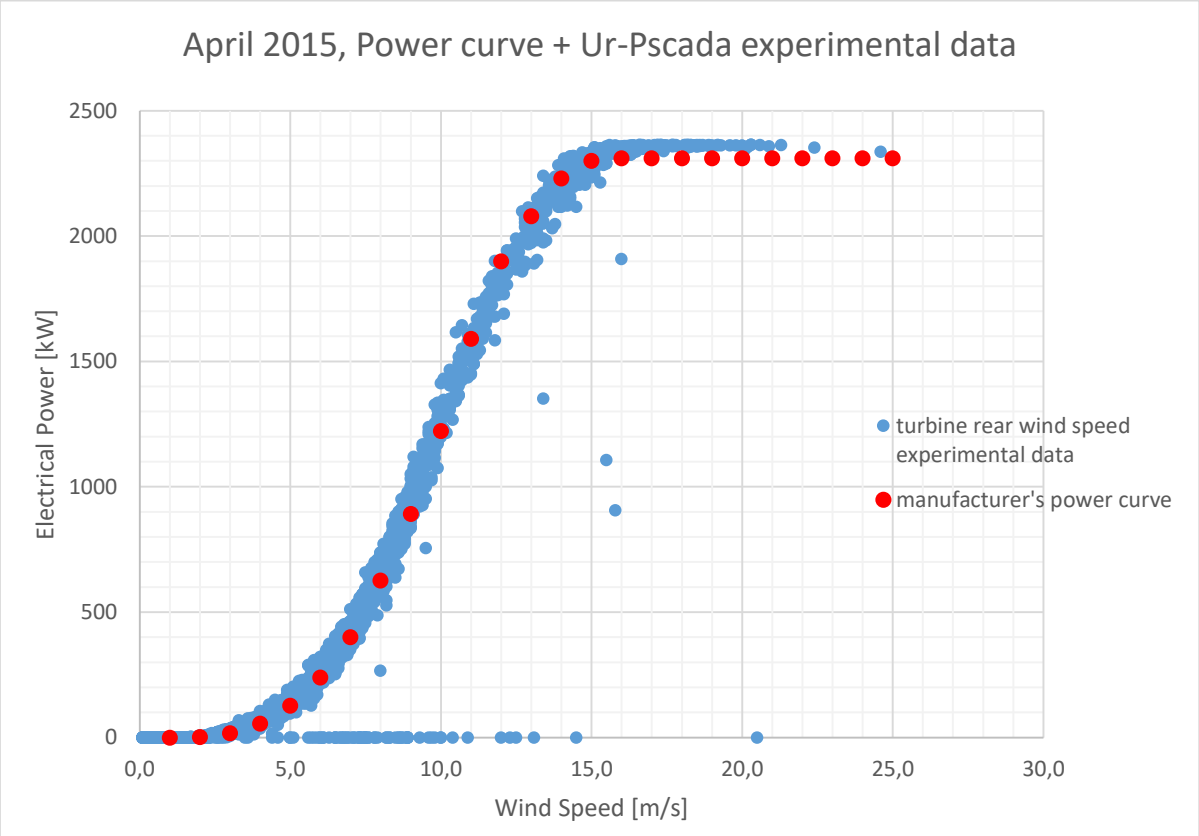

Figure 69: **Power curve + Ur-Pscada experimental data, April 2015.**

Both the April and the March-December charts show too favourable Ur-P points, in terms of power production, with comparison to the manufacturer's power curve. Using these non-addressed data as an actual power curve would produce wrong energy yield estimations, and wrong efficiency estimations. The Ur value is lower than its associated front hub wind speed: the wind has been slowed down flowing through the wind turbine, yielding part of its kinetic energy, according to the Betz law principles.

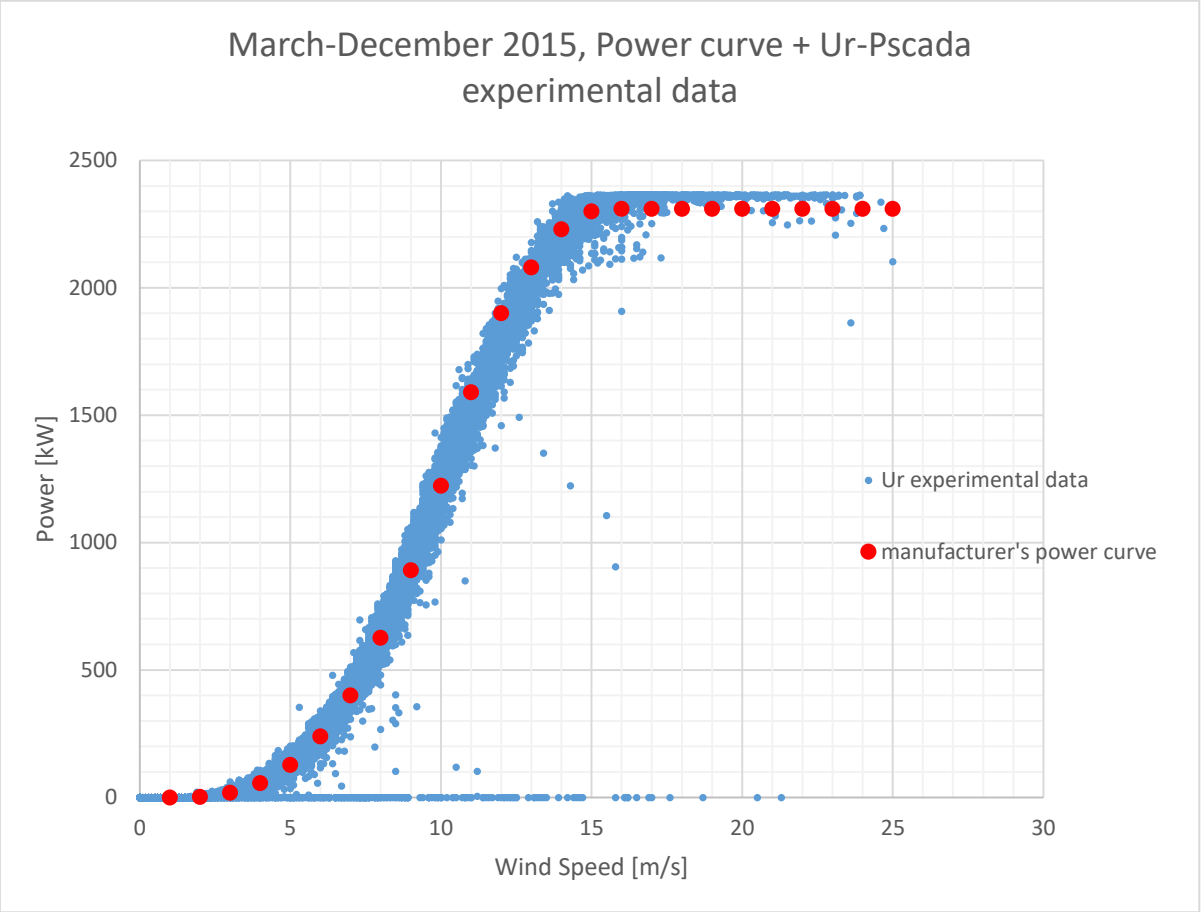

Figure 70: **Power curve + Ur-Pscada experimental data, March-December 2015.**

Chapter 2.4: Experimental power curves Front hub wind speed-Pscada; turbulence and air density assessment

2.4.1 General assessment

For each 10 min i interval, it's possible to plot Uanem wind speeds, and their associated P electrical active power. P is presented as Pscada, electrical power measured by the SCADA measurement system. The resulting power curve associates the *front hub wind speed,*with the produced electrical power. In order to obtain that, only the points respecting the following condition are considered:

- Uanem>Ur

Data are furtherly discriminated on the basis of 3 turbulence intervals, and on air density.

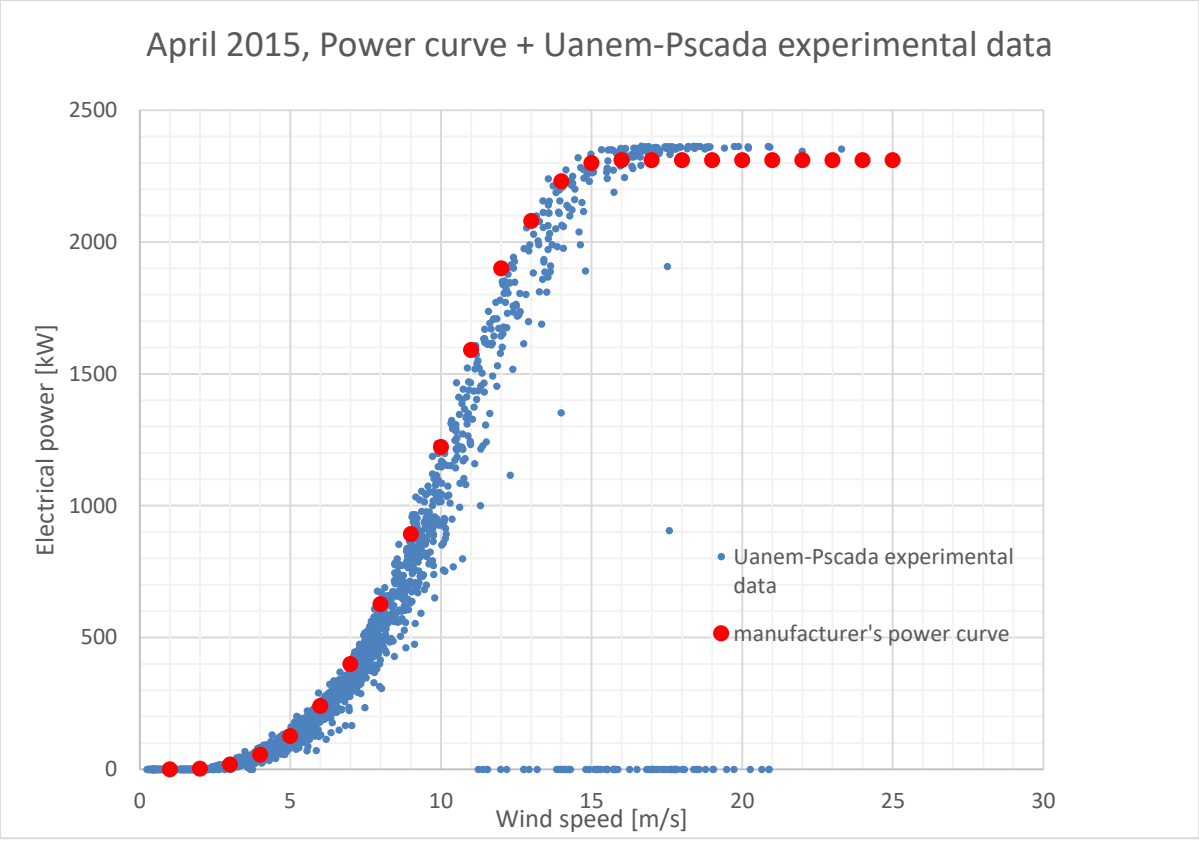

Figure 71: **Power curve + Uanem-Pscada experimental data, April 2015.**

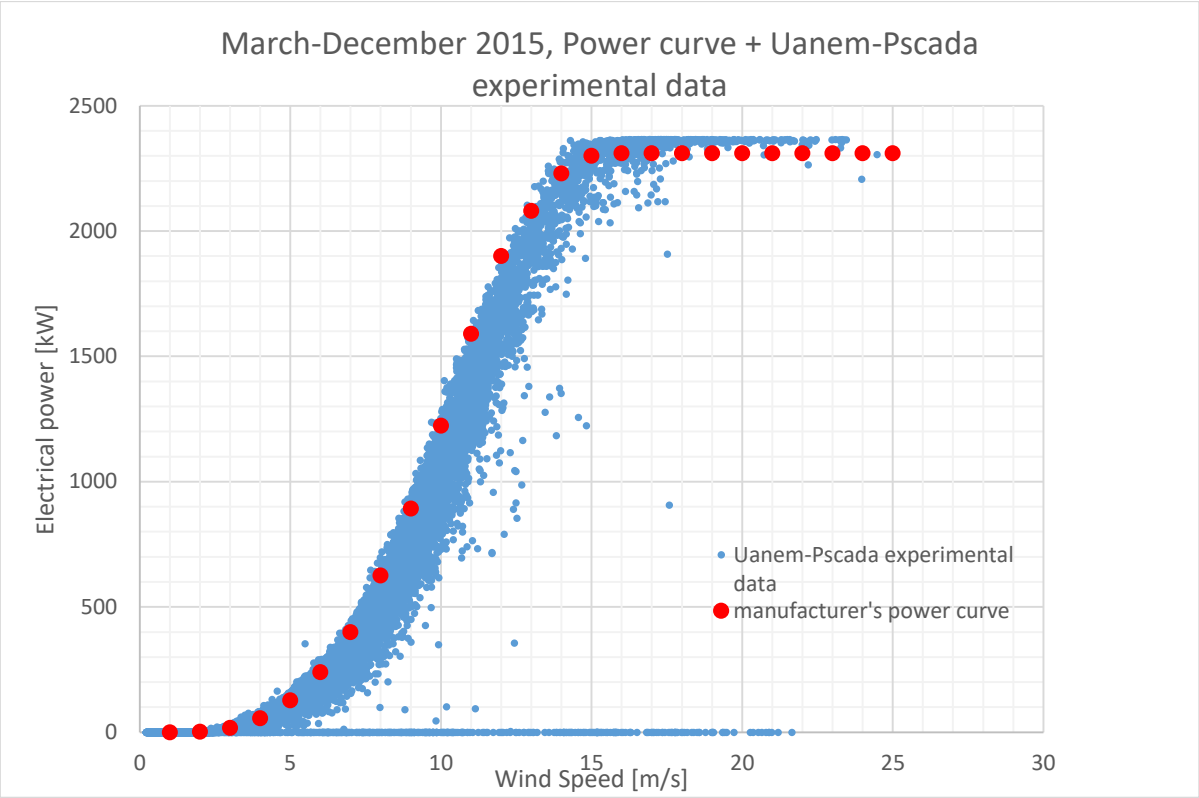

Figure 72: **Power curve + Uanem-Pscada experimental data, March-December 2015.**

2.4.2 Turbulence assessment

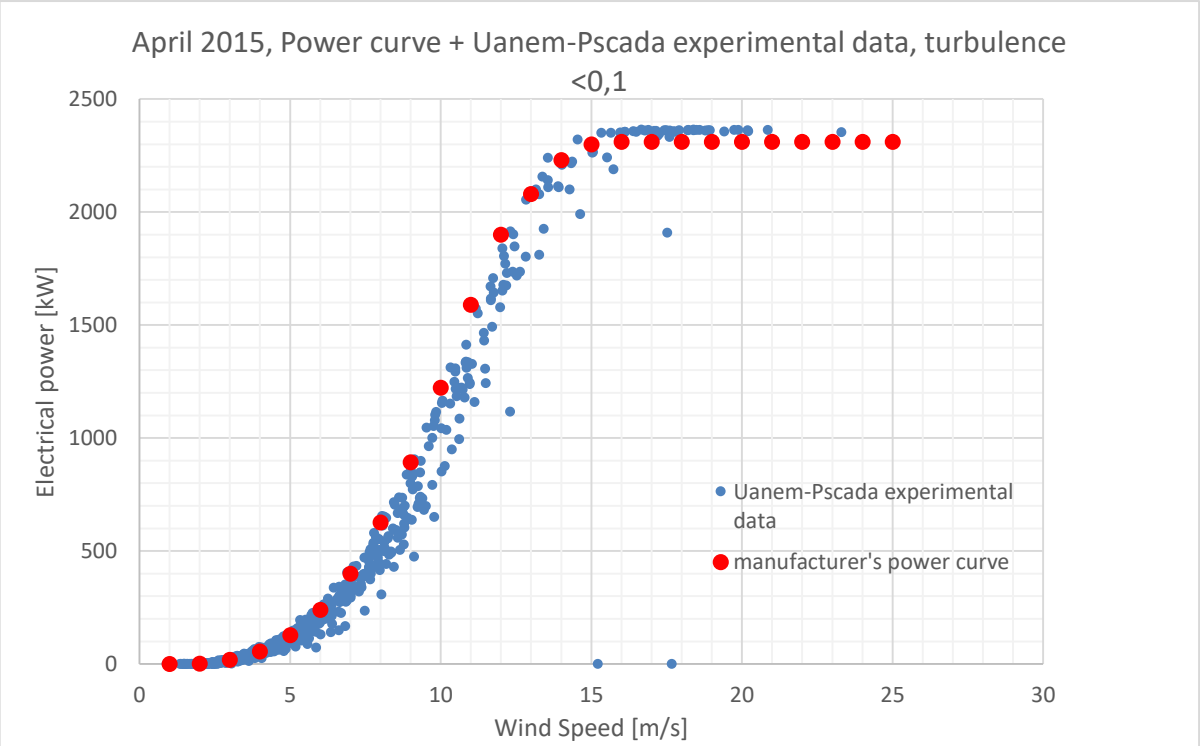

Figure 73: **Power curve + Uanem-Pscada experimental data, turbulence <0.1, April 2015.**

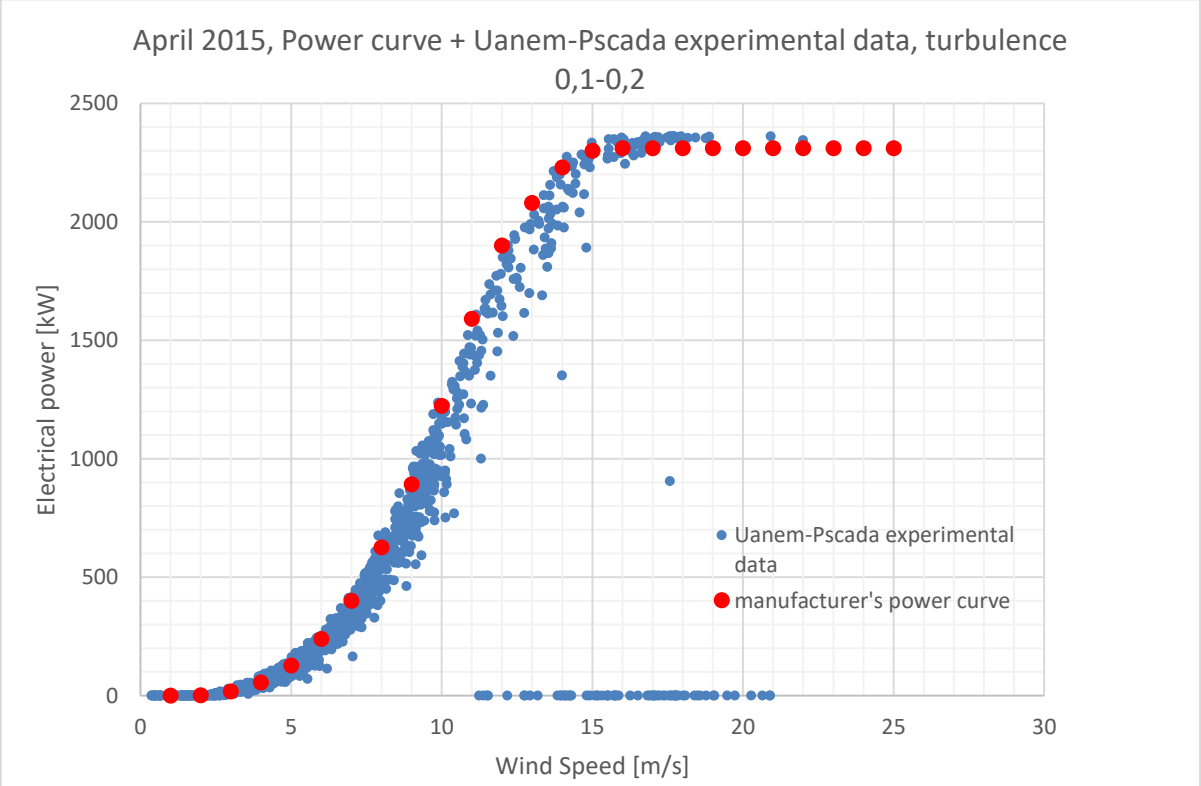

Figure 74: **Power curve + Uanem-Pscada experimental data, turbulence 0.1-0.2, April 2015.**

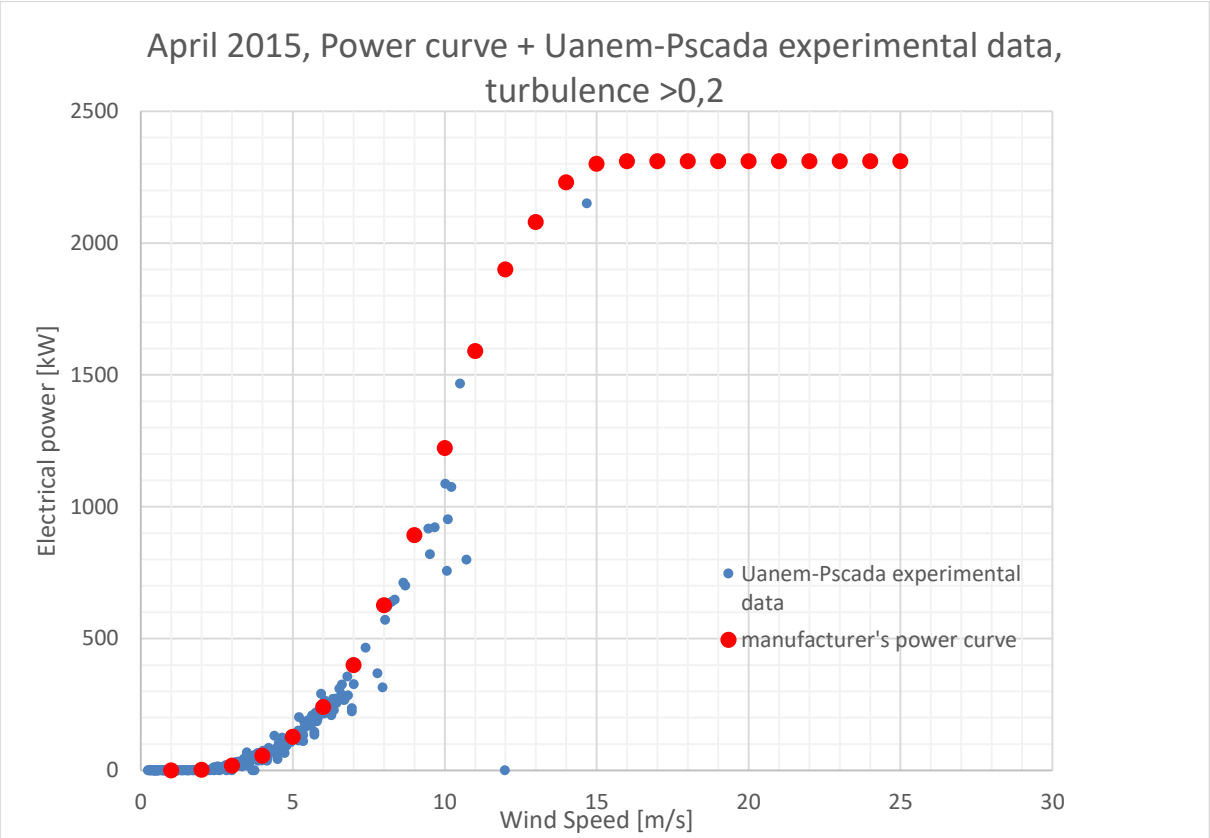

Figure 75: **Power curve + Uanem-Pscada experimental data, turbulence >0.2, April 2015.**

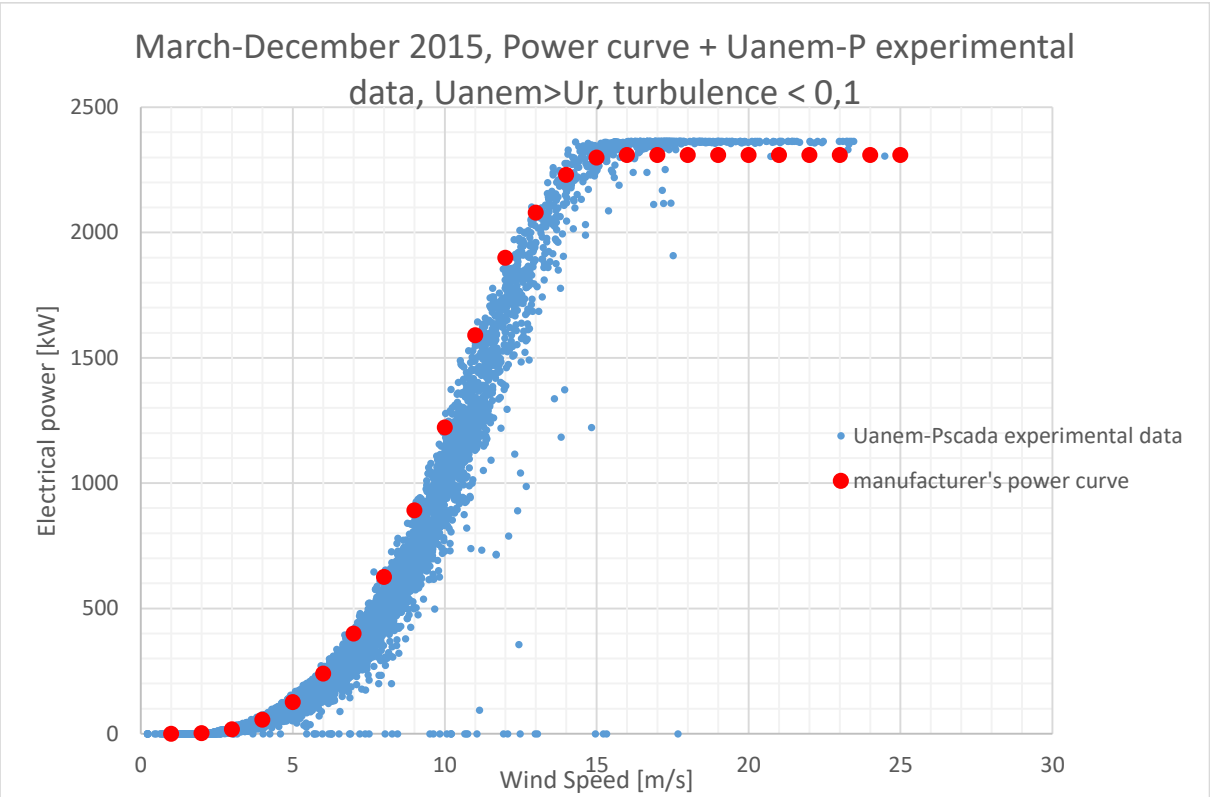

Figure 76: **Power curve + Uanem-Pscada experimental data, Uanem>Ur, turbulence <0.1, March-December 2015.**

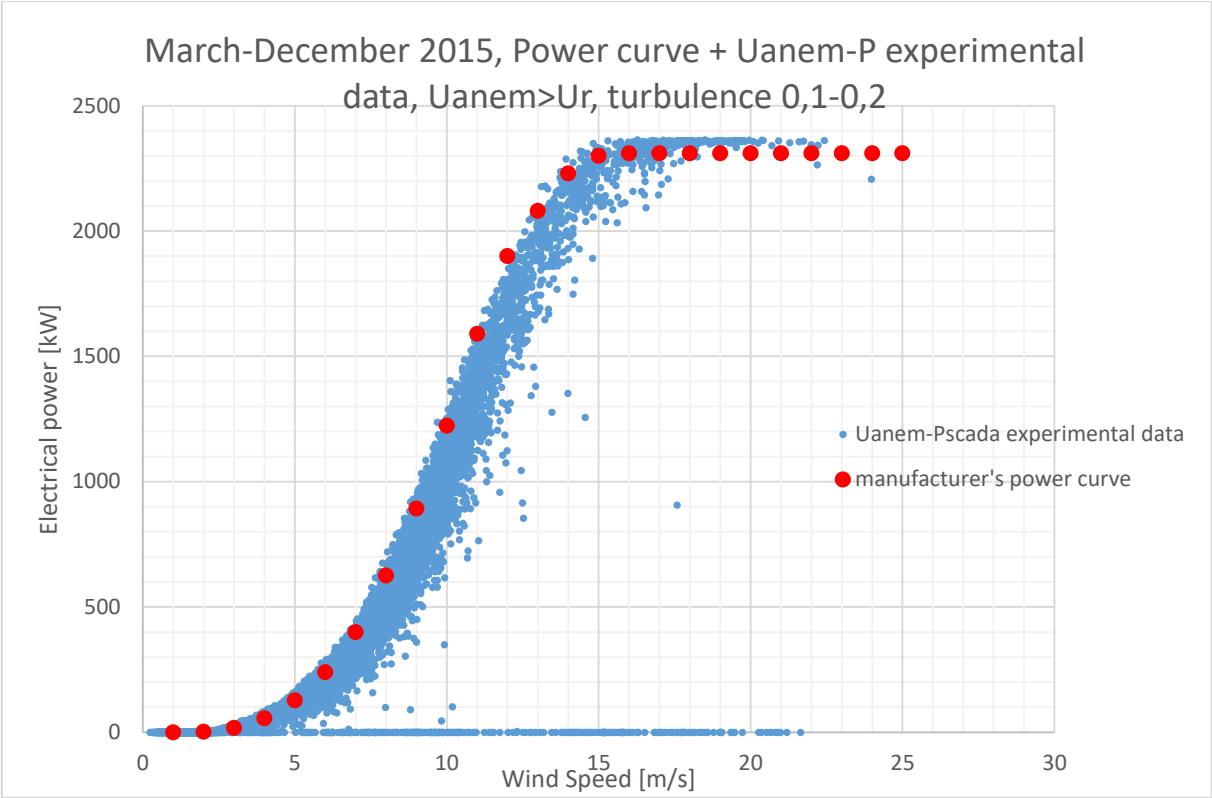

Figure 77: **Power curve + Uanem-Pscada experimental data, Uanem>Ur, turbulence 0.1-0.2, March-December 2015.**

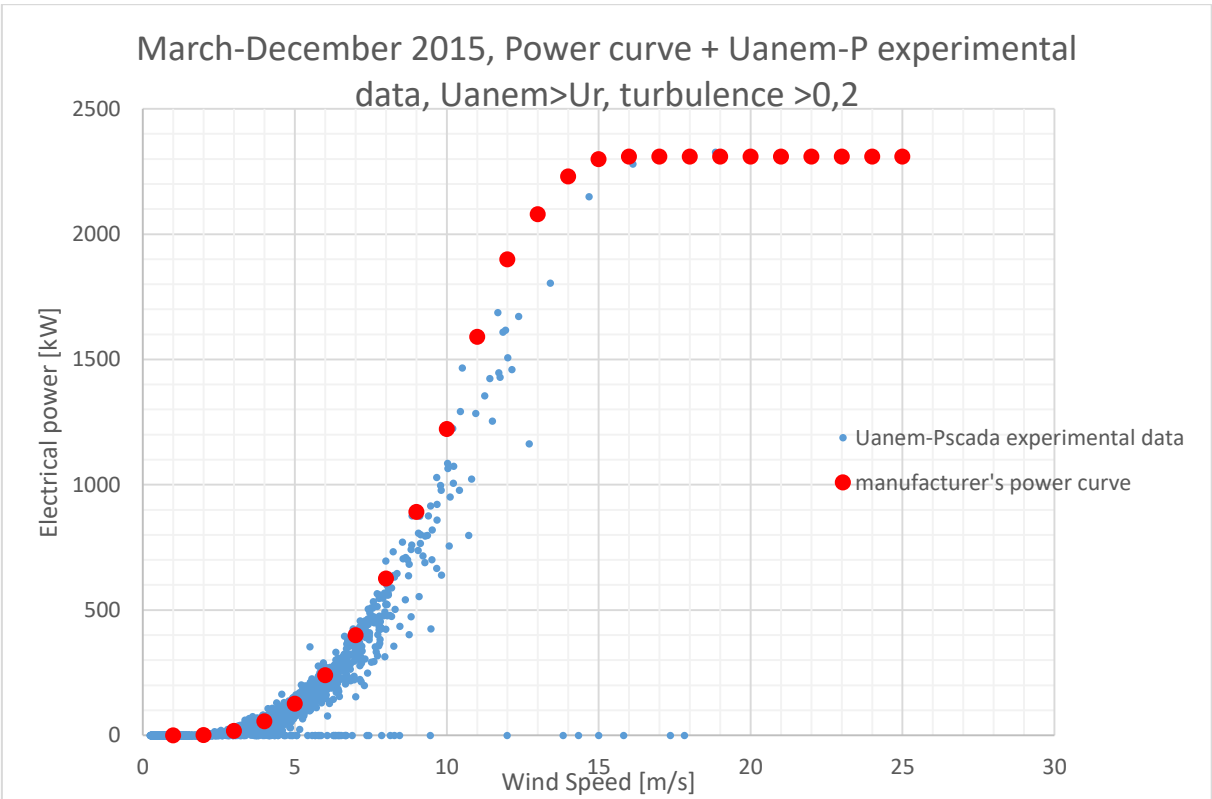

Figure 78: **Power curve + Uanem-Pscada experimental data, Uanem>Ur, turbulence >0.2, March-December 2015.**

The most straightforward conclusion regarding these curves is that, in both April and March-December cases, points characterized by turbulence>0.2 are concentrated on a low-medium wind speed range. Under 4 m/s and under 80-100 kW, the measurement system errors are predominant, thus part of these data should not be considered totally reliable.

Moreover, above wind speeds of 14 m/s, a higher electrical power, with reference to the manufacturer's curve power, can be noticed. The deviation is inside the range of 80 kW, and it's possible to speculate it's due to the measurement system altogether. This particular aspect will be furtherly analysed in the conclusions chapter.

Noticeably, the majority of the experimental points are translated to the left, with comparison to the manufacturer's curve. Given that the manufacturer's curve is calculated in more favourable conditions, standard conditions (sea level, 1013,15 hPa, 15 °C), more aspects can have an influence, in terms of this electrical power reduction, with reference to a particular wind speed.

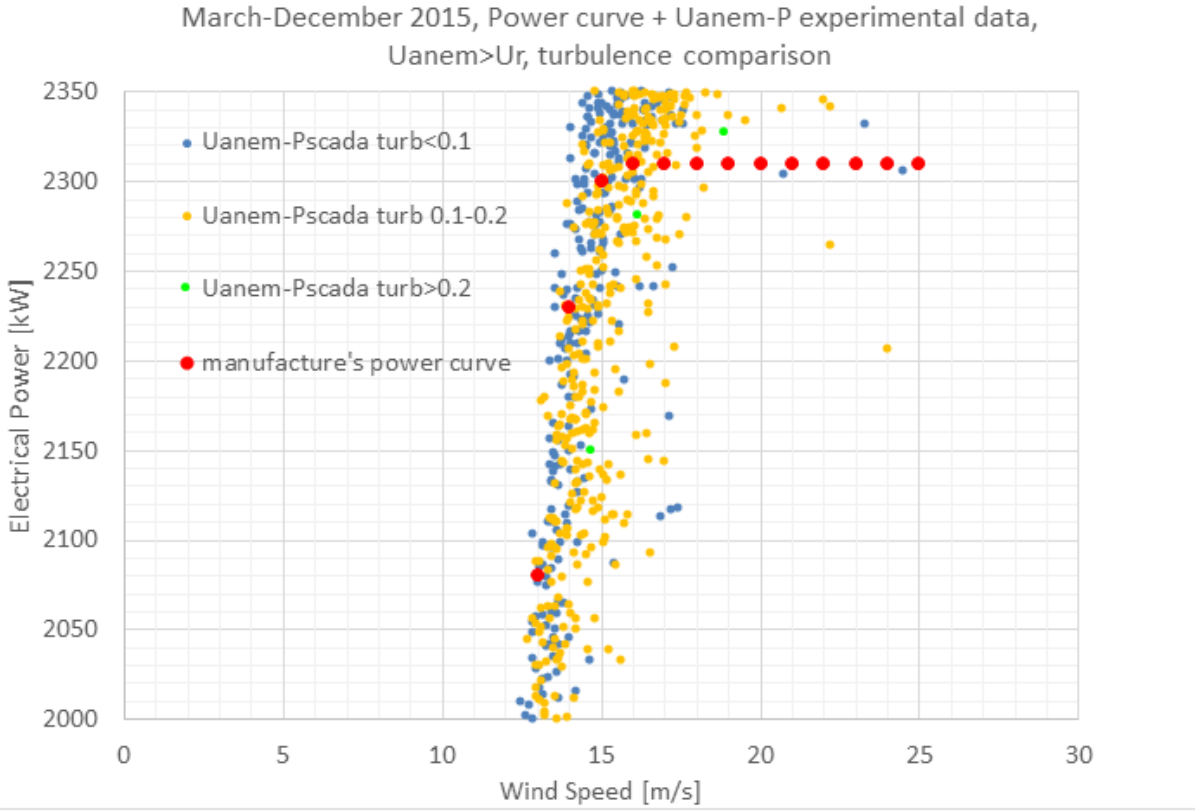

Figure 79: **Power curve + Uanem-Pscada experimental data, Uanem>Ur, turbulence comparison, March-December 2015.**

It can be noticed how points with turbulence between 0.1-0.2 produces the bigger deviation with comparison to the manufacturer's power curve at medium-high wind speeds.

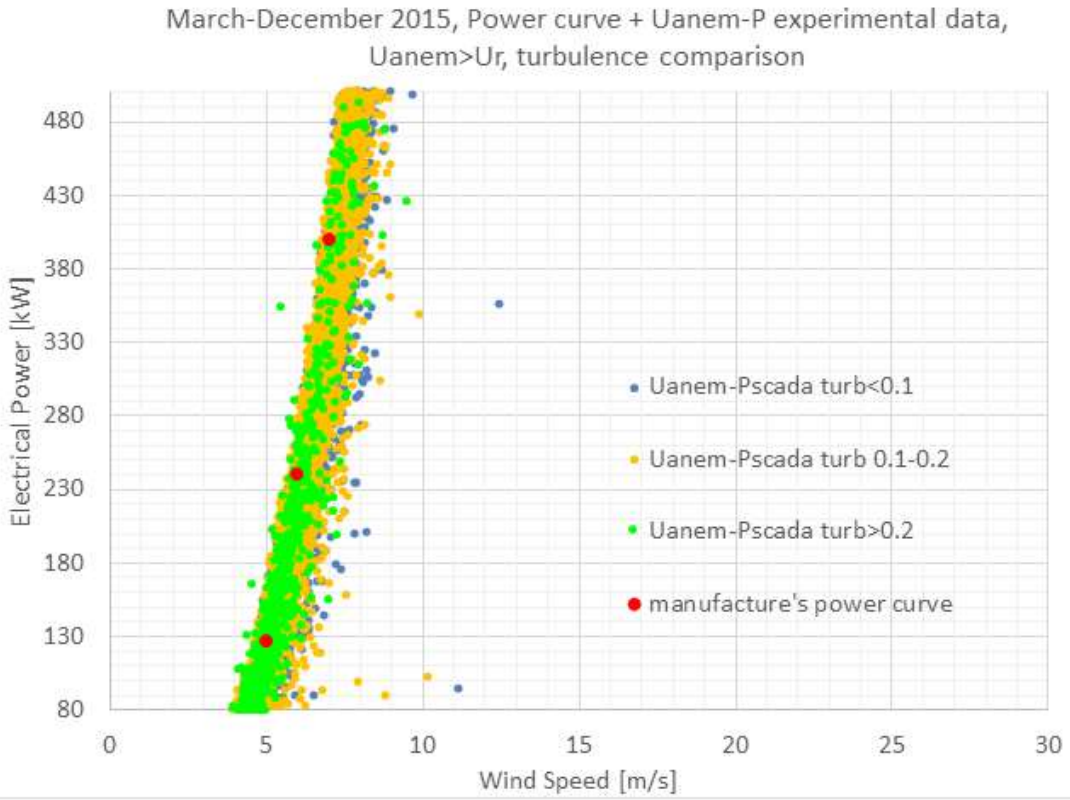

Figure 80: **Power curve + Uanem-Pscada experimental data, Uanem>Ur, turbulence comparison, March-December 2015.**

On the other hand, turbulent data (turbulence >0.2) tends to be concentrated around wind speeds of 5 m/s. However, they don't produce significantly oriented power deviations, with comparison to the manufacturer's power curve and to less turbulent points.

2.4.3 Air density assessment

It is possible to produce a Uanem-Pscada chart with reference to air density. The longer period, March-December 2015, has been taken into consideration, in order to get sufficient points and to reduce as much as possible the influence of specific monthly conditions on the results. The minimum obtained air density is on the order of 1.06 [kg/m^3]. The max obtained air density is on the order of 1.20 [kg/m^3]

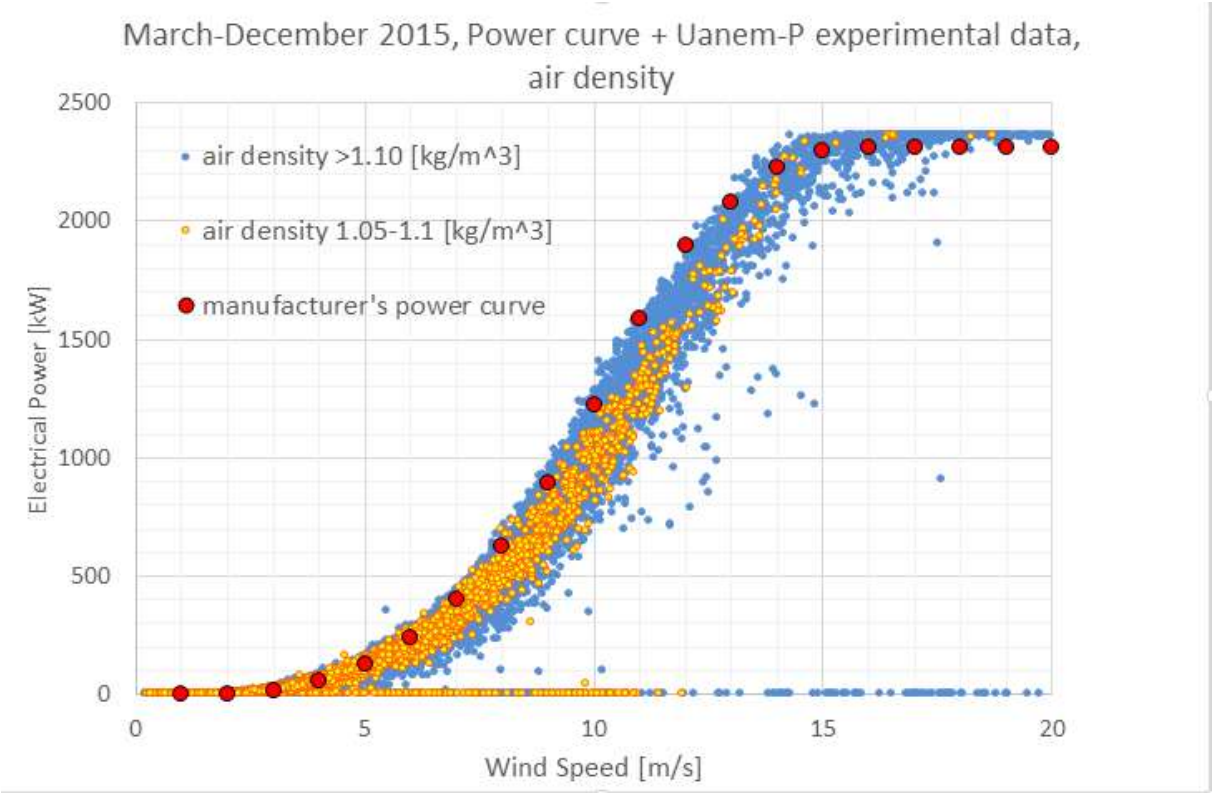

Figure 81: **Power curve + Uanem-Pscada experimental data, air density, March-December 2015.**

The chart clearly shows that the lower density points cloud tend to be associated to a lower electrical power for wind speeds above 8-10 [m/s]. The present result is consistent with literature [43].

However, it should be noticed that points dispersion, with reference to the manufacturer's power curve, is not very dependant on air density. In simple words, higher air density does not seem to be associated with a more narrow points cloud.

[43] Hau, *Wind Turbines fund., p.570-573*

Exploring in a more accurate way the reasons of the points dispersion can't be properly done with only the experimental data used in the present study case. On the other hand, 3 possibly strong causes should be investigated:

- Blade soiling: increase on the blade surface roughness are a major cause of deviations from the manufacturer's power curve[44]. Northern Sardinia is characterized by a dry, sandy environment, and rain can be absent even for months, during summer. Also,dead insects on the blades can't be excluded as a concurrent cause of soiling.
- Complex terrain: local topography can have a strong influence on wind flow directions components, turbulence, and eventually cause a noticeable deviation from the manufacturer's power curve[45]. It should also be noticed that the station anemometer is located 156m far from the wind turbine: small but significant local variations in the air flow between the station and the turbine can't be totally excluded.
- Lower air density, with reference to the MSL standard conditions density used to calculate the manufacturer's power curve: ρair=1.225 kg/m^3. In our study case, the average air density is 1.127 kg/m^3. According to the Betz law, on-site average air density would produce an 8% lower aerodynamic power at the same conditions, with reference to MSL standard conditions.

[44] Hau, *Wind Turbines fund., p.575-576*
[45] Hau, *Wind Turbines fund., p.569-570*

Chapter 2.5: Station anemometer- turbine rear wind speed direct

Linear correlations

With reference to the same time interval

In the proposed study case, the easiest correlation between *station anemometer* Uanem and *turbine rear* Ur wind speeds is to build a correlation chart in which each point is referred to a specific 10-min i interval. The horizontal axis represents Ur, while the vertical axis represents Uanem. Plotting every $(Ur_i;Uanem_i)$ point, a linear trend y=mx+a can be obtained through Excel.

2.5.1 All-points correlation

With no particular data discrimination (Uanem>Ur has NOT been imposed), it is hard to find any particular trend in the Ur-Uanem direct correlation.

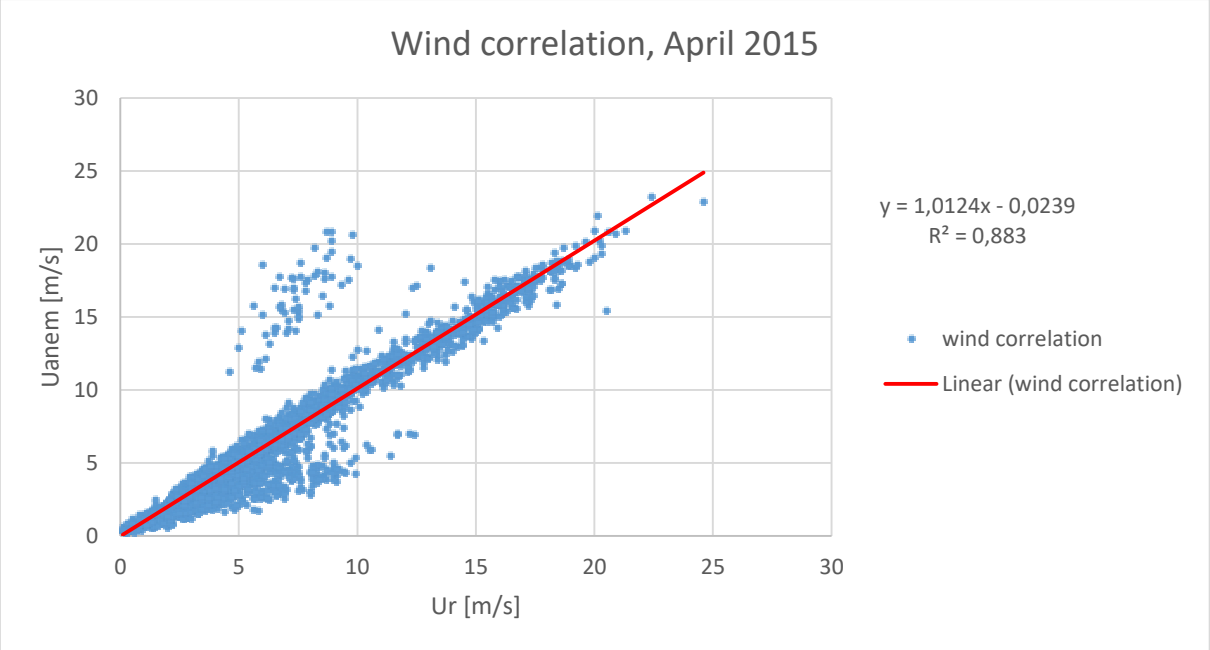

Figure 82: **Wind Correlation, April 2015.**

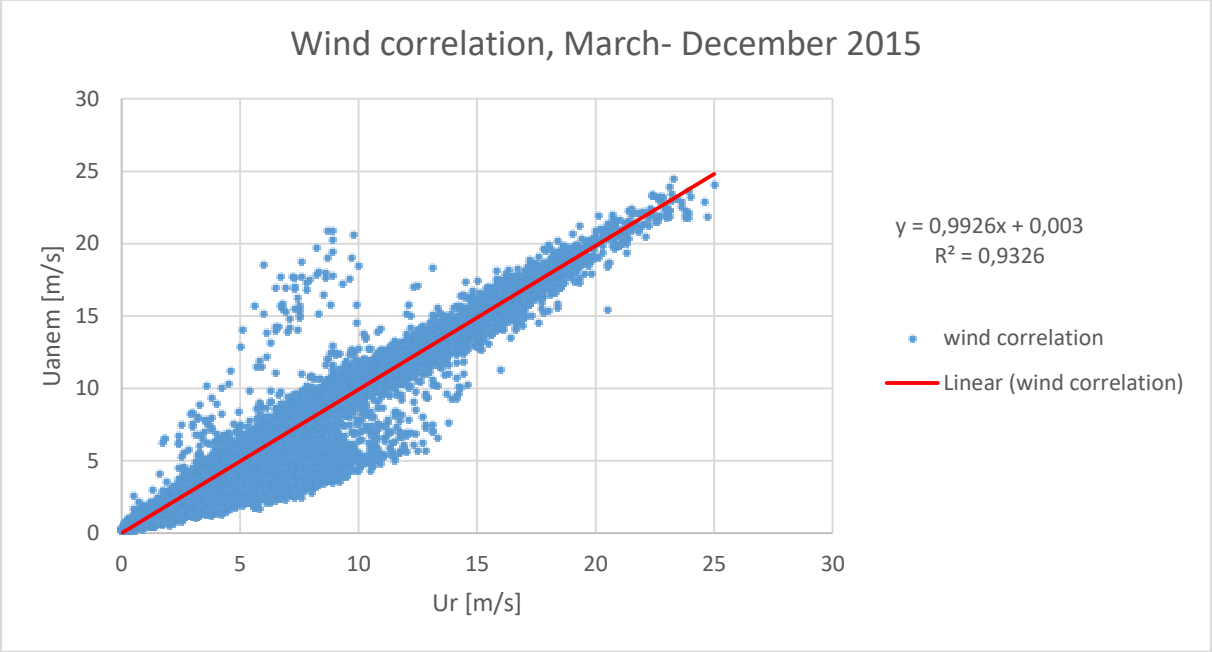

Figure 83: **Wind Correlation, March-December 2015.**

2.5.2 Linear correlation with turbulence and Uanem>Ur assessment

A further step is to discard all the points where Ur wind speed exceeds Uanem wind speed. In fact, due to the nature of energy converter of a wind turbine, we would expect to have a higher *front hub* wind speed, with reference to the *turbine rear* wind speed.

However, the Uanem wind speed is not necessarily equal to the *front hub* wind speed. Depending on the wind direction, the wind can hit the turbine *before* the station anemometer. Moreover, on other directions, wind speed measurements can be affected by the slowing effect of other wind turbines of the wind farm.

Last but not least, the non-instantaneous nature of the wind data (average value of a 10 min interval) can affect the fact that a *turbine rear* measurement would be higher than the *station anemometer* measurement.

The following condition is imposed:

$$Uanem_i > Ur_i$$

A second condition, regarding turbulence, is imposed:

$$turb\ (Uanem_i) < 0.18$$

Thus, the correlation chart is modified, and a certain number of points is discarded. We obtain a different trendline.

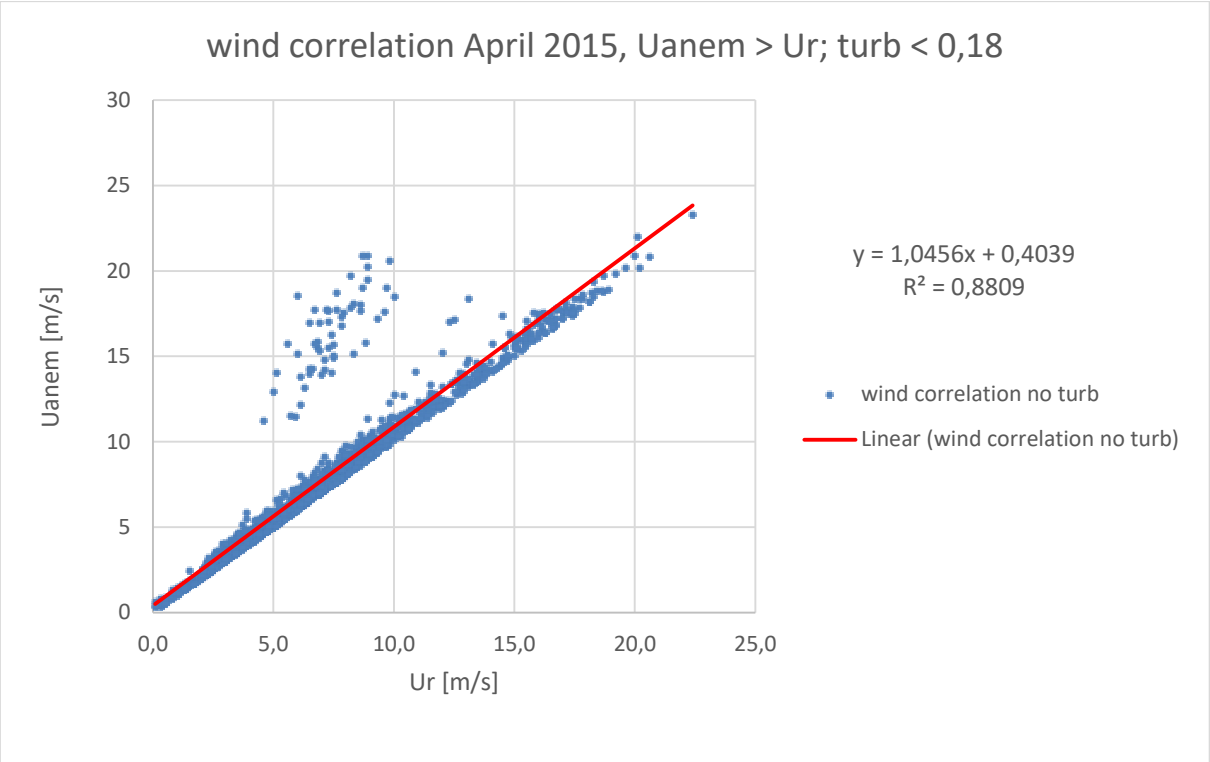

Figure 84: **Wind Correlation, Uanem>Ur, turbulence<0.18, April 2015.**

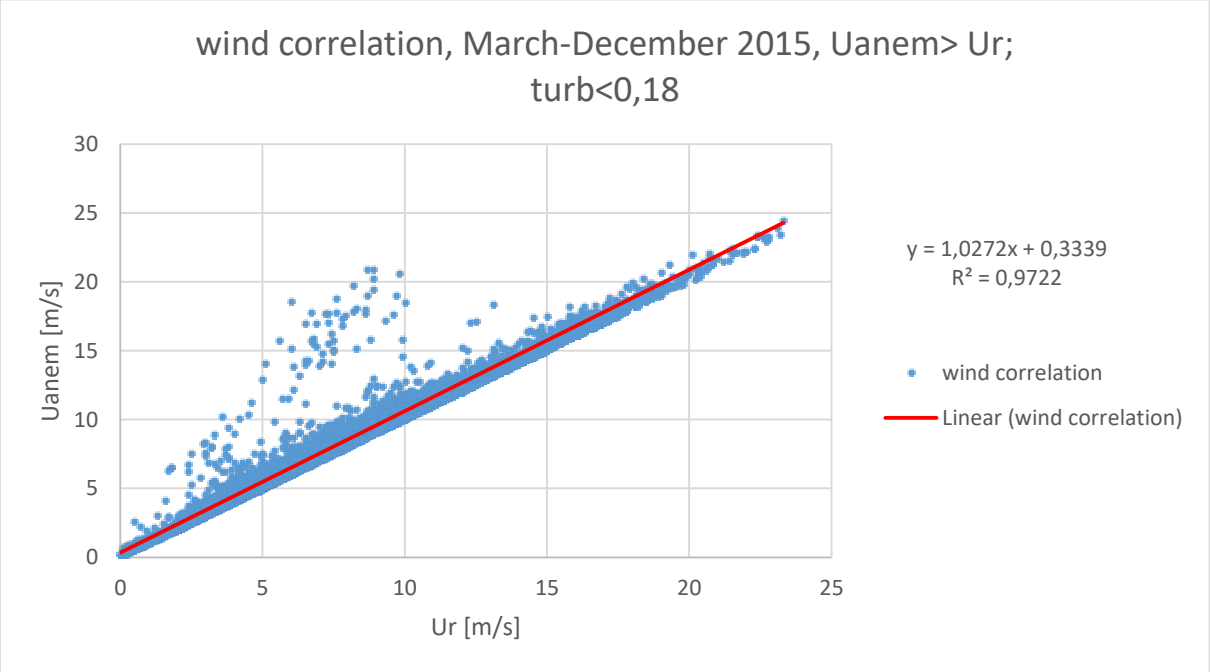

Figure 85: **Wind Correlation, Uanem>Ur, turbulence<0.18, March-December 2015.**

2.5.3 Linear correlation only main direction

In the last case, only the points corresponding to the main wind direction are used for the correlation. With reference to the conducted wind direction analysis, both for April, 2015, and for the period March-December 2015, the main direction is WNW

Eventually, the following conditions are applied:

- Wind direction WNW (main direction)
- Uanem > Ur
- Turbulence <0,18

Some lines of the excel worksheet are presented as example. The “valid for correlation” test is confirmed when the 3 cited conditions are true.

Uanem [m/s]	Ur [m/s]	Uanem> Ur TRUE(1), FALSE(0)	date, time	Danem [°]	Dmain WNW	turb(Uanem) < 0,18	VALID FOR CORR
0,855	1	FALSE	01/03/2015 00.00	153,0267	FALSE	TRUE	FALSE
0,35	0,2	TRUE	01/03/2015 00.10	101,98	FALSE	FALSE	FALSE
0,715	0,8	FALSE	01/03/2015 00.20	13,85727	FALSE	FALSE	FALSE
0,783	0,9	FALSE	01/03/2015 00.30	60,16653	FALSE	TRUE	FALSE
1,336	1,5	FALSE	01/03/2015 00.40	81,11674	FALSE	FALSE	FALSE
1,588	1,8	FALSE	01/03/2015 00.50	81,99473	FALSE	FALSE	FALSE
1,491	1,6	FALSE	01/03/2015 01.00	67,77296	FALSE	TRUE	FALSE
1,127	1,1	TRUE	01/03/2015 01.10	60,99889	FALSE	TRUE	FALSE
1,09	1,3	FALSE	01/03/2015 01.20	90,61464	FALSE	FALSE	FALSE
1,801	2,2	FALSE	01/03/2015 01.30	111,4245	FALSE	TRUE	FALSE
2,002	2,1	FALSE	01/03/2015 01.40	110,2087	FALSE	TRUE	FALSE
2,166	2,1	TRUE	01/03/2015 01.50	110,3467	FALSE	TRUE	FALSE
1,867	2,1	FALSE	01/03/2015 02.00	105,9687	FALSE	TRUE	FALSE
2,2	2	TRUE	01/03/2015 02.10	113,5193	FALSE	TRUE	FALSE
2,045	2,1	FALSE	01/03/2015 02.20	114,0163	FALSE	TRUE	FALSE
1,995	1,9	TRUE	01/03/2015 02.30	120,9164	FALSE	TRUE	FALSE
1,495	1,6	FALSE	01/03/2015 02.40	124,0858	FALSE	FALSE	FALSE
1,425	1,6	FALSE	01/03/2015 02.50	118,0252	FALSE	TRUE	FALSE

Table 5: **Linear correlation assessment example.**

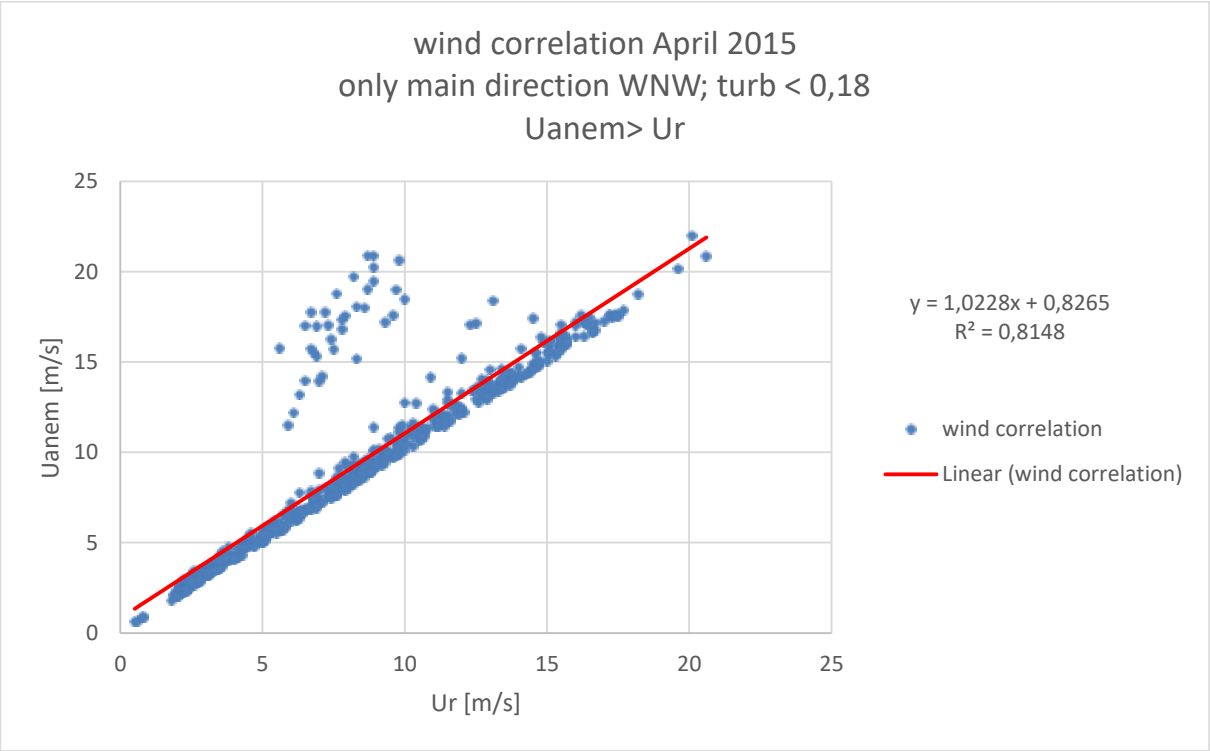

Figure 87: **Wind Correlation, only main direction (WNW), Uanem>Ur, turbulence<0.18, April 2015.**

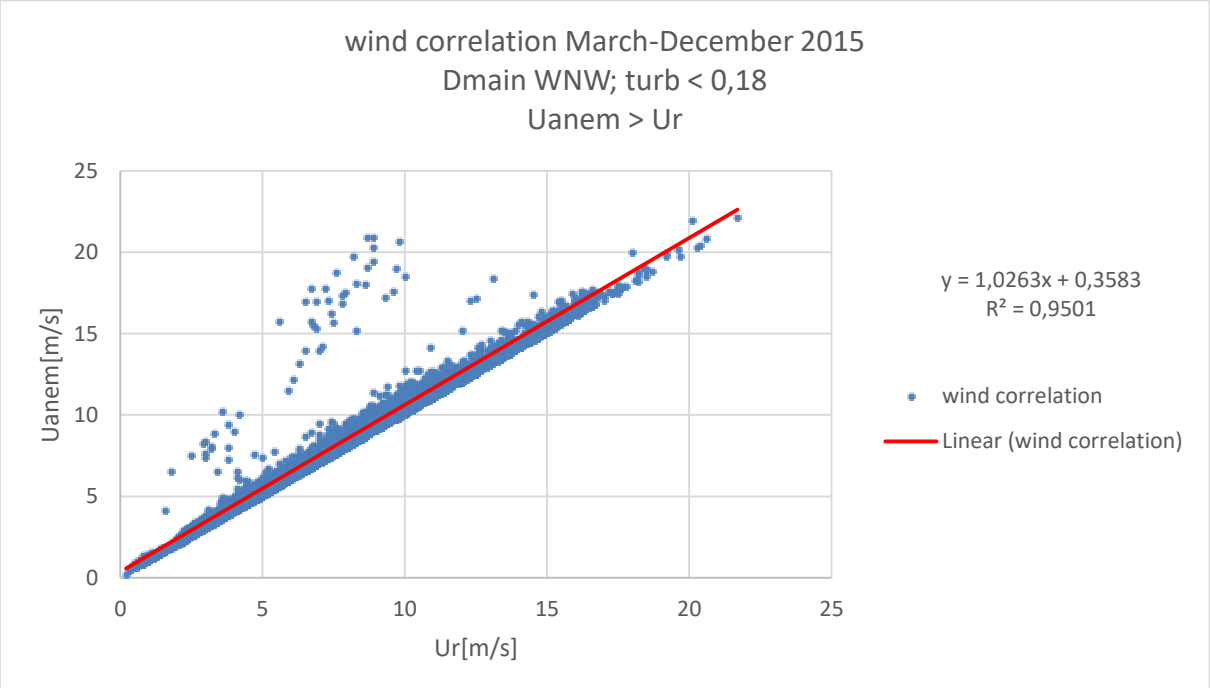

Figure 88: **Wind Correlation, only main direction (WNW), Uanem>Ur, turbulence<0.18, March-December 2015.**

Chapter 2.6: Manufacturer's power curve turbine rear wind speed-Pscada correlations, 5% non-exceeding probability method[46]

with reference to the same power interval, using a Gamma distribution empirical cumulative distribution function (ECDF)

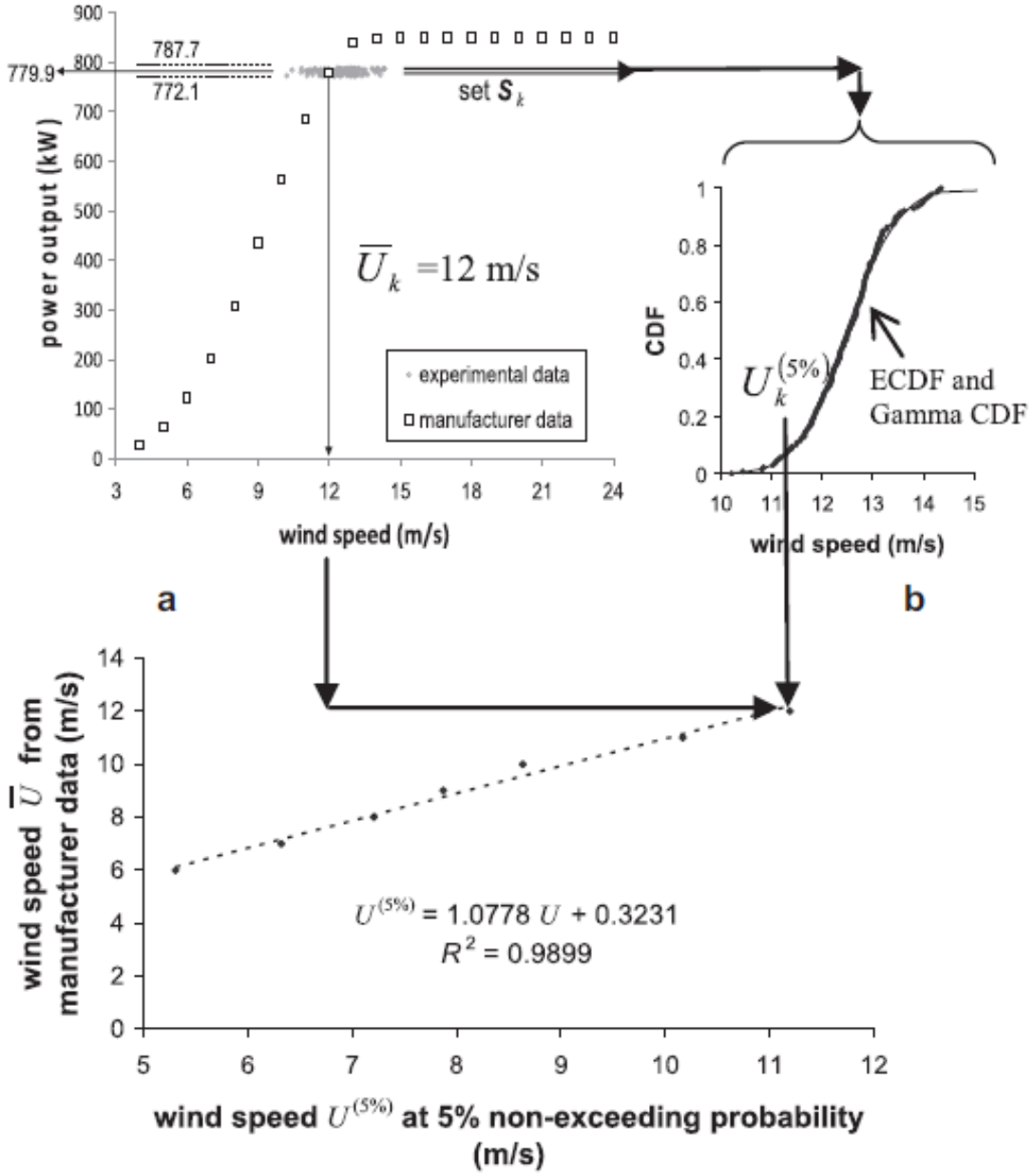

Figure 89: **Illustration of the 5% non-exceeding probability correlation method. Data shown are from a different study case.**
Source: F.Spertino et al., DFIG equiv. mismatch assessment, p.340 Renewable Energy 48, 2012.

[46] F.Spertino et al., DFIG equiv. mismatch assessment, Renewable Energy 48, 2012

In the proposed method, a medium-speed wind range is used. From the manufacturer's power curve, k=7 points are taken, between 6 and 12 [m/s]. Upc is the wind speed with reference to the power curve, Ppc(Upc) is the electrical power with reference to the chosen Upc. The power curve is not continuous: 25 Upc-Ppc points are provided by the manufacturer.

Considering the wind speed-power data provided by the *Ur wind speed sensor* together with the P(Ur) SCADA power measurement system, we obtain a data series. Every *turbine rear* Ur_i wind speed (the average 10-min i-interval turbine rear wind speed) comes together with the electrical power Pi SCADA measurement (average electrical power referred to the same i interval). These data are shown in the following chart, together with the manufacturer's power curve.

The aim of the correction method is to address the mismatch between this experimental series and the manufacturer's power curve in a more statistical way, compared to a simple direct linear mismatch addressing.

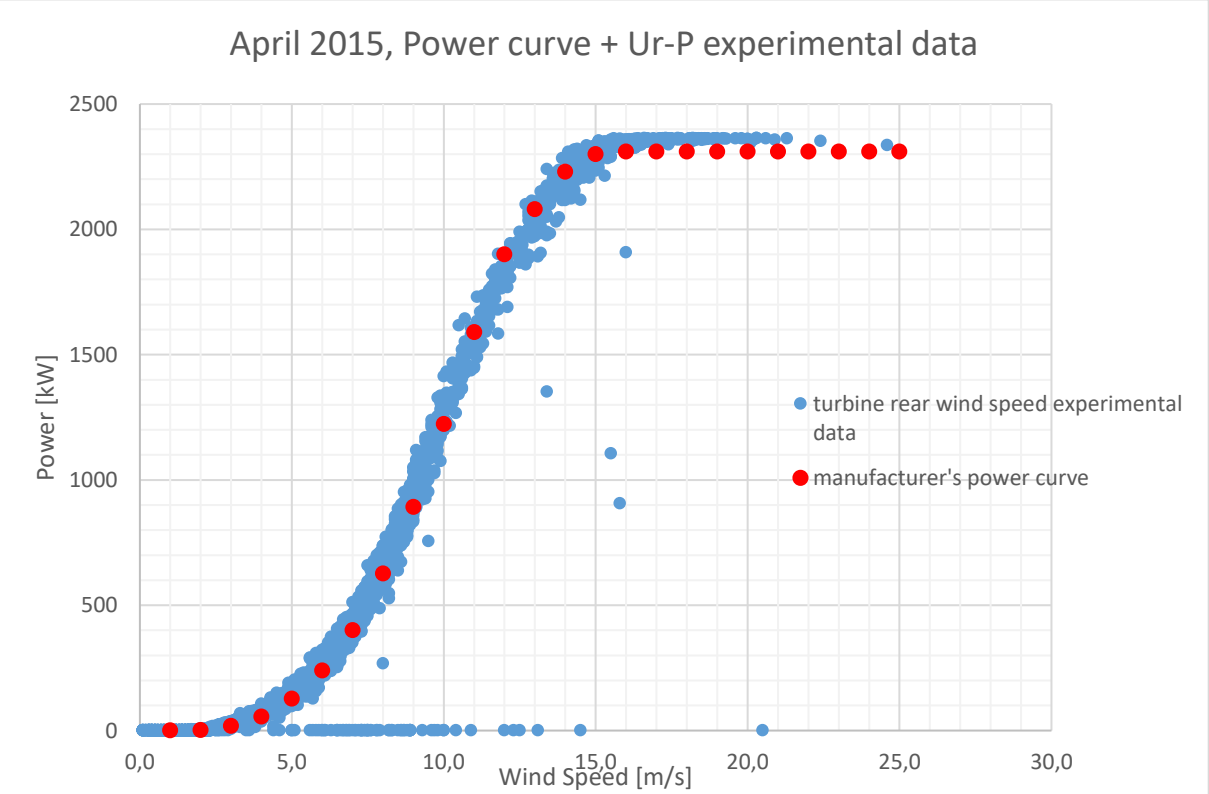

Figure 90: **Power curve + Ur-P experimental data, April 2015.**

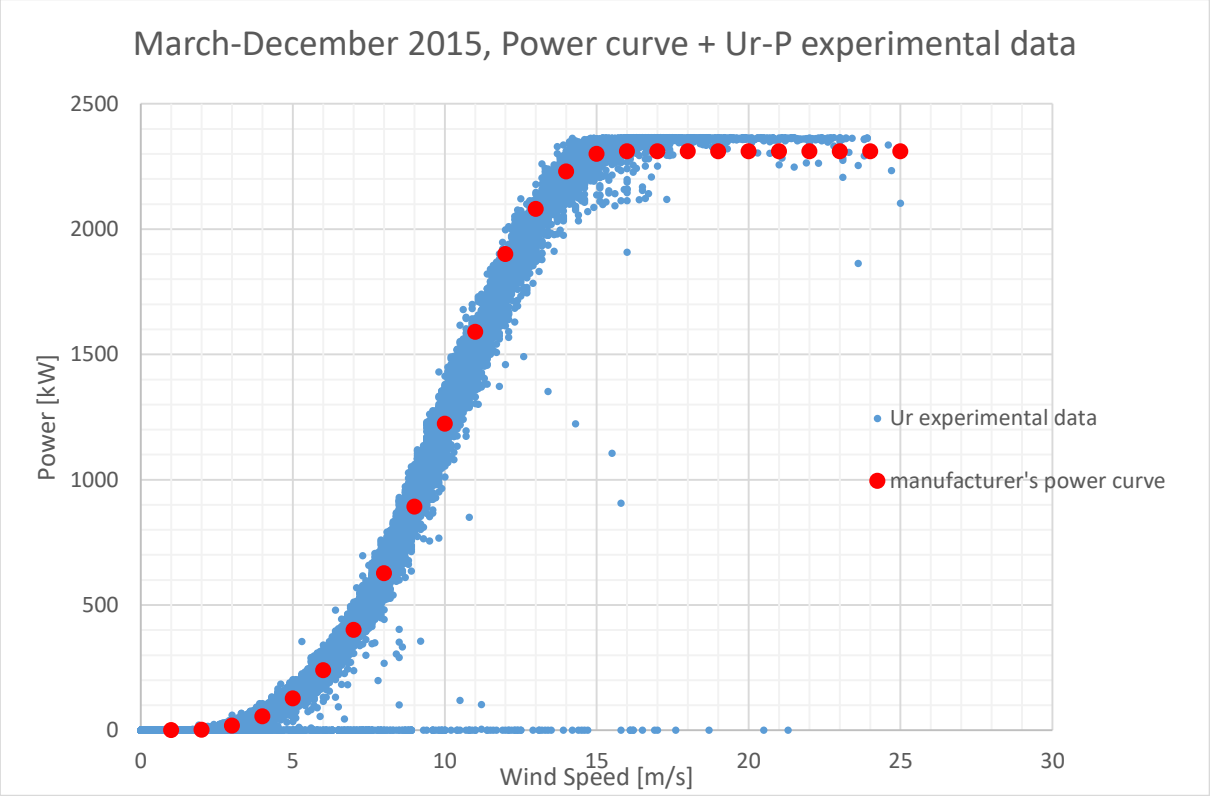

Figure 91: **Power curve + Ur-P experimental data, March-December 2015.**

To build the correction method, the following condition is to be true, regarding experimental Ur, P(Ur) data:

- Turbulence <0.18

For every power curve Ppc_i point, it's possible to define a threshold ε. E should be small, in order to define a small interval around Ppc_i. We define:

$$\varepsilon = 0.01 * Ppc_i$$

Around Ppc_i, a small set of experimental points S_i is defined:

$$S_i = \{\{Ur, P(Ur)\}: P(Ur) \in [Ppc_i - \varepsilon, Ppc_i + \varepsilon]\}$$

Every S_i data set is characterised by its mean avg(S_i) and by its variance var(S_i).

Considering the points of a specific S_i set as random variables, it's possible to obtain an equivalent gamma probability function.

The Gamma probability distribution is defined as:

$$f(U) = \frac{U^{a-1}}{b^a \Gamma(a)} * e^{-U/b}$$

In which $\Gamma(.)$ is the Gamma function, $b = var(S_i)/mean(S_i)$, $a = mean(S_i)/b$.

From the described Gamma probability distribution function, the value $U_i^{5\%}$ is obtained, corresponding to a 5% non-exceeding probability. $U_i^{5\%}$ is representative of the S_i data set, in order to build a correlation with the Upc_i point from the manufacturer's power curve.

Repeating the procedure for the 7 i point, thus for the corresponding S_i data sets, 7 $U_i^{5\%}$ are obtained. Every $U_i^{5\%}$ is plotted against the corresponding Upc_i wind speed value of the power curve. 7 points are plotted, and a linear trend y=mx+a can be obtained.

April,2015	Upc[m/s]	6	7	8	9	10	11	12
	Ppc [kW]	240	400	626	892	1223	1590	1900
	treshold+ [kW]	237,6	396	619,74	883,08	1210,77	1574,1	1881
	treshold- [kW]	242,4	404	632,26	900,92	1235,23	1605,9	1919
	no of points Si	7	14	8	4	8	5	12
	mean	5,8286	6,9143	7,975	8,875	9,8625	11,16	12,875
	var	0,0124	0,0429	0,0136	0,0292	0,039821	0,043	1,132955
gamma distr	b	0,0021	0,0062	0,0017	0,0033	0,004038	0,003853	0,087996
	a	2743,9	1115,5	4686,4	2700,5	2442,627	2896,409	146,3127
	U 5%	**5,647**	**6,577**	**7,784**	**8,596**	**9,537**	**10,821**	**11,176**

Table 6: **Ur5% calculation, April 2015.**

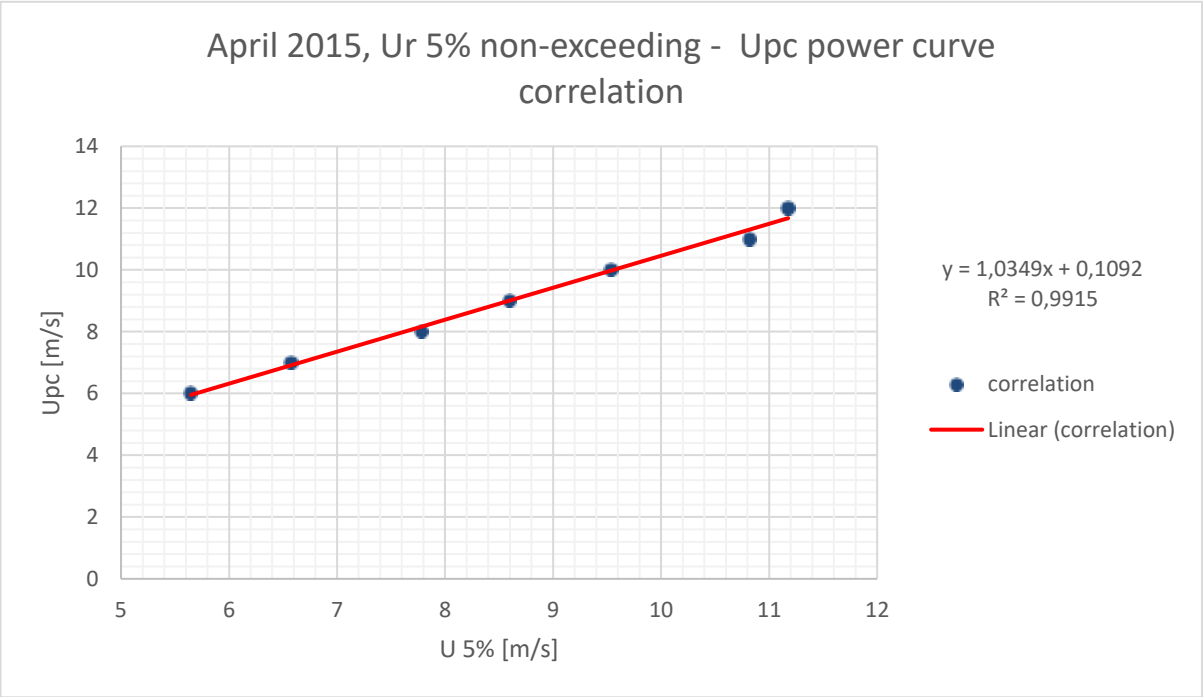

Figure 92: **Ur5% non-exceeding, Upc power curve correlation, April 2015.**

March-Dec 2015	Upc[m/s]	6	7	8	9	10	11	12
	Ppc [kW]	240	400	626	892	1223	1590	1900
	treshold+ [kW]	237,6	396	619,74	883,08	1210,8	1574,1	1881
	treshold- [kW]	242,4	404	632,26	900,92	1235,2	1605,9	1919
	no of points Si	111	138	125	90	105	68	101
	mean	5,88018	6,93623	7,9688	8,9067	9,9552	11,1868	12,5
	var	0,03306	0,02787	0,0362	0,0368	0,2342	0,05639	0,226
gamma distr	b	0,00562	0,00402	0,0045	0,0041	0,0235	0,00504	0,01808
	a	1045,93	1725,98	1754,4	2155,1	423,12	2219,28	691,3717
	U 5%	**5,58434**	**6,66392**	**7,6585**	**8,5935**	**9,1728**	**10,7991**	**11,72846**

Table 7: **Ur5% calculation, March-December 2015.**

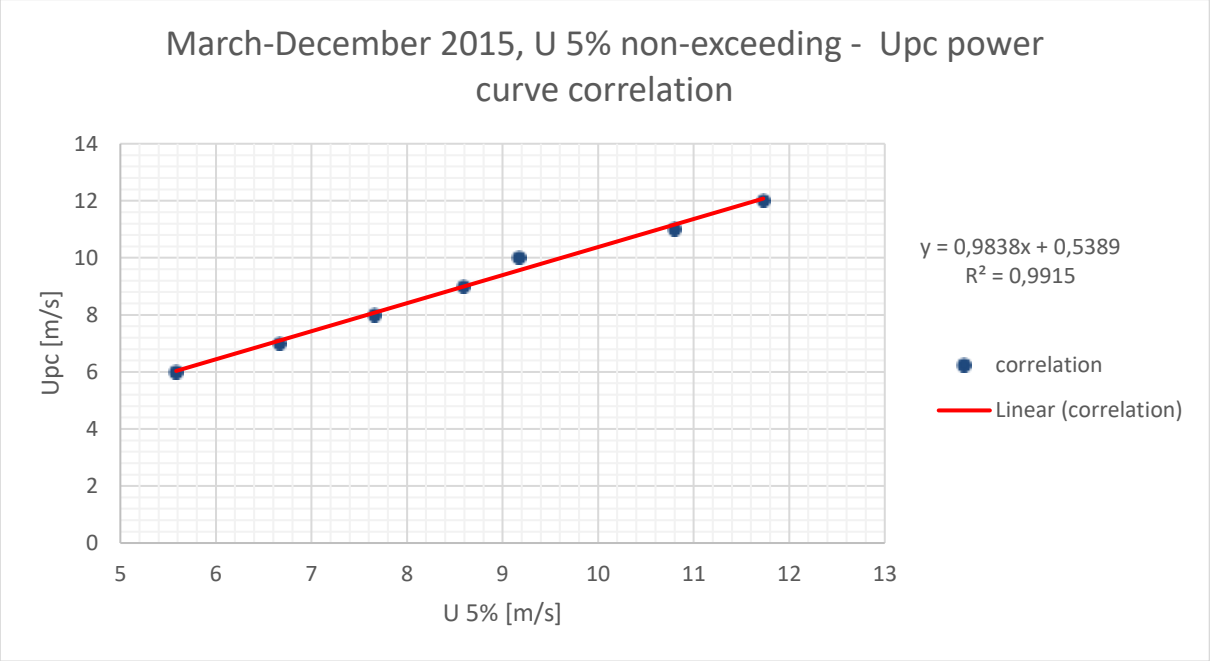

Figure 93: **Ur5% non-exceeding, Upc power curve correlation, March-December 2015.**

Both for April and March-December, a clear linear trend in the U5%-Upc chart has been found: it's coherent, because a U5% *lower* than its associated Upc was attended. Of course, in every Ur-Pscada chart, the Ur-Pscada points cloud left border is located on the *left* of the manufacturer's power curve. U5%, as it is defined, in the interval where it is defined, is sufficiently close to the *left* border of the Ur-Pscada points cloud.

In simple words, correcting every Ur-Pscada point using the U5%-Upc linear trend means obtaining a U'-Pscada corrected series of points, with its *left* border sufficiently close to the manufacturer's power curve.

This type of mismatch addressing is proper: it will produce a U'-Pscada point series similar to the experimental Uanem-Pscada series (which associates *front hub wind speed* and its relative electrical power). In a certain sense, the U'-Pscada corrected series represents an *estimation* of the Uanem-Pscada series.

Chapter 2.7: Experimental data mismatch assessment

Every presented mismatch assessment procedure produced a different linear equation y=mx+a. m and a coefficients are used to "correct" the original experimental Ur turbine rear wind speed data, thus obtaining U', representative of the front hub wind speed. The electrical power associated to Ur, P(Ur) and P'(U') associated to U' are, of course, the same, as the aim of the method is to obtain a U' which is a valid estimation of the *front hub wind speed*.

$$P(Ur_i) = P'(U'_i)$$

. P(Ur) is the electrical power associated to the *turbine rear wind speed* Ur. P'(U') is the electrical power associated to the *estimated front hub wind speed* U'. Both are to be intended as average quantities with reference to the 10-min interval i.

$$U' = a * U + b$$

a and b are the coefficients of the equation y=mx+b obtained for each mismatch assessment method.

2.7.1 April, 2015

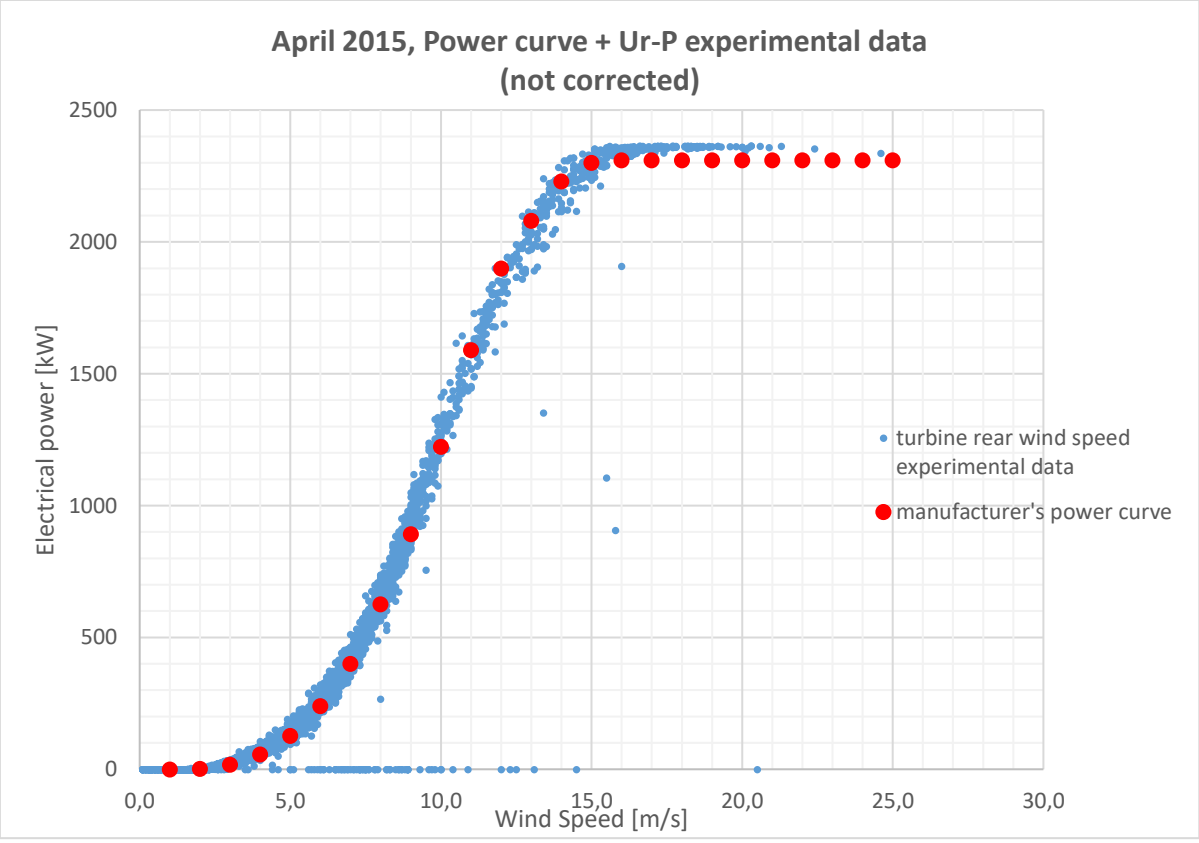

Figure 94: **Power curve + Ur-P experimental data (not corrected), April 2015.**

2.7.1.1 Direct linear correlation correction method

The correlation equation is y = 1.0456x+0.4039. Thus,

$$U' = 1.0263 * U + 0.3583$$

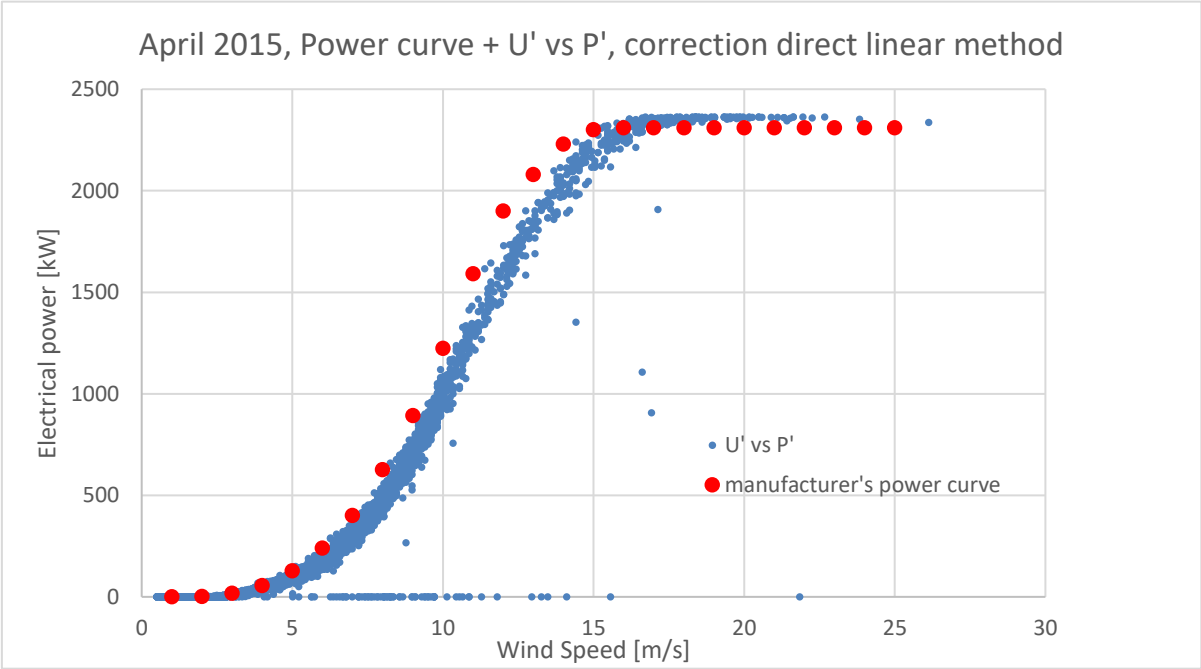

Figure 95: **Power curve + U' vs P', correction direct linear method, April 2015.**

2.7.1.2 Direct linear correlation correction method only main direction

The correlation equation is y = 1.0228x+0.8265. Thus,

$$U' = 1.0228 * U + 0.8265$$

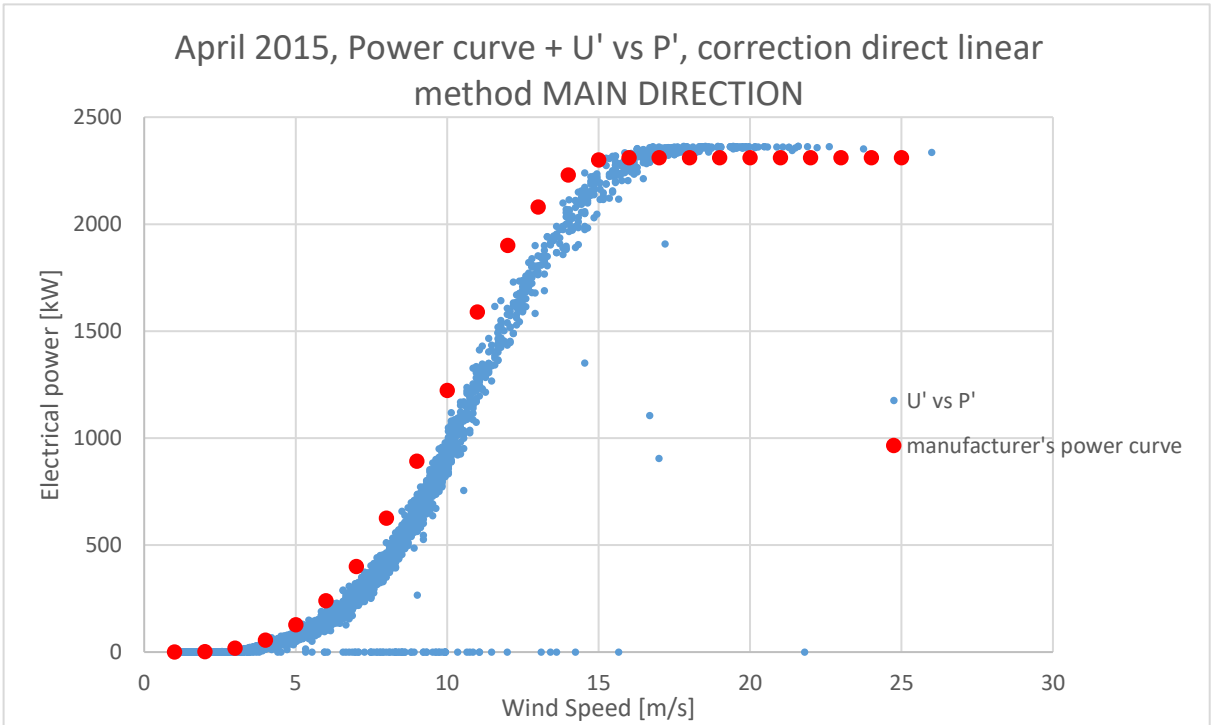

Figure 96: **Power curve + U' vs P', correction direct linear method, main direction, April 2015.**

2.7.1.3: 5% non-exceeding correction method

The correlation equation is y = 1.0349x+0.1092. Thus,

$$U' = 1.0349 * U + 0.1092$$

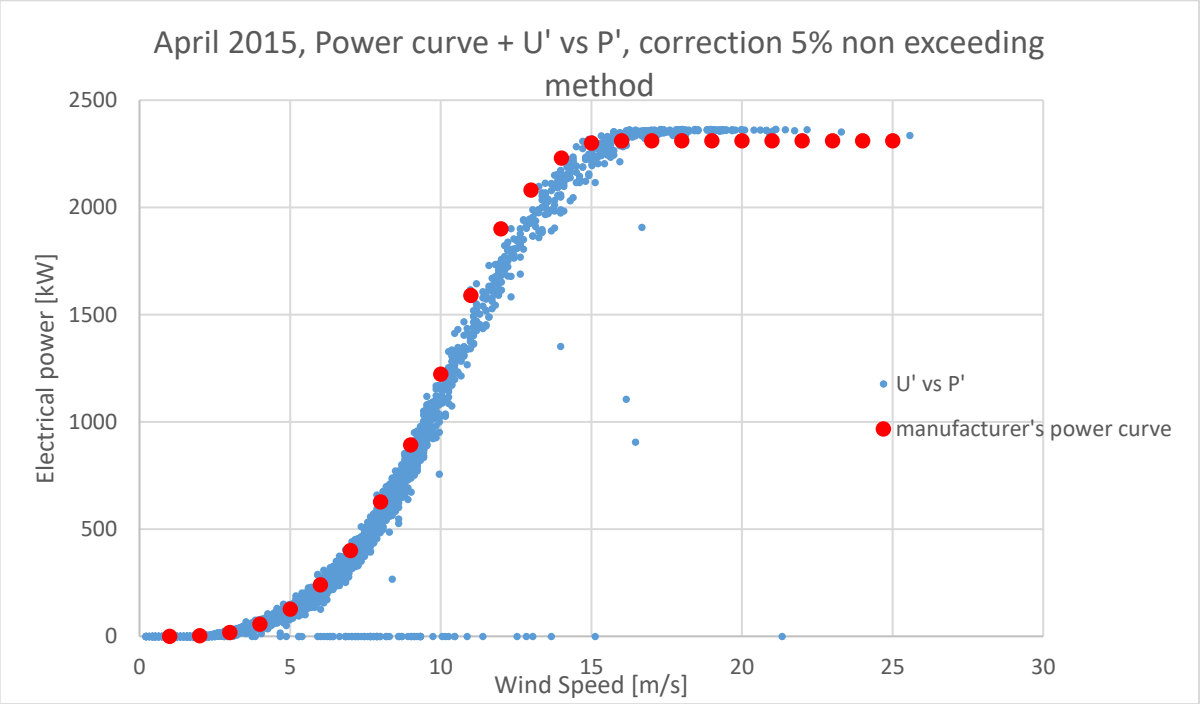

Figure 97: **Power curve + U' vs P', correction 5% non exceeding method, April 2015.**

2.7.1.4 Conclusions

The correction operated with the 5% non-exceeding method produced the best result, more specifically with reference to the Uanem-Pscada power curve.

It is safe to assume that the 5% non-exceeding method produces a closer correction of Ur, with reference to Uanem, than a direct linear correction method.

2.7.2 March-December 2015

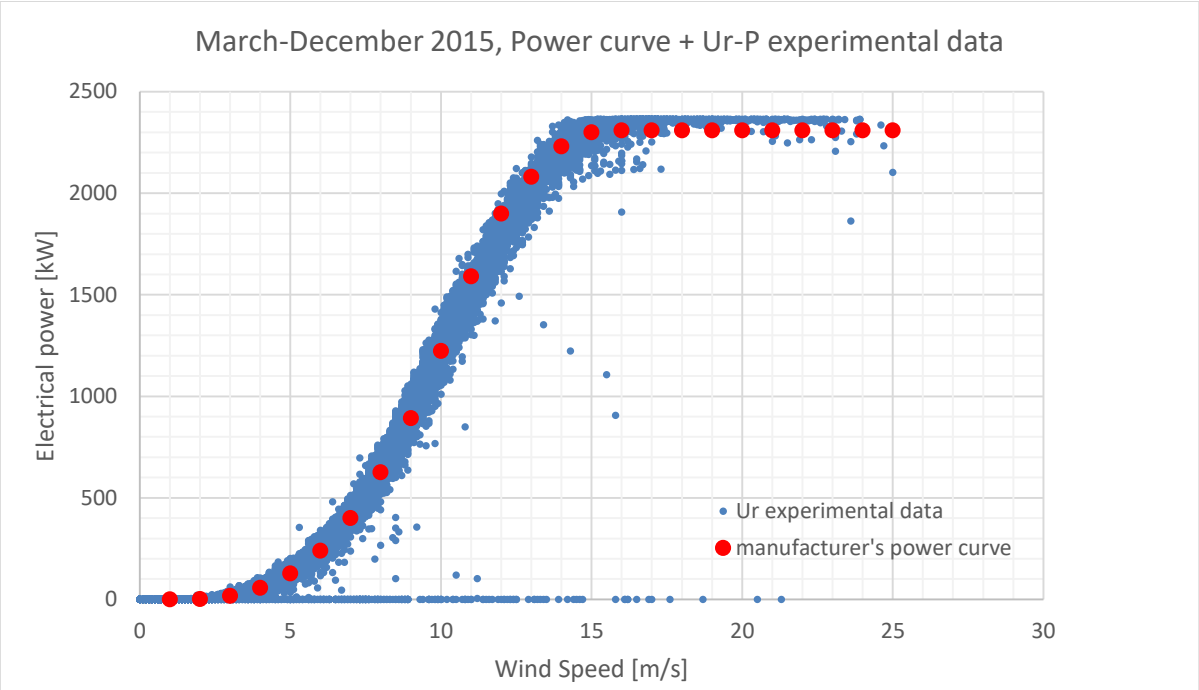

Figure 98: **Power curve + Ur-P experimental data, March-December 2015.**

2.7.2.1 Direct linear correlation correction method

The correlation equation is y = 1.0272x+0.3339. Thus:

$$U' = 1.0272 * U + 0.3339$$

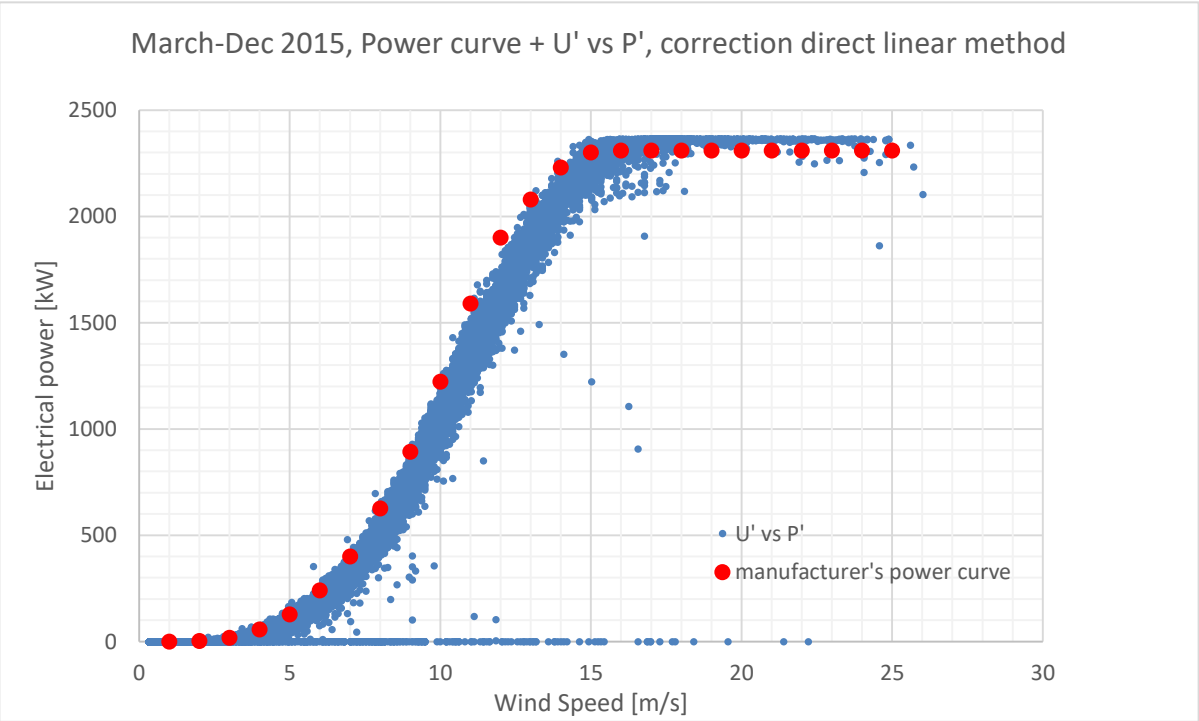

Figure 99: **Power curve + U' vs P', correction direct linear method, March-December 2015.**

2.7.2.2 Direct linear correlation correction method only main direction

The correlation equation is y = 1.0263x+0.3583. Thus,

$$U' = 1.0263 * U + 0.3583$$

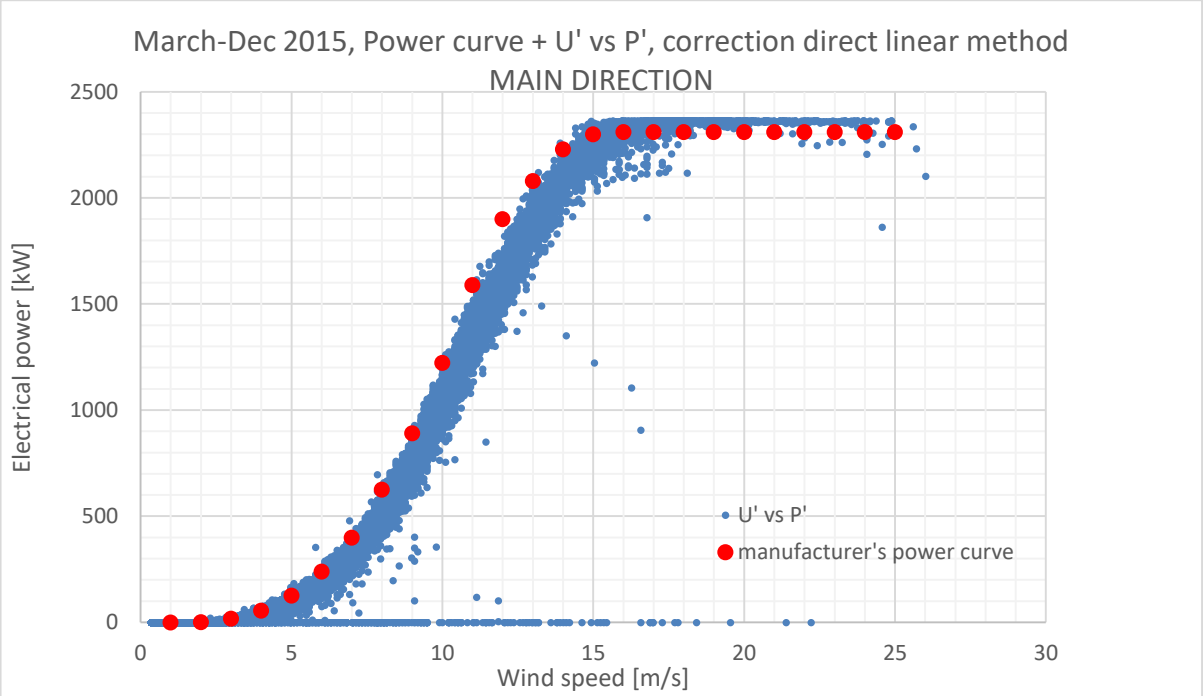

Figure 100: **Power curve + U' vs P', correction direct linear method, main direction, March-December 2015.**

2.7.2.3: 5% non-exceeding correction method

The correlation equation is y = 0.9838x+0.5389. Thus,

$$U' = 0.9838 * U + 0.5389$$

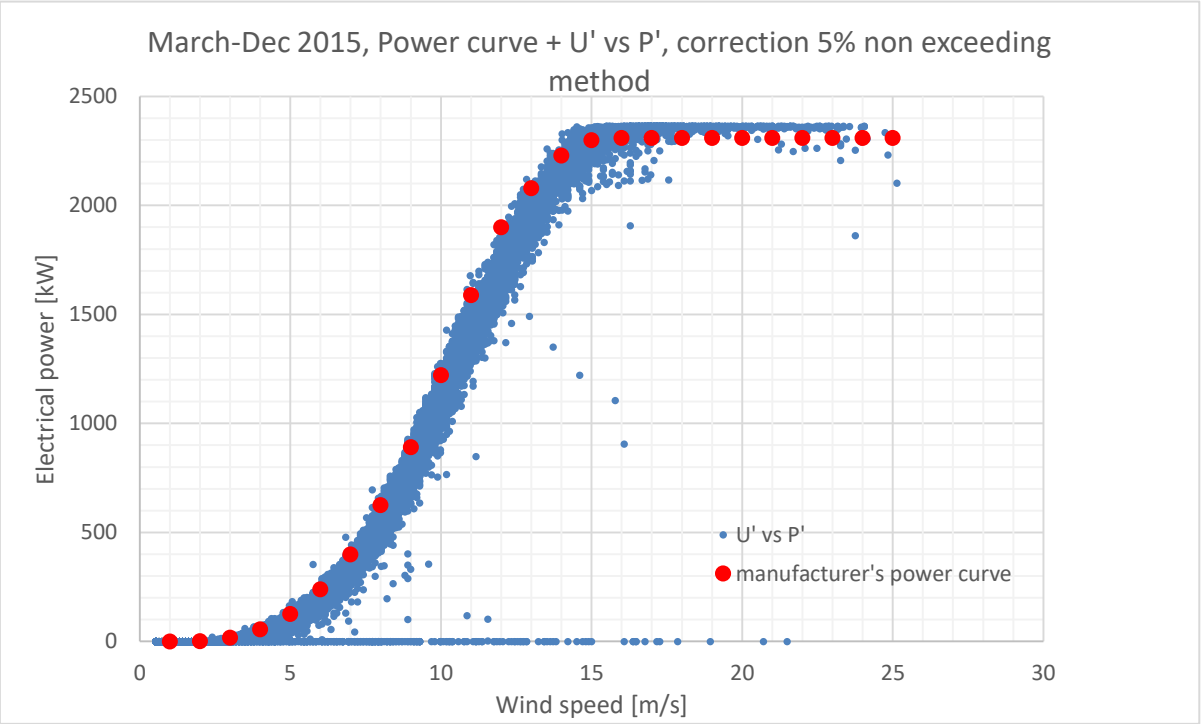

Figure 101: **Power curve + U' vs P', correction 5% non exceeding method, March-December 2015.**

2.7.2.4 Conclusions

Regarding March-December 2017, both the direct linear and the 5% non-exceeding method produce good results, with reference to the Uanem-Pscada experimental power curve . However, the 5% non-exceeding method will be preferred, being more accurate from statistical point of view, also to be used in efficiency calculations.

Chapter 2.8 Wind turbine average efficiency estimation[47][48]

The corrected wind speeds data set U' and its associated electrical power P'(U')= Pscada can be used to operate an estimation of the wind turbine average efficiency.

The aerodynamic power Pair_in5% is calculated through the following formula:

$$Pair\_in5\% = \frac{1}{2}\rho_{air}\frac{\pi}{4}D^2U'^3$$

Where ρ_{air} [kg/m^3] is the air density, and D [m] is the rotor diameter.

The air density ρ_{air} is determined thanks to the experimental data of temperature Ti and pressure Pi, for each 10-min i interval:

$$\rho_{air} = P/(R \cdot T)$$

Where R=287,15 [J/(kg·K)] is the air constant.

The average efficiency of the 10-min i interval can be obtained as:

$$\eta_{air\_in5\%} = Pscada/Pair\_in5\%$$

The average efficiency on the established time period $(\sum_{i=1}^{n} i)/(6 * 24)$ days, composed of n 10-min i intervals, can be estimated as:

$$\eta_{air\_in5\%\_tot} = \sum_{i=1}^{n} Pscada_i \Big/ \sum_{i=1}^{n} Pair\_in5\%_i$$

These efficiencies can be compared to the experimental efficiencies obtained using the actual station anemometer wind speeds Uanem. For each i interval.

$$Pair\_in = \frac{1}{2}\rho_{air}\frac{\pi}{4}D^2Uanem^3$$

$$\eta_{air\_in} = \frac{Pscada_i}{Pair\_in_i}$$

[47] F.Spertino et al., DFIG equiv. mismatch assessment, Renewable Energy 48, 2012
[48] F.Spertino et al, Operational Characteristics of a 27-MW Wind Farm from Experimental Data, IEEE 2008

For the total time period:

$$\eta_{air\_in\_tot} = \sum_{i=1}^{n} Pscada_i \Big/ \sum_{i=1}^{n} Pair\_in_i$$

A further data filtration is applied. Working with the actual station anemometer data, it's necessary to ensure that the station anemometer wind speed Uanem is bigger than the corresponding Ur: if the condition is not verified, Uanem can't be considered as the *front hub wind speed*, and thus it can't be used into efficiency calculations. Furthermore, $\eta_{air\_in5\%}$ and η_{air_in} have to be smaller than 59% (Betz limit), and Pscada must be greater than 80 kW (on a nominal power of 2300 kW), to avoid an excessive influence of the measurement system errors.

- Uanem>Ur
- η<59%
- Pscada>80 kW

In the charts, the efficiencies are compared to the manufacturer's Cp. The standard deviation of the efficiencies is presented as estimation of the efficiencies dispersion with reference to the average value.

2.8.1 Total efficiencies

April, 2015	
tot efficiency Pscada/Pair_in	tot efficiency Pscada/Pair_in5%
33,14%	33,61%

March-Dec 2015	
tot efficiency Pscada/Pair_in	tot efficiency Pscada/Pair_in5%
35,52%	37,38%

March-Dec 2015	**turbulence <0,1**
tot efficiency Pscada/Pair_in	tot efficiency Pscada/Pair_in5%
32,37%	34,74%

March-Dec 2015	**turbulence 0,1-0,2**
tot efficiency Pscada/Pair_in	tot efficiency Pscada/Pair_in5%
38,02%	39,44%

March-Dec 2015	**turbulence >0,2**
tot efficiency Pscada/Pair_in	tot efficiency Pscada/Pair_in5%
41,95%	41,57%

The total efficiencies Pscada/Pair_in are pretty high for an inland installed wind turbine, and they demonstrate the goodness of the wind farm site, in terms of wind resource. High efficiencies demonstrate that the turbine works in its higher Cp region for a significant number of 10 min i intervals.

A very peculiar aspect that should be noticed is that efficiency increases with the turbulence index It. This result shouldn't be taken as a univocal causal effect, because measurements are not distributed similarly with reference to the wind speed range. However, it is expected that a wind characterized by a higher It, under the same conditions, produces a higher aerodynamical power Pair_in, with comparison to a lower It: turbulences creates peaks of wind speed that, according to Betz law (depending on the third power of wind speed) carry more aerodynamical power than what expressed by the average 10-min wind speed value[49]. In simple words, it is possible that, in this study case, using the 10-min wind speed average value brings to an underestimation of a turbulent wind.aerodynamical power

The total efficiency Pscada/Pair_in5% should be interpreted as an estimation of the total efficiency Pscada/Pair_in. The estimation is good, the values are very close.

[49] Hau, *Wind Turbines fund., p.573-574*

2.8.2 Average wind speed conversion efficiencies

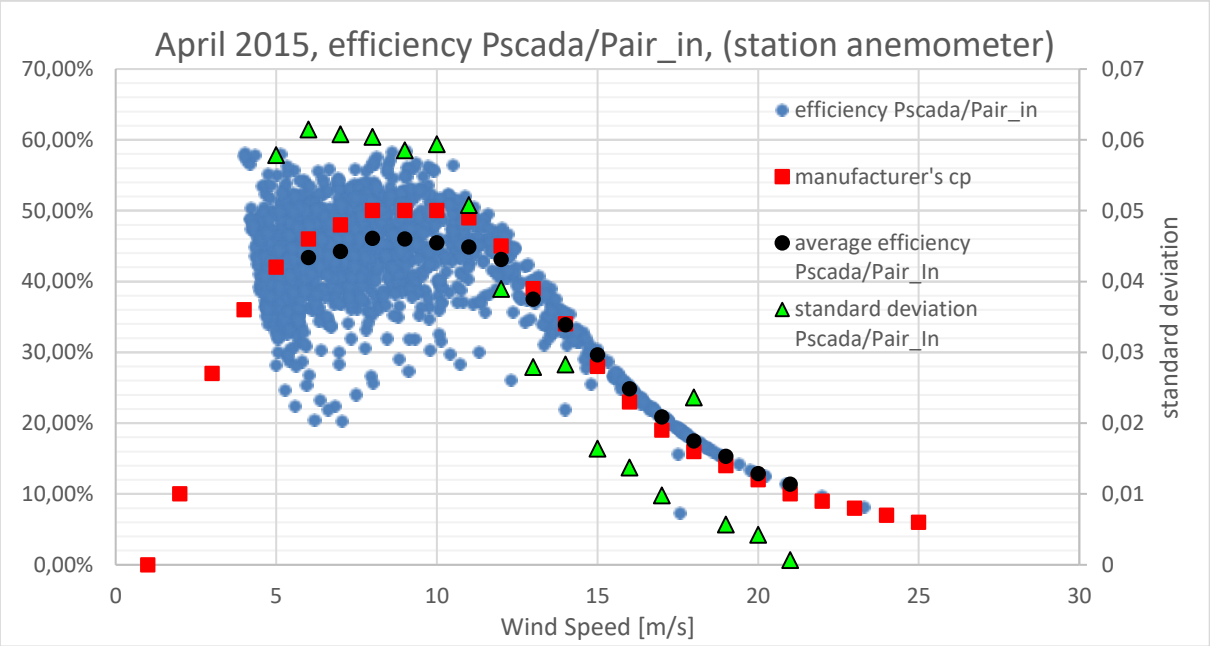

Figure 102: **Efficiency Pscada/Pair_in (station anemometer), April 2015.**

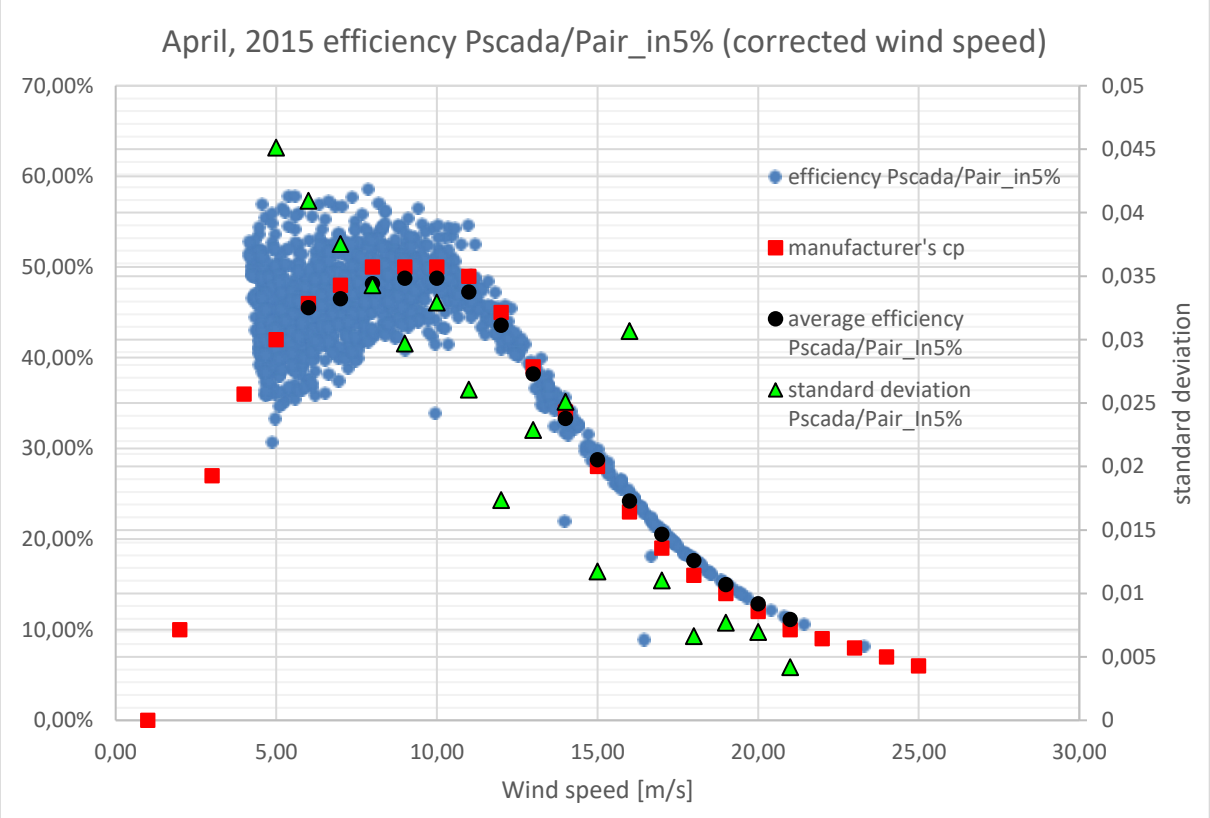

Figure 103: **Efficiency Pscada/Pair_in5% (corrected wind speed), April 2015.**

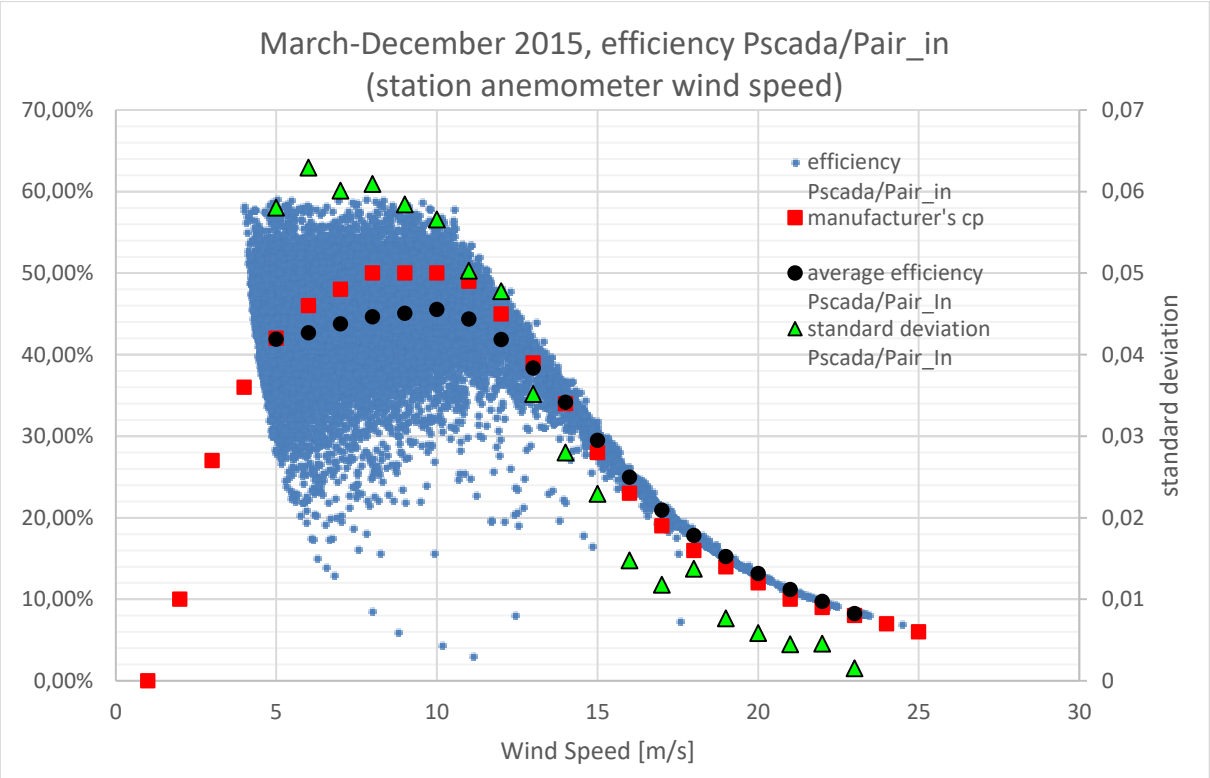

Figure 104: **Efficiency Pscada/Pair_in (station anemometer), March-December 2015.**

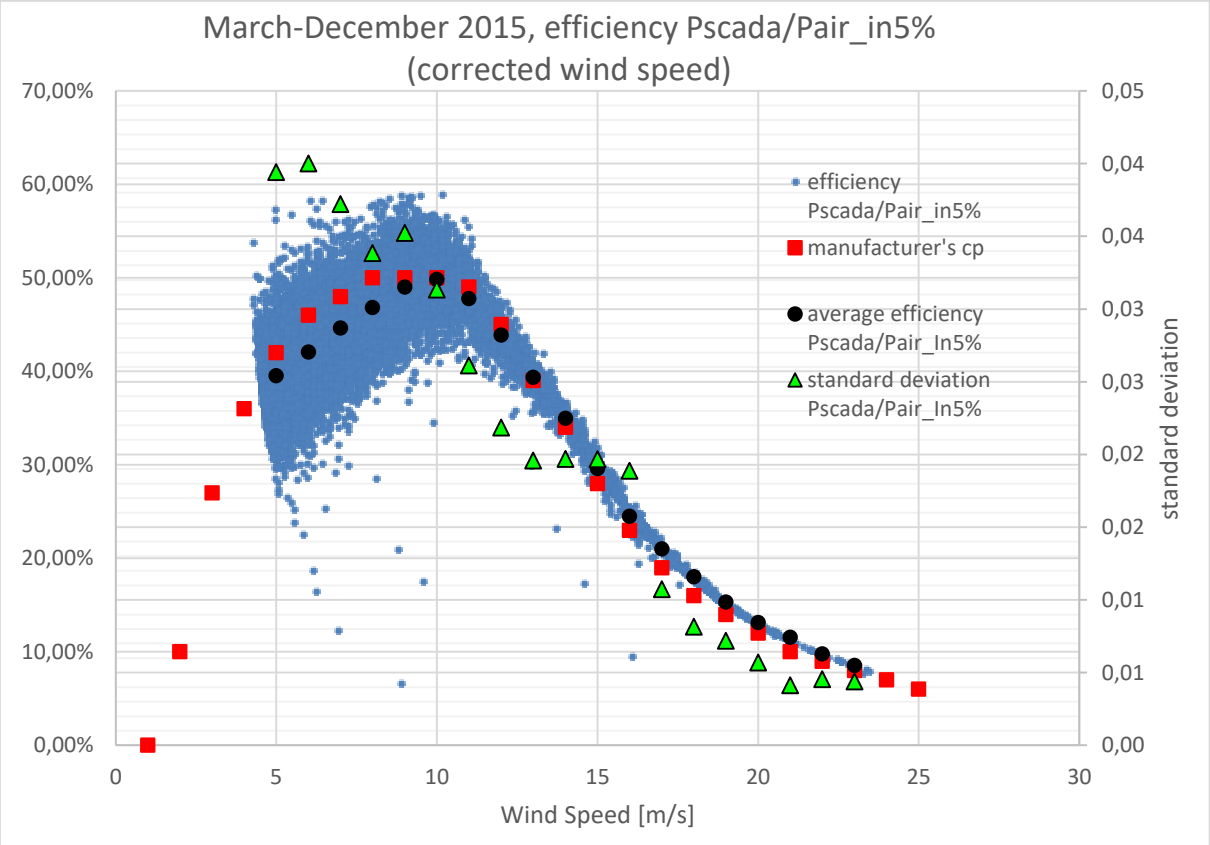

Figure 105: **Efficiency Pscada/Pair_in5% (corrected wind speed), March-December 2015.**

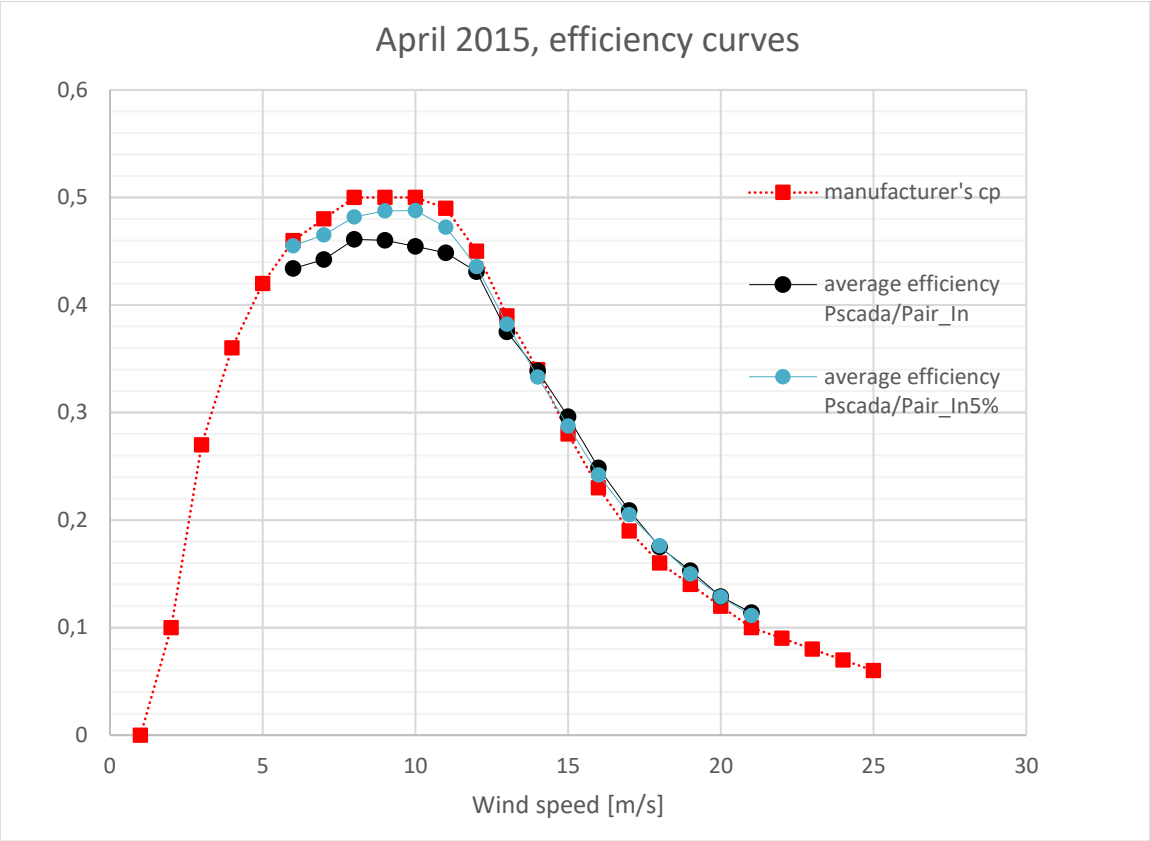

Figure 106: **Efficiency curves, April 2015.**

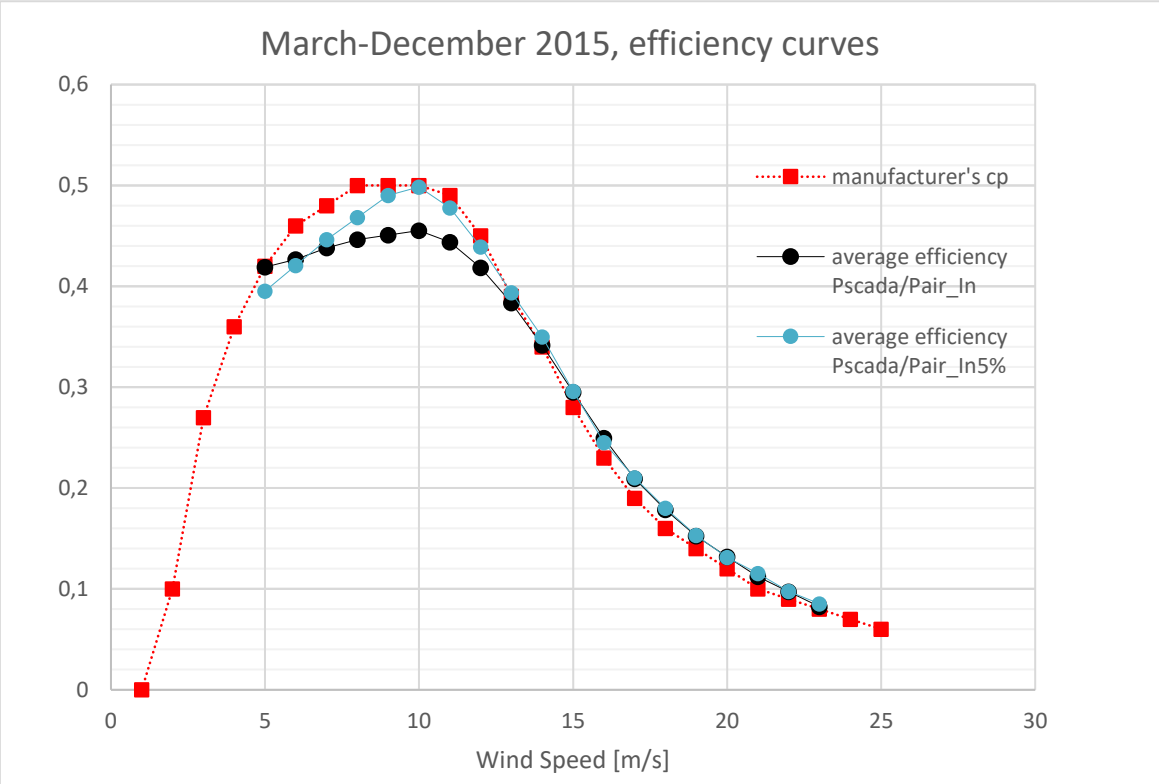

Figure 107: **Efficiency curves, March-December 2015.**

Taking into consideration the single 10-min i efficiency Pscada_Pair_in, obtained using the real, station anemometer measured (Uanem) wind speed, it produces a more dispersed efficiency points cloud, with comparison to the corrected-data efficiency points Pscada_Pair_in5%, a concept expressed through the standard deviation with reference to the specific wind speed.

The average efficiency Pscada/Pair_in shows to be lower than the manufacturer's Cp curve. Not surprisingly, it is consistent with what already obtained with regards to the Uanem-Pscada chart: the power measurements for a specific wind speed showed to be lower than the manufacturer's power curve, with the exception of wind speeds higher than 14 m/s (a problem with the SCADA measuring system has been supposed).

In simple words, according to the Betz law and to the definition of efficiency, if a specific Uanem produces less electrical power (Pscada) than what expected from the manufacturer's power curve, its efficiency conversion (of aerodynamic power into electrical power) will be lower. Extending this concept for a sufficient number of i 10-min intervals characterized by a specific wind speed, the average efficiency for that wind speed, with comparison to the manufacturer's Cp, will be lower. Calculations shows that this is true for wind speeds lower than 14 m/s.

For wind speeds higher than 14 m/s, the average efficiency Pscada/Panem shows to be higher than the manufacturer's Cp. On this fact, the influence of a problem with the SCADA measuring system overestimating Pscada can't be excluded.

With regards to the corrected data efficiency Pscada/Pair_in5% and considering how it was calculated, the main goal would be to obtain a similar pattern with reference to the Pscada/Pair_in obtained with the "real" station anemometer data. This is partially true: however, the correction produces a less dispersed efficiency points cloud, as it is demonstrated by a lower standard deviation.

Eventually, the average Pscada/Pair_in5% shows to be higher, more optimistic than the Pscada/Pair_in "real" average efficiency. This fact probably implies that the hypothesis of associating every Ur5% (5% gamma non-exceeding turbine rear wind speed) and its relative P(Ur5%) to an equal Ppc power on the manufacturer's power curve is too optimistic, and it produces a slightly too optimistic correction in terms of average efficiency.

It should also be stated that the 5% method correction is derived from a linear equation.

This linear equation has been obtained through the linear association of the Ur5%-Upc points. These points are not necessarily perfectly disposed on a line: using the linear association implies an error in the correction.

As it has been stated with regards to the Pscada/Pair_in “real” average efficiency, for wind speeds higher than 14 m/s the average Pscada/Pair_in5% efficiency shows to be higher than the manufacturer’s Cp. Once again, the influence of a problem with the SCADA measuring system overestimating Pscada can’t be excluded.

Eventually, the corrected data average efficiency Pscada/Pair_in5% shows to be a good, slightly more optimistic estimation of the “real” average efficiency Pscada/Pair_in, confirming the goodness of the 5% non-exceeding correction method.

Chapter 2.9: Conclusions

All conclusions will be referred to the March-December 2015 period, if not stated otherwise.
The study examined a noticeably good wind farm site in Northern Sardinia, Italy: the main wind direction is clearly WNW (20,2% relative frequency) with a remarkable WNW average wind speed of 7.28 m/s, with reference to the March-December 2015 period.
Thanks to the station anemometer and to the SCADA power measurement, it has been possible to characterize experimental *front hub wind speed-electrical power* points, compare them to the manufacturer's power curve, and make further consideration with regards to turbulence and air density. Experimental points are consistent with the power curve, however, a considerable power deviation is observed: the plotted points describes a lower power production than the manufacturer's curve. More turbulent points concentrates nearer to the power curve at low wind speeds (4-7,5 m/s), points with turbulence between 0.1-0.2 creates more dispersion at higher wind speeds (>14 m/s). With regards to air density, lower air density points deviates significantly from the manufacturer's power curve for medium high wind speeds (>10 m/s). The power deviation, on the whole wind speed interval, can't be properly explained with turbulence and air density variations. More causes have been hypothesized to justify this deviaton:

- Blade soiling, typical of a dry, sandy environment.
- Complex terrain effects on wind.
- Lower on-site air density, with reference to standard MSL conditions used to calculate manufacturer's power curve

Front hub wind speed (from the station anemometer) and *turbine rear wind speed* (from the turbine's back nacelle) have been correlated with direct linear relations, and with the 5% non-exceeding method.
The 5% non-exceeding method appears to produce the better estimation of the *front hub wind speed*, requiring only the *turbine rear wind speed* and the manufacturer's power curve, with no need of any unperturbed wind speed sensor.
Turbine rear wind speed has been corrected with the 5% method, and corrected data has been used to produce total 10-months efficiency estimations, and average electrical conversion efficiencies (Cp) with reference to different wind speeds. Efficiencies have been compared to to experimental efficiencies obtained through the station anemometer's data and to manufacturer's Cp curve.

On March-December 2015, according to a total measured efficiency of 35.52%, the site proved to be very good in terms of wind resource (significantly hitting the higher Cp range of the turbine). The estimated efficiency, obtained through the 5%method corrected wind speed, is 37.38% for the same period. The estimation is close, but the 5% method shows to be slightly too optimistic, the trend being confirmed even on turbulence efficiency analysis. However, a difference lower than 2% could be acceptable, considering instrument's errors and the aleatory nature of the wind resource.

Electrical power/aerodynamic power 10-min efficiencies have been studied, with reference to their wind speed, both using *measured front hub wind speed* and *corrected wind speed*. Efficiencies calculated through measured wind speed show a higher dispersion with reference to their average values (obtained for different wind speeds), with a standard deviation up to 0.062. Efficiency points calculated through *corrected wind speed* have a lower dispersion with reference to their average values (obtained for different wind speeds), with a standard deviation up to 0.040. In both cases, dispersion dramatically decreases for wind speeds higher than 13 m/s

Measured average efficiency points show to be lower than the manufacturer's Cp for wind speeds lower than 13 m/s, confirming the wind speed-electrical power analysis. However, for wind speeds higher than 15 m/s, the average efficiency points are equal or slightly higher than the manufacturer's Cp: errors in the SCADA measurement system have been hypothesized.

The estimated average efficiency, obtained with the *corrected wind speed*, produced an overestimation, with reference to the measured average efficiency, for wind speeds higher than 7 m/s.

For wind speeds exceeding 14m/s, the measured average efficiency and the estimated average efficiency produces the same values.

In conclusion, the 5% non-exceeding probability correction method showed to be effective in both *turbine rear wind speed* correction and the following efficiency estimation. The method is sufficiently simple and efficient to be used on commercial application. However, its slight overestimation of efficiency should be considered.

With reference to this specific case, a further analysis on blade soiling, complex site topography and other potential site-related causes would be interesting to better explain the experimental power deviation with reference to the manufacturer's power curve.

References

Burton, Jenkins: *Wind energy Handbook*, Wiley, 2011. ISBN: 978-0-470-69975-1

Ackermann: *Wind power in power systems,* Wiley, 2012. ISBN: 9780470974162

Wei Tong: *Wind power generation and wind turbine design,* WIT press, Southampton 2010. ISBN: 978-1-84564-205-1

Hau: *Wind Turbines. Fundamentals, technologies, application economics,* Springer, Berlin-Heidelberg 2013. ISBN: 978-3-642-27150-2

Vittal, Ayyanar: *Grid integration and dynamic impact of wind energy,* Springer, New York 2013. ISBN:978-1-4419-9322-9

Marchis: *Storia delle macchine,* Laterza, Bari 2005

Spertino: *Generazione fotovoltaica ed eolica di energia elettrica (university course),* Politecnico di Torino, Turin 2013.

F.Spertino P.Di Leo, I. Ilie, G.Chicco, *DFIG equivalent circuit and mismatch assessment between manufacturer and experimental power-wind speed curves*, Renewable Energy 48, 2012

G.Chicco, P.Di Leo, I.Ilie, F.Spertino, *Operational Characteristics of a 27-MW Wind Farm from Experimental Data, IEEE 2008,* 978-1-4244-1633-2/08/.00

F.Piccinnu, prova finale laurea triennale ingegneria energetica, *Analisi statistica dei dati anemometrici e calcolo della producibilità di una turbina eolica*, Politecnico di Torino, Torino 2017

Rosłaniec: *Energy conversions (university course),* Warsaw University of Technology, Warsaw 2016.

Enercon website and E70 data sheets http://www.enercon.de/en/products/ep-2/e-70/

The European wind atlas http://www.wasp.dk/dataandtools#wind-atlas__european-wind-atlas

Wikipedia: https://en.wikipedia.org/wiki/Main_Page

Ringraziamenti

Il mio più grande grazie va alla mia famiglia allargata, che mi ha sostenuto e incoraggiato durante questi anni. E' solo grazie a voi, al vostro sostegno morale e materiale, al vostro supportare le mie scelte, se sono potuto arrivare a questo importante traguardo. Un grazie a mia madre Piera, a mio padre Walter e a mio fratello Roberto. Grazie a mia nonna Giovanna Maria e a mio nonno Giovanni, ai miei zii Alberto, Giannino, Margherita, che sono andati ben oltre il loro ruolo familiare. Un grazie ed un pensiero a mia nonna Gavina, che mi ha trasmesso tanto nei pochi bellissimi anni trascorsi insieme: mi piace pensare che, da lassù, sorrida alla vista del suo nipotino. Grazie, a tutti voi, con tutto il cuore. Siete le persone più importanti della mia vita.

Grazie a zio Cosimo e a zia Tina, per tutti i bei momenti condivisi insieme, da sempre.

Un ringraziamento a diddino Franco, a diddina Vincenzina e a mio cugino Michele: grazie per la fiducia, l'affetto, e per rappresentare una delle ancore che mi legano alla mia terra.

Ringrazio Antonio, l'amico di una vita. Mi sei sempre stato accanto e ci sarai sempre; tra noi, persino le parole sono superflue.

Grazie a Riccardo, che ha illuminato la mia vita in un momento difficile, e che conosce di me forse più di chiunque altro. Sei una delle persone a me più care.

Grazie al mio caro amico Mikhail: i tuoi consigli, i tuoi discorsi, perfino il tuo sarcasmo mi hanno fatto crescere moltissimo. Mi mancano terribilmente le nostre serate insieme a Varsavia.

Un grazie sentito a Pasquale: i tuoi consigli, la tua perseveranza, il tuo aiuto sono stati fondamentali. Ti sono molto grato.

Un ringraziamento particolare a Olga, che mi ha reso una persona un pochino migliore, e a cui devo tanto.

Grazie agli amici di sempre, Chiara, Giovanni, Virginia, Jerica.

Grazie ai migliori coinquilini e amici che si possano desiderare, Chiara, Michele, ed Enrico.

Un ringraziamento ai miei compagni di avventure al Politecnico e non solo, Riccardo, Francesca, Antonio, Giulia, Federico, Moira, Andrea.

Grazie a tutte le persone che hanno reso speciale la mia avventura polacca, in particolare a Flavio, Małgorzata, Roman, Roberto, Davide e Justyna.

Ringrazio il mio Relatore, Prof. Filippo Spertino, per la grande fiducia che ha riposto in me, per la pazienza e i buoni consigli che ho avuto modo di apprezzare.

Ringrazio infine il Warsaw University of Technology per avermi accolto, ospitato e per avermi dato così tanto. E' stato semplicemente l'anno più bello della mia vita. In particolare, grazie al Prof. Łukasz Rosłaniec per aver reso ancora migliore il mio anno a Varsavia, e avermi trasmesso quel qualcosa in più di cui ho imparato a fare tesoro.